



Understanding Whole-Plant Nonstructural Carbohydrate Storage in a Changing World

Citation

Furze, Morgan E. 2019. Understanding Whole-Plant Nonstructural Carbohydrate Storage in a Changing World. Doctoral dissertation, Harvard University, Graduate School of Arts & Sciences.

Permanent link

<http://nrs.harvard.edu/urn-3:HUL.InstRepos:42029588>

Terms of Use

This article was downloaded from Harvard University's DASH repository, and is made available under the terms and conditions applicable to Other Posted Material, as set forth at <http://nrs.harvard.edu/urn-3:HUL.InstRepos:dash.current.terms-of-use#LAA>

Share Your Story

The Harvard community has made this article openly available.
Please share how this access benefits you. [Submit a story](#).

[Accessibility](#)

Understanding whole-plant nonstructural carbohydrate storage in a changing world

A dissertation presented by

Morgan E. Furze

to

The Department of Organismic and Evolutionary Biology

in partial fulfillment of the requirements
for the degree of

Doctor of Philosophy

in the subject of

Biology

Harvard University
Cambridge, Massachusetts
April 2019

© Morgan E. Furze 2019

All rights reserved

Understanding whole-plant nonstructural carbohydrate storage in a changing world

ABSTRACT

Nonstructural carbohydrates (NSCs) play a critical role in plant physiology and metabolism. They serve as building blocks for growth, fuel for respiration, and solutes for cellular regulation, but they can also be stored in the form of sugars and starch, with allocation timescales spanning minutes to decades. When stored, this reserve acts as a “food pantry” that enables sessile, long-lived plants to survive during unfavorable environmental conditions when their ability to make new NSCs is impaired. While there is growing evidence linking NSCs with stress tolerance and survival, critical questions about the size of the carbohydrate “food pantry” and how quickly it is used up and replenished remain unresolved. This knowledge gap hinders our ability to predict plant resilience to biotic and abiotic stress in a changing world, which has broader implications for understanding both short-term and long-term C storage and cycling at the whole-plant and ecosystem levels.

In Chapter 1, I compared carbohydrate storage in temperate species at Harvard Forest (Petersham, MA) to determine the size and seasonal dynamics of whole-tree NSC reserves over the course of a year. These field-based NSC data were then scaled up to the forest ecosystem level and compared to estimates from commonly used ecosystem and land surface models. In Chapter 2, I built upon this work by characterizing the radial patterns in the concentration and age of NSCs within organs to gain insight into the availability of NSC reserves.

In Chapter 3, I combined a long-term warming experiment with ^{13}C -CO₂ pulse labeling and compound-specific isotope analysis to trace sugars throughout whole-trees in the field (Richmond,

NSW). This allowed for the assessment of carbon dynamics in response to warming representative of future temperature predictions for Australia.

In Chapter 4, I quantified the seasonal dynamics of NSCs in boreal species at SPRUCE (Bovey, MN), a large-scale global change experiment using open-top chambers. This initial work explored shrubs and trees outside of the chambers and will inform long-term plant responses to elevated CO₂ and temperature within the chambers.

Overall, this dissertation provides insight into whole-plant carbon storage and allocation under current and future climatic conditions.

Contents

INTRODUCTION	1
CHAPTER 1: Whole-tree nonstructural carbohydrate storage and seasonal dynamics in five temperate species	8
CHAPTER 2: Seasonal fluctuation of nonstructural carbohydrates within tree organs reveals the metabolic availability of older stemwood reserves	21
CHAPTER 3: Carbon isotopic tracing of sugars throughout whole-trees exposed to climate warming	55
CHAPTER 4: Seasonal patterns of nonstructural carbohydrate reserves in four woody boreal species	83
APPENDIX A: Detours on the phloem sugar highway: stem carbon storage and remobilization	95

Acknowledgments

To my committee members, mentors, and collaborators, past and present, thank you for fostering my curiosity of the natural world, providing invaluable guidance and encouragement, and giving me the opportunity and tools to develop as a scientist.

To my labmates and plant peers, thank you for your boundless support and enthusiasm, for infusing my life with positivity, and for teaching me that green is the color of life.

To my friends, family, and fitness community, thank you for navigating graduate school with me, and providing outlets to destress and enjoy life. A special thanks to my roommates for literally everything, and to my grandparents for voicing their love.

To my brother and sister-in-law, thank you for guiding me through life, embracing my idiosyncrasies, providing laughter and friendship, and holding me to my 6-year timeline.

To my parents, thank you for your unconditional love, support, trust, and patience. You gave me the opportunity, tools, and guidance to succeed and have supported all of my pursuits without question. Thank you for always being there for me.

To my best friend, thank you for enriching my life, believing in me, pushing me to challenge myself, and motivating me with Mao's homestyle pork and pickle chips. You were my favorite part of graduate school.

For Dianne

Introduction

Adapted from Appendix A:

Furze, ME, Trumbore, S, Hartmann, H. 2018. Detours on the phloem sugar highway: stem carbon storage and remobilization. *Current Opinion in Plant Biology* 43: 89-95.

Plants are organisms that can live for decades, centuries, and even millennia. This long lifespan increases a plant's risk of encountering stressful conditions where normal functioning is disturbed and metabolism has to rely on stored resources (McDowell, 2011). Because plants are autotrophic organisms, storage of primary metabolites like nonstructural carbohydrates (NSC) is particularly important for survival during biotic and abiotic stress. These reserves are allocated to various organs and processes operating on timescales ranging from minutes to decades, each contributing to the plant's overall carbon (C) balance (Hartmann & Trumbore, 2016).

NSCs exist in essentially all components of living vegetative tissues of the plant; they can be found in vacuoles, plastids, and the cytosol of cells, as well as in the apoplast (Secchi & Zwieniecki, 2016). Large amounts of NSCs are stored long-term in amyloplasts of ray and axial parenchyma cells. Because secondary growth in woody plants produces new cell layers interspersed with living parenchyma cells every year, the resulting tissues provide storage capacities for different temporal horizons: : small branches and fine roots are thought to serve as seasonal storage, while large branches, coarse roots, and tree stems are used for decadal storage (Hartmann & Trumbore, 2016). Only the heartwood, comprising the innermost region of woody organs, does not contain living cells and therefore NSCs in the heartwood are presumed to be inaccessible (Spicer, 2005).

Supply and demand of NSCs is often asynchronous, for example, during leaf out in temperate deciduous species or during more unpredictable events such as drought, pest outbreaks, and

disturbance. In such cases, plants must often allocate previously stored NSCs throughout their bodies, both between and within organs, to maintain proper function. In trees, stems are the linkage between the main photosynthetic source, the canopy, and one of its major heterotrophic sinks, the root system. Secondary growth in stems produces layers of cells each growing season, divided into xylem, which transports mainly water and nutrients from the soil to the canopy and transport phloem, which redistributes recently fixed (younger) and previously stored (older) NSCs vertically between organs. During the last decades, evidence has accumulated that the transport phloem is not an ‘express’ highway, but rather a leaky pipe where NSCs passively diffuse out and are actively loaded back into companion cells during long distance vertical transport (De Schepper *et al.*, 2013).

These inverse flows are thought to serve as short term buffers for imbalances between sources and sinks, but can also facilitate lateral exchange of NSCs between the phloem and stem parenchyma (Minchin *et al.*, 1993; McQueen *et al.*, 2005). Ray cells extend radially throughout the xylem and connect to the phloem, allowing for both the lateral storage and remobilization of NSCs into and out of the stem (Ziegler, 1964). Recently, radiocarbon signatures of sugars and starch have demonstrated lateral storage by net inward mixing of younger NSCs into the stem in many temperate tree species (Richardson *et al.*, 2015; Trumbore *et al.*, 2015). The use of mixed-aged NSCs for respiration or growth of stem resprouts supports the idea of remobilization of previously stored reserves (Carbone *et al.*, 2013; Muhr *et al.*, 2013).

However, processes regulating the exchange of NSCs along the transport pathway, and the degree to which timescales of NSC storage result from physical transport and isolation (i.e. flow rates into and out of rays) versus active regulation remain poorly understood. Coupling this with our limited knowledge of the spatial and temporal distribution of NSCs throughout whole-trees yields an incomplete picture of C storage and allocation, which hinders our ability to predict species’ resilience and forecast forest ecosystem responses to global change (Le Roux *et al.*, 2001). Herein, I explore

whole-plant C storage and allocation, particularly in trees, by measuring the size, age, and seasonality of NSCs in belowground and aboveground organs of various temperate, boreal, and subtropical species using colorimetric analyses and isotopic techniques.

First, I compared carbohydrate storage in five temperate tree species at Harvard Forest (Petersham, MA) to determine the size and seasonal dynamics of whole-tree NSC reserves and the contribution of individual organs. (Chapter 1). NSC concentrations in the branches, stem, and roots were measured over the course of a year. These concentrations were scaled up to the whole-tree and whole-forest levels using allometric equations. I then compared my measurement of whole-forest NSC storage to estimates of whole-forest NSC storage generated by ecosystem and land surface simulation models. I found that the size of whole-tree NSC reserves differed between species based on traits like leaf habit and wood anatomy. NSC reserves were minimally drawn down across the seasons at the whole-tree level, but substantially drawn down at the organ level, particularly in the branches. By comparing my measurement of whole-forest carbohydrate storage with those estimated by simulation models, I found that simulation models generally overpredict NSC storage by 100%. Overprediction of NSC reserves consequently makes trees appear more resilient to stress than they actually are.

Second, I built upon the work in Chapter 1 by investigating the distribution of NSCs within individual organs to gain insight into the availability of reserves in deeper tissues to support plant function (Chapter 2). I measured the radial patterns of NSCs in aboveground and belowground organs over the course of a year, and estimated the mean age of sugars within and between different organs in a subset of trees using the radiocarbon bomb spike approach. My results highlight the dynamic nature of NSC pools, even in older stem rings.

Third, I explored how carbohydrate transport and utilization will respond to a warmer world. I conducted a warming and isotopic pulse-chase experiment on an endemic Eucalypt species growing in a whole-tree chamber system (Richmond, NSW) to test whether warming increases the speed of

carbohydrate dynamics (Chapter 3). Whole trees were pulse-labeled with ^{13}C - CO_2 to follow recently assimilated C through different organs and sugars using compound-specific isotope analysis. I then compared the concentrations and turnover rates of individual sugars between ambient and warmed ($+3^\circ\text{C}$) treatments. Trees dynamically allocated ^{13}C -labeled sugars from the leaves to the roots. However, there was not a significant treatment effect on C dynamics, as sugar concentrations and turnover rates were not altered by warming. My results suggest that an endemic Eucalypt was able to acclimate to warming representative of future temperature predictions for Australia and provide insight into the physiological and environmental controls on whole-tree C balance.

Then, I quantified the seasonal dynamics of NSC reserves in four woody boreal species at the SPRUCE facility (Bovey, Minnesota), a global change ecosystem manipulation in which open-top chambers are set in a boreal peat bog and receive various degrees of elevated CO_2 and temperature (Chapter 4). My initial work quantified NSC storage in trees and shrubs growing outside of the chambers, and these baseline data will inform long-term measurements within the chambers. The overarching goal is to determine how different temperature (ambient to $+9^\circ\text{C}$) and CO_2 (ambient and 2x ambient) treatments influence NSC storage and whether this varies between species. I found that NSC storage dynamics differed between species as well as between shrubs and trees.

Finally, I reviewed our current knowledge of C storage and allocation in tree stems (Appendix A). To date, research and models emphasize the role of tree stems as “express” sugar highways. However, recent investigations using isotopic markers suggest that there is considerable storage and exchange of phloem-transported sugars with older NSC reserves within the stem. We suggest that stems play an important role not only in long-distance transport, but also in the regulation of the tree’s overall C balance, and isotopic tools hold promise for improving our quantitative understanding of C partitioning.

Taken together, this body of work advances our understanding of whole-plant C storage and allocation. This knowledge is essential for highlighting the important role of NSCs in processes ranging from the organism to ecosystem level. At the organism level, NSCs are not only critical for plant physiology and metabolism, but also their storage may influence species' resilience by serving as a buffer against biotic and abiotic stress. At the ecosystem level, NSCs are an important component of the global C cycle, and should be taken into consideration when modeling C fluxes and predicting the C capture potential of forests. Thus, resolving how carbohydrates flow through plants contributes to our basic understanding of C physiology and provides a foundation for improving our ability to predict how forest ecosystem will respond to a changing world.

References

- Carbone MS, Czimeczik CI, Keenan TF, Murakami PF, Pederson N, Schaberg PG, Xu X, Richardson AD. 2013. Age, allocation and availability of nonstructural carbon in mature red maple trees. *New Phytologist* 200:1145-1155.
- De Schepper V, De Swaef T, Bauweraerts I, Steppe K. 2013. Phloem transport: a review of mechanisms and controls. *Journal of Experimental Botany* 64:4839-4850.
- Hartmann H, Trumbore S. 2016. Understanding the roles of nonstructural carbohydrates in forest trees—from what we can measure to what we want to know. *New Phytologist* 211: 386–403.
- Le Roux X, Lacoite A, Escobar-Gutiérrez A, Le Dizès S. 2001. Carbon-based models of individual tree growth: a critical appraisal. *Annals of Forest Science* 58:469-506.
- McDowell NG. 2011. Mechanisms linking drought, hydraulics, carbon metabolism, and vegetation mortality. *Plant Physiology* 155:1051-1059.
- Minchin PEH, Thorpe MR, Farrar JF. 1993. A simple mechanistic model of phloem transport which explains sink priority. *Journal of Experimental Botany* 44:947-955.
- McQueen JC, Minchin PEH, Thorpe MR, Silvester WB. 2005. Short-term storage of carbohydrate in stem tissue of apple (*Malus domestica*), a woody perennial: evidence for involvement of the apoplast. *Functional Plant Biology* 32:1027-1031.
- Muhr J, Angert A, Negrón-Juárez RI, Muñoz WA, Kraemer G, Chambers JQ, Trumbore SE. 2013. Carbon dioxide emitted from live stems of tropical trees is several years old. *Tree Physiology* 33:743-752.
- Richardson AD, Carbone MS, Huggett BA, Furze ME, Czimeczik CI, Walker JC, Xu X, Schaberg PG, Murakami P. 2015. Distribution and mixing of old and new nonstructural carbon in two temperate trees. *New Phytologist* 206:590-597.
- Secchi F, Zwieniecki MA. 2016. Accumulation of sugars in the xylem apoplast observed under water stress conditions is controlled by xylem pH. *Plant, Cell & Environment* 39:2350-2360.
- Spicer R. 2005. Senescence in secondary xylem: heartwood formation as an active developmental program. In: Holbrook NM, Zwieniecki MA, eds. *Vascular transport in plants*. Academic Press, 457–475.

Trumbore S, Czimczik CI, Sierra CA, Muhr J, Xu X. 2015. Non-structural carbon dynamics and allocation relate to growth rate and leaf habit in California oaks. *Tree Physiology* 35:1206-1222.

Ziegler H. 1964. Storage, mobilization and distribution of reserve material in trees. In Zimmermann MH, ed. *The formation of wood in forest trees*. Academic Press, 303-320.

1

Whole-tree nonstructural carbohydrate storage and seasonal dynamics in five temperate species

Reprinted from:

Furze, ME, Huggett, BA, Aubrecht, DM, Stolz, CD, Carbone, MS, Richardson, AD. 2018. Whole-tree nonstructural carbohydrate storage and seasonal dynamics in five temperate species. *New Phytologist* 221: 1466-1477.

Open access article and supplement available at <https://doi.org/10.1111/nph.15462>

Whole-tree nonstructural carbohydrate storage and seasonal dynamics in five temperate species

Morgan E. Furze¹ , Brett A. Huggett², Donald M. Aubrecht¹, Claire D. Stolz¹, Mariah S. Carbone^{3,4}  and Andrew D. Richardson^{3,5} 

¹Department of Organismic and Evolutionary Biology, Harvard University, 26 Oxford St, Cambridge, MA 02138, USA; ²Department of Biology, Bates College, Lewiston, ME 04240, USA;

³Center for Ecosystem Science and Society, Northern Arizona University, Flagstaff, AZ 86011, USA; ⁴Department of Biological Sciences, Northern Arizona University, Flagstaff, AZ 86011, USA; ⁵School of Informatics, Computing, and Cyber Systems, Northern Arizona University, Flagstaff, AZ 86011, USA

Author for correspondence:

Morgan E. Furze

Tel: +1 617 495 5891

Email: mfurze@fas.harvard.edu

Received: 24 May 2018

Accepted: 25 August 2018

New Phytologist (2018)

doi: 10.1111/nph.15462

Key words: carbon allocation, carbon balance, Harvard Forest, nonstructural carbohydrates (NSCs), temperate trees, whole-tree NSC storage.

Summary

- Despite the importance of nonstructural carbohydrates (NSC) for growth and survival in woody plants, we know little about whole-tree NSC storage. The conventional theory suggests that NSC reserves will increase over the growing season and decrease over the dormant season. Here, we compare storage in five temperate tree species to determine the size and seasonal fluctuation of whole-tree total NSC pools as well as the contribution of individual organs.
- NSC concentrations in the branches, stemwood, and roots of 24 trees were measured across 12 months. We then scaled up concentrations to the whole-tree and ecosystem levels using allometric equations and forest stand inventory data.
- While whole-tree total NSC pools followed the conventional theory, sugar pools peaked in the dormant season and starch pools in the growing season. Seasonal depletion of total NSCs was minimal at the whole-tree level, but substantial at the organ level, particularly in branches. Surprisingly, roots were not the major storage organ as branches stored comparable amounts of starch throughout the year, and root reserves were not used to support springtime growth.
- Scaling up NSC concentrations to the ecosystem level, we find that commonly used, process-based ecosystem and land surface models all overpredict NSC storage.

Introduction

Existing primarily as nonstructural carbohydrates (NSCs), and to a lesser degree as lipids and sugar alcohols, nonstructural carbon (C) plays a critical role in the physiology and metabolism of forest trees. NSCs are stored in essentially all living vegetative tissues in the form of soluble sugars and insoluble starch and can be subsequently drawn upon to maintain proper tree function. They serve as building blocks for growth, fuel for respiration, and solutes for osmoregulation and osmoprotection (reviewed in Hartmann & Trumbore, 2016). As such, NSCs are allocated to various functions and stored in various organs on timescales spanning minutes to decades, allowing trees to persist when respiration exceeds photosynthesis during recurring annual events like springtime leaf out in deciduous species as well as during more unpredictable stressors like drought.

As trees rely on and replenish stored NSCs throughout the year, seasonal variation in storage is driven by the balance between sources and sinks. Depletion occurs when photosynthesis is low or demands are high, and refilling occurs under the reverse conditions (Chapin *et al.*, 1990). Based on the conventional theory of annual NSC reserve dynamics in temperate forest

woody plants, NSCs are expected to increase throughout the growing season when photosynthesis is high and NSC reserves accumulate as growth slows, and decrease throughout the dormant season when photosynthesis is absent and NSC reserves are drawn upon for respiration (Kozlowski, 1992). However, our understanding of NSC storage – at the whole-tree level – remains limited. Specifically, we lack a detailed understanding of how the size and seasonal fluctuation of whole-tree total NSC storage as well as the contributions of individual organs to these dynamics differ among temperate forest trees.

While previous studies have estimated total NSC storage at the whole-tree level (Gholz & Cropper, 1991; Barbaroux *et al.*, 2003; Hoch *et al.*, 2003; Würth *et al.*, 2005; Gough *et al.*, 2009; Richardson *et al.*, 2015; Smith *et al.*, 2017), whole-tree total NSC storage has not been assessed throughout the year with high temporal resolution. Generating estimates of whole-tree total NSC storage requires a detailed assessment in which NSC concentrations are frequently measured across organs, scaled up to the whole-organ level, and then summed together. These estimates are essential for understanding how C flows throughout trees over time and will help to interpret NSC dynamics as a product of the complex integration of source-sink functions, storage

© 2018 The Authors

New Phytologist © 2018 New Phytologist Trust

This is an open access article under the terms of the Creative Commons Attribution License, which permits use, distribution and reproduction in any medium, provided the original work is properly cited.

New Phytologist (2018) **1**
www.newphytologist.com

strategies, and different biological roles of sugars and starch (reviewed in Martínez-Vilalta *et al.*, 2016).

Moreover, previous work supports the need to measure a wider range of both belowground and aboveground organs, as a single organ is not a good indicator of NSC storage at the whole-tree level (Richardson *et al.*, 2013). NSC concentrations differ between organs, making it impossible to estimate whole-tree storage based on concentration measurements from a single organ. Also, the seasonal dynamics may be different for each organ (Hoch *et al.*, 2003), reflecting an organ's contribution to physiological and metabolic processes at different times throughout the year as well as its physiological specialization. For example, roots may have a higher storage capacity due to a larger proportion of ray and axial parenchyma cells (Lens *et al.*, 2000; Pratt *et al.*, 2007), with NSC reserves allocated towards new springtime growth. Thus, some organs may preferentially store NSCs more so than other organs, with this role shifting seasonally.

In addition to contributions by individual organs, a species' ecology also drives the seasonal dynamics of whole-tree total NSC storage. Differences in NSC storage and allocation are influenced by leaf habit (Hoch *et al.*, 2003; Palacio *et al.*, 2007; Richardson *et al.*, 2015) and wood anatomy (Barbaroux & Bréda, 2002). For example, past studies often report higher storage requirements for deciduous than evergreen species (Dickson, 1989; Kozłowski, 1992; Hoch *et al.*, 2003). Similar differences in storage are also evident based on wood anatomy, with larger reserves for ring-porous compared to diffuse-porous species (Barbaroux & Bréda, 2002). These findings motivate the estimation

of whole-tree total NSC storage across multiple species, which in turn fosters a more robust estimation of total NSC storage at the ecosystem level.

Furthermore, our understanding of the seasonal dynamics of whole-tree total NSC storage is limited (Würth *et al.*, 2005; Smith *et al.*, 2017). While total NSC concentrations at the organ level have been found to be only weakly seasonal (Hoch *et al.*, 2003; Richardson *et al.*, 2013; Hoch, 2015), a detailed within-year study is needed to assess seasonality at the whole-tree level. By examining whole-tree total NSC pools during periods of varying supply and demand over the course of a year, we can resolve the contribution of individual organs, as well as characterize seasonal fluctuations of sugar and starch pools to determine both the size and timing of annual minima/maxima. Although not yet quantified, a minimum threshold of NSC storage may be required to maintain proper tree function (Adams *et al.*, 2013). Thus, a detailed within-year study not only provides foundational insights into the role of NSCs in whole-tree and ecosystem C balance, but also informs future studies that seek to investigate the influence of interannual variation and associated stressors (i.e. drought) on storage dynamics.

Here we characterize whole-tree total NSC storage in five temperate tree species. We collected belowground and aboveground woody organs each month, measured their sugar and starch concentrations, and then scaled these data up to the whole-tree level (Fig. 1). Our objective was to quantify whole-tree total NSC storage over the course of a year to test the conventional theory, which suggests that NSC reserves will increase over the growing

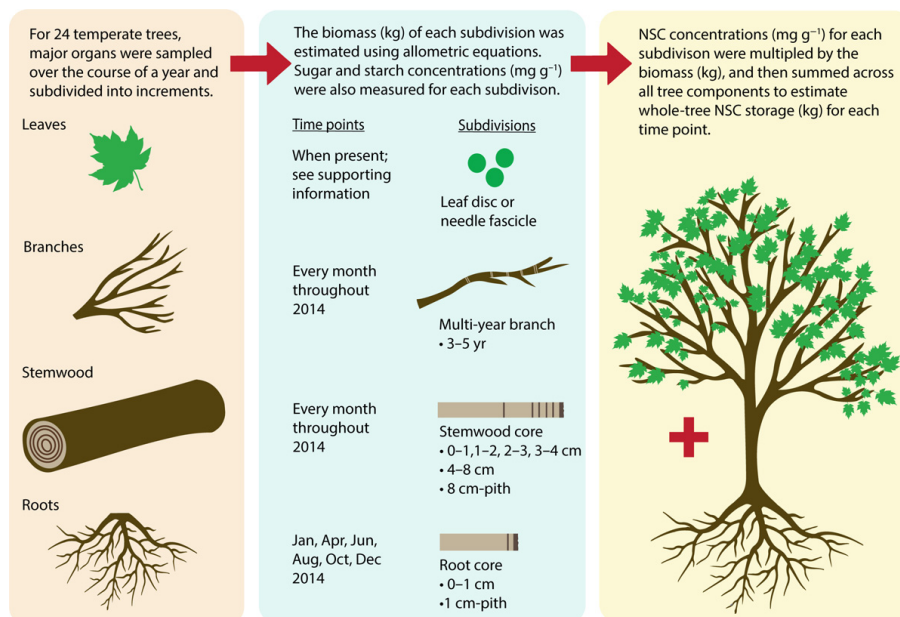


Fig. 1 Summary of field sampling and allometric scaling from nonstructural carbohydrate (NSC) concentrations to whole-tree NSC pools.

season and decrease over the dormant season. Specifically, we addressed the following questions: (1) How big are whole-tree total NSC pools? (2) Do these pools vary across the seasons and if so, what is the degree of seasonal fluctuation? (3) What is the contribution of individual organs to whole-tree storage? (4) Do the above storage dynamics differ between coexisting temperate tree species? Additionally, to understand the role of storage in the context of ecosystem-level C fluxes and annual woody biomass production, we estimated ecosystem-level total NSC storage using forest stand inventory data and compared this with predictions from a suite of commonly used, process-based ecosystem and land surface models.

Materials and Methods

Study site

Harvard Forest, is an oak-dominated, mixed temperate forest located in Petersham, MA, USA (42.53°N, 72.17°W). We selected 24 mature trees for this study belonging to the following species: red oak (*Quercus rubra* L., $n=6$), white pine (*Pinus strobus* L., $n=6$), red maple (*Acer rubrum*, $n=6$), paper birch (*Betula papyrifera*, $n=3$), and white ash (*Fraxinus americana* L., $n=3$). These trees represent the dominant species in this area of Harvard Forest and are broadly representative of the forests in the northeastern USA. Importantly, they cover various forms of leaf habit, wood anatomy, and shade tolerance. White pine is an evergreen conifer, whereas the other species are deciduous broadleaf trees. Of the deciduous broadleaf species, red oak and white ash are ring-porous, and red maple and paper birch are diffuse-porous. White ash and paper birch are shade-intolerant species, while the others are of intermediate shade tolerance.

Throughout the study year 2014, phenological observations (O'Keefe, 2015) as well as environmental conditions (Boose, 2018) were recorded at Harvard Forest and provide context for NSC dynamics reported herein. In brief, our study species exhibited 50% budburst by mid-May. In the autumn, leaves began to drop by the start of October and deciduous species were barren by mid-November. A comprehensive analysis of phenological events across tree species and over time at Harvard Forest is provided in Richardson & O'Keefe (2009). Furthermore, Harvard Forest has a mean annual temperature of 7.1°C and a mean annual precipitation of 1100 mm. Air temperature and precipitation data recorded by an on-site meteorological station in 2014 as well as for the period 2002–2017 are displayed in Supporting Information Fig. S1.

Field collection

In January 2014, we measured diameter at breast height (DBH) and tree height (Table S1) for all sampled trees. Each month throughout 2014, a stemwood core to the pith was collected from each tree with a standard 4.3-mm increment borer (Haglöf Company Group, Långsele, Sweden), starting at breast height on the south or southwest face of each tree with each subsequent core collected in a zigzag pattern (*c.* 7.5 cm over, 7.5 cm up; 18 cm

average core depth). In addition to a monthly stemwood core, we collected sunlit branches from the top of the canopy, which was accessed using a bucket lift. Sunlit leaves were also gathered when present, but were not necessarily taken from the sampled branch. We collected coarse root cores in January, April, June, August, October, and December 2014. The first root sample was taken at 20 cm along the root from the base of the tree, and subsequent cores were taken in a zigzag pattern. Samples were kept on dry ice in the field during each collection and then stored at -80°C .

Laboratory preparations and NSC analyses

It has been shown that NSC concentrations often decline with increasing stem depth (Hoch *et al.*, 2003), yielding NSC concentrations in the heartwood that are generally very low. Therefore, scaling to the whole-stem requires that this variation be accounted for. Although other work has scaled up by differentiating between sapwood and heartwood (Würth *et al.*, 2005), we subdivided the stemwood cores into smaller pieces to obtain a finer resolution. Coarse roots were also subdivided, and branchwood was homogenized across multiple years of growth. Therefore, across trees, we consistently subdivided organs for NSC analysis (Methods S1).

Importantly, NSCs were measured in both 'inactive' and 'active' tissues due to our approach of subdividing entire organs. Given the diameter of the sampled roots ($c. \geq 5$ cm diameter) and branches (*c.* 1–1.5 cm diameter, multi-year 3–5 yr old), 'inactive' heartwood may have been present in the roots, but perhaps absent or minimal in the branches depending on the species. Less than 20% of NSCs in the stem and 10% of NSCs in the whole tree were stored in the stem heartwood. Inclusion of the heartwood in pool estimates did not affect the seasonal dynamics of NSC storage in the stem (Methods S2).

Samples were freeze-dried (FreeZone 2.5; Labconco, Kansas City, MO, USA, and Hybrid Vacuum Pump, Vacuubrand, Wertheim, Germany) and ground (mesh 20, Thomas Scientific Wiley Mill, Swedesboro, NJ, USA; SPEX SamplePrep 1600; MiniG, Metuchen, NJ, USA). To measure sugar concentrations (adapted from Chow & Landhäusser, 2004), 10 mg of previously freeze-dried and ground tissue was freeze-dried overnight and then extracted with 80% hot ethanol followed by colorimetric analysis with phenol–sulfuric acid. The resulting bulk sugar extract was read at 490 nm on a microplate reader (Epoch Microplate Spectrophotometer; Bio-Tek Instruments, Winooski, VT, USA) or a spectrophotometer (Thermo Fisher Scientific GENESYS 10S UV-Vis, Waltham, MA, USA). Sugar concentrations (expressed as mg sugar per g dry wood) were calculated from a 1 : 1 : 1 glucose–fructose–galactose (Sigma Chemicals, St Louis, MO, USA) standard curve.

To determine starch concentrations, the remaining tissue was solubilized in NaOH and then digested with an α -amylase/amyloglucosidase digestive enzyme solution. Glucose hydrolysate was determined using a PGO-colour reagent solution (Sigma Chemicals) and read at 525 nm. Starch concentrations (expressed as mg starch per g dry wood) were calculated based on a glucose (Sigma Chemicals) standard curve. When conducting NSC

analyses, we included at least one internal laboratory standard (red oak stemwood, Harvard Forest, Petersham, MA, USA) per analysis. Additional information about NSC measurements are provided in Methods S1.

Allometric scaling from sugar and starch concentrations to whole-organ and whole-tree pools

We estimated the dry wood biomass of each organ (branch, stemwood, and root; Table S2) and organ subdivisions using allometric scaling theory (Jenkins *et al.*, 2004; see Methods S2 for details of calculations). The species-specific allometric equations used were developed for North American trees > 2.5 cm DBH, which made them appropriate for the species and size range of trees in this study. To reiterate, subdividing organs allowed us to account for variation in NSC concentrations within an organ (i.e. radial decline of NSCs in stemwood). We then paired the sugar and starch concentrations for each sample (i.e. subdivisions of each organ) with the estimate of that component's woody biomass. This was done for each sample per tree, and then the amounts were summed to estimate whole-tree total NSC storage for each month. In this case, the whole-tree total NSC pool is the sum of coarse root, stemwood, and branch reserves.

Jenkins *et al.* (2004) does not provide equations and coefficients for distinguishing between coarse and fine roots. Thus, only coarse roots were sampled and coarse root biomass was estimated in this study (Methods S2). A lack of partitioning of roots into different diameter size classes may ultimately lead to underestimation or overestimation of NSC storage in the root system. Uncertainty estimates for fine roots are provided in Richardson *et al.* (2015).

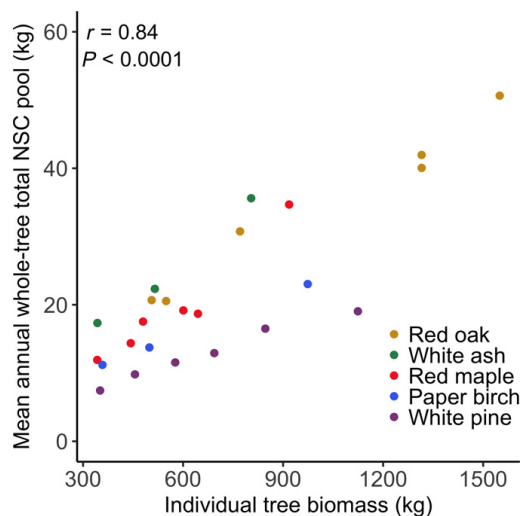


Fig. 2 Relationship between tree biomass and mean annual whole-tree total nonstructural carbohydrate (NSC) pools for 24 trees sampled at Harvard Forest in 2014. Strength of association was evaluated using Pearson's correlation, $\alpha = 0.05$.

For a subset of trees, we also included the NSC pool in foliage, but our calculations indicated that this was a minor portion of the whole-tree total NSC pool (Methods S3). Additionally, trees in our sample were all of similar DBH and ultimately biomass based on allometric equations. Therefore, biomass did not significantly differ between species (Fig. S2) and storage differences reflect NSC concentrations. However, there was a positive correlation between individual tree biomass and whole-tree total NSC pool size (Fig. 2), so biomass was included as a covariate in our statistical analyses. Data from this project are available for download and public use (Furze *et al.*, 2018).

Estimating ecosystem-level total NSC storage

In 2014, a biomass inventory of the Prospect Hill Tract at Harvard Forest was conducted for live trees > 10 cm DBH in 34, 10 m radius plots (Munger & Wofsy, 2018). Using these data and species-specific allometric equations, we estimated the biomass of each tree and its organs (foliage, branch, stemwood, and root) for over 600 trees from 14 deciduous broadleaf and evergreen conifer species (Methods S4). Measured total NSC concentrations from our five study species were used as estimates for the most similar tree species and paired with woody biomass to obtain whole-tree total NSC storage. We then summed together whole-tree total NSC storage of individual trees to estimate total NSC storage per unit ground area for this temperate forest, and examined this value in the context of annual woody biomass production, eddy flux tower measurements, and model-based predictions of total NSC storage at Harvard Forest. See caption of Fig. 6 for process-based model assumptions. When comparing results, assume that NSCs are *c.* 40% C to convert from kg NSC m² to kg C m².

Statistical analyses

While stemwood and branches were sampled every month, roots were sampled in January, April, June, August, October, and December 2014. Therefore, statistical analyses were conducted for these 6 months when whole-tree total NSC, sugar, and starch pools were complete and represent the sum of root, stem, and branch reserves. Statistical analyses for organ-level dynamics used 6-month data for roots and 12-month data for stemwood and branches. All statistical analyses were performed in R v.3.3.2 and linear mixed-effects (lme) models were fit by maximum-likelihood using the nlme package. All models contain fixed effects (specified below), individual tree as a random effect, and whole-tree or whole-organ biomass as a covariate. For significant mixed-effects models, differences between pairs of means were evaluated with Tukey's honest significant difference (HSD), $\alpha = 0.05$.

To compare whole-tree total NSC pool size between our five temperate species, as well as to determine if whole-tree total NSC pools varied across seasons according to the conventional theory, we used a linear mixed-effects (lme) model to analyze whole-tree total NSC (sum of sugar and starch pools) pool size among sampling months and species (month \times species; Fig. 3). The same

analysis was repeated for both whole-tree sugar and starch pools (month \times species; Fig. 4). For significant interaction effects, whole-tree total NSC, sugar, and starch pools were assessed across sampling months for each individual species (month; shaded bands in Figs 3, 4; Table S3).

Next, we sought to determine if pool size and seasonal patterns differed at the organ level by assessing total NSC, sugar, and starch pools in the branches, stemwood, and roots (Fig. 5). For each pool type, we used a lme model to analyze pool size among organs and species (organ \times species, Table S4). For significant interaction effects, total NSC, sugar, and starch pools were assessed among organs for each individual species (organ; Table S5). Finally, to determine if organ-level storage varied across the seasons, we used a lme model to analyze total NSC, sugar, and starch pools for each organ among sampling months and species (month \times species; Table S6). Again, for significant interaction effects, each pool type was assessed across sampling months for each individual species and organ (month; Table S7).

Results

Whole-tree total NSC pools

The ranking of species from largest to smallest whole-tree total NSC pool was red oak, white ash, red maple, paper birch, and white pine, and pool size significantly differed between species ($P < 0.0001$; Fig. 3). These results support the idea that species fall along a gradient according to leaf habit and wood anatomy,

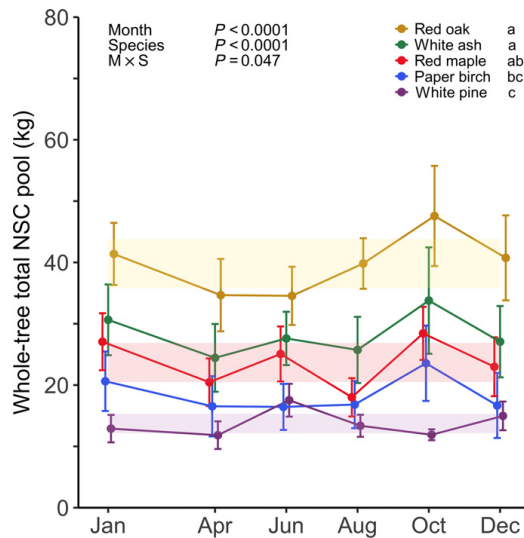


Fig. 3 Seasonal dynamics of whole-tree total nonstructural carbohydrate (NSC) pools for five temperate tree species sampled at Harvard Forest in 2014. Error bars denote ± 1 SE of the mean. Lowercase letters indicate significance of differences among species. Shaded bands for individual species represent the 95% confidence interval around the linear mixed-effects (lme) model estimated mean whole-tree total NSC pool.

with deciduous ring-porous species (red oak and white ash) having larger whole-tree total NSC reserves than both deciduous diffuse-porous (red maple and paper birch) and evergreen conifer (white pine) species.

In general, whole-tree total NSC pools built up over the growing season and declined over the dormant season, which is in line with the conventional theory ($P < 0.0001$; Fig. 3). However, the effect of sampling month on whole-tree total NSC pools depended on species ($P = 0.047$). The whole-tree total NSC pool tended to peak in October for each deciduous species and in June for evergreen white pine (Table S3). This finding suggests that leaf habit may also influence seasonal dynamics as whole-tree total NSC pools peak at different times of the year for deciduous and evergreen species. However, while the timing of peak storage at the whole-tree level may differ between species, the magnitude

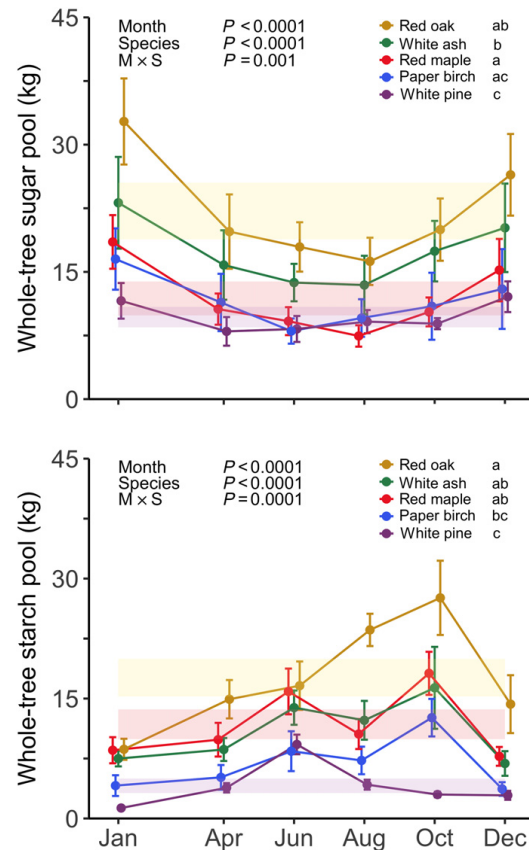


Fig. 4 Seasonal dynamics of whole-tree sugar (top) and starch (bottom) pools for five temperate tree species sampled at Harvard Forest in 2014. Error bars denote ± 1 SE of the mean. Lowercase letters indicate significance of differences among species. Shaded bands for individual species represent the 95% confidence interval around the lme model estimated mean whole-tree sugar or starch pool.

of seasonal NSC fluctuation was similar. During the growing season, deciduous species exhibited an *c.* 28% increase in whole-tree total NSC pools from the mean minimum in April to the mean maximum in October. This increase was comparable for white pine from April to June (32%).

Whole-tree sugar and starch pools

Whole-tree sugar and starch pools differed between species (both $P < 0.0001$; Fig. 4). Whole-tree sugar pools were largest for the ring-porous species red oak and white ash. In most cases, whole-tree starch pools for deciduous species were larger than that of

white pine. In general, NSCs were more often stored as sugars rather than starch throughout the year, but most deciduous species retained substantial reserves in the form of starch by the end of the growing season.

In general, whole-tree sugar pools decreased over the first half of the year and replenished during the second half of the year, peaking in the winter; whereas whole-tree starch pools slowly increased throughout the year reaching a peak in October (both $P < 0.0001$; Fig. 4). However, the effect of sampling month on whole-tree sugar and starch pools depended on species (sugar $P = 0.001$; starch $P = 0.0001$). Whole-tree sugar pools followed the expected pattern for all species, whereas whole-tree starch

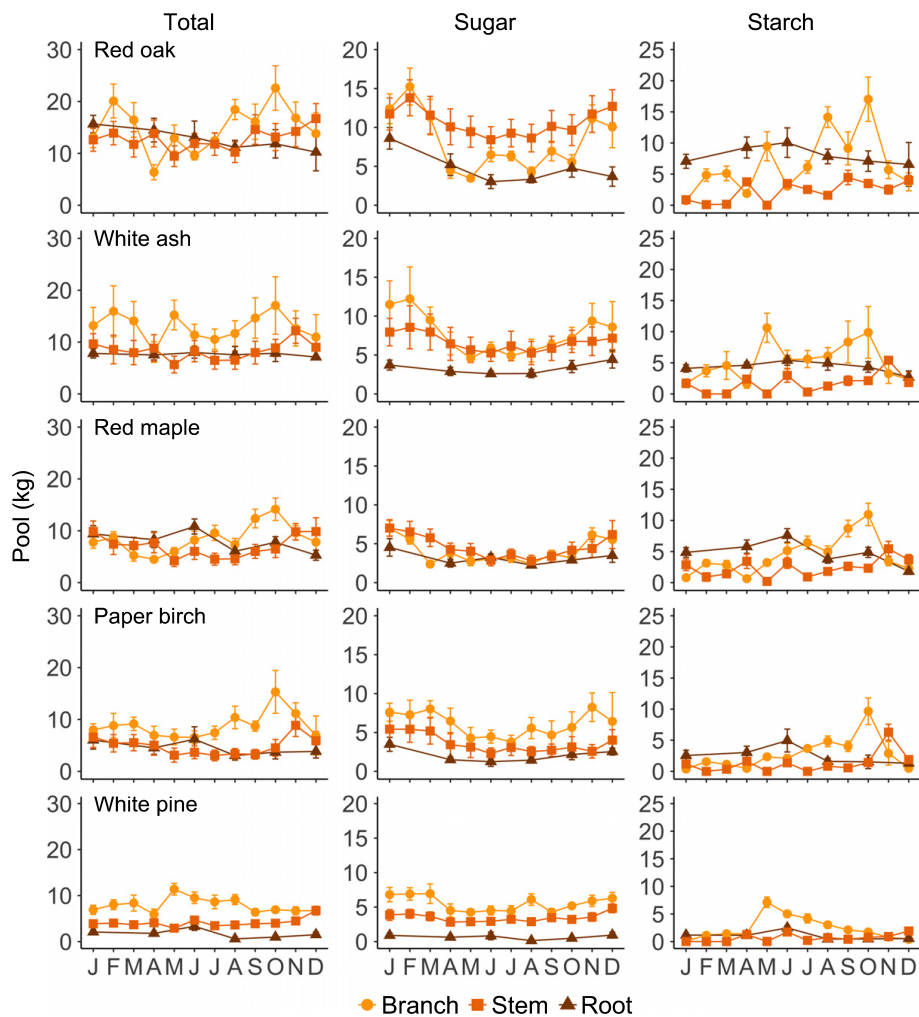


Fig. 5 Seasonal dynamics of whole-organ total nonstructural carbohydrate (NSC) (left), sugar (middle), and starch (right) pools for five temperate tree species (rows) sampled monthly at Harvard Forest in 2014. Error bars denote ± 1 SE of the mean. Note the difference in y-axis scale between columns.

pools tracked the patterns for total NSC pools, specifically the peak in October for the deciduous species and in June for evergreen white pine (Fig. 4; Table S3).

Storage and seasonality in organs

The distribution of total NSCs, sugars, and starch differed between organs (all $P < 0.0001$; Fig. 5; Table S4). Despite stemwood having the largest biomass, branches were the largest reservoir of total NSCs and sugars, followed by roots, and then stemwood. For starch, branches and roots had comparable storage which was larger than that of stemwood. However, the partitioning between organs depended on species (Table S4), and starch storage did not always differ between organs, particularly for paper birch (Table S5).

The seasonal patterns of sugar and starch pools (Table S6) often differed between organs, possibly reflecting different functional roles of sugars and starch in each organ and/or different organ contributions to processes occurring at different times of the year. In general, sugar pools were lower in the growing season than in the dormant season, particularly in aboveground organs. By contrast, while branch and stem starch pools tended to peak at the onset of the dormant season in deciduous species, root starch, and root total NSC pools in general, remained fairly stable throughout the year. However, root total NSC and starch pools declined between June and August for red maple, and root sugar pools declined between January and April for red oak and red maple (Table S7).

The percentage of sugars and starch in each organ relative to whole-tree total NSCs varied throughout the year (Table S8). As noted above, whole-tree total NSC pools tended to peak in October for each deciduous species and in June for white pine. At these times of maximal storage, organ contributions to the whole-tree total NSC pool were *c.* 25% root, 25% stemwood, and 50% branch for deciduous species and 20% root, 25% stem, and 55% branch for white pine. However, the distribution of sugars and starch differed across these woody organs. Between 70% and 90% of whole-tree sugar was in aboveground organs. The majority of whole-tree starch was stored in the branches of deciduous species in October (red oak 63%, white ash 57%, red maple

60%, and paper birch 77%), with far less in the roots (*c.* 30% in red oak, white ash, and red maple, and 13% in paper birch).

Estimation of ecosystem-level total NSC storage and seasonality

We estimated the belowground and aboveground tree biomass of the site to be *c.* 28.5 kg m⁻², which is in agreement with previous estimates conducted at Harvard Forest using multiple allometry methods (Ahmed *et al.*, 2013). Combining this forest biomass estimate with measured total NSC concentrations from our five study species, we estimated average total NSC storage across the year at the ecosystem level to be 0.41 kg C m⁻² or 1.03 kg NSC m⁻². Of this total, 0.59 kg m⁻² was sugars and 0.44 kg m⁻² was starch. Partitioning total NSC storage across organs showed that the majority of NSCs were stored in the branches (0.40 kg m⁻²), followed by stemwood (0.27 kg m⁻²) and roots (0.32 kg m⁻²), with substantially less stored in foliage (0.04 kg m⁻²).

Additionally, estimated ecosystem-level total NSC storage was in line with the allocation of assimilated C to various forest C pools (Table 1). Based on these estimates, stored NSCs at the ecosystem level could support woody biomass production for an entire year. Importantly, when comparing our results with predictions from ecosystem and land surface models, we find that all process-based simulation models overpredict total NSC storage and seasonal depletion of NSC reserves at the ecosystem level for Harvard Forest (Fig. 6).

Discussion

Size of whole-tree pools, and differences among species

At the whole-tree level, the amount of NSCs stored differed between species. In general, our results showed that whole-tree total NSC storage fell along a gradient with larger pools for ring-porous species compared with diffuse-porous and evergreen. This finding is not surprising considering that deciduous species are thought to rely on stored reserves for springtime growth (Kramer & Kozlowski, 1979; Piispanen & Saranpää, 2001), and more

Table 1 Forest stand-level characteristics at Harvard Forest.

Component	Estimate	From	Reference
Total NSC	0.41 ± 0.05 kg C m ⁻²	2014	Furze <i>et al.</i> (2018); Munger & Wofsy (2018)
Sugar	0.24 ± 0.05 kg C m ⁻²	2014	Furze <i>et al.</i> (2018); Munger & Wofsy (2018)
Starch	0.18 ± 0.06 kg C m ⁻²	2014	Furze <i>et al.</i> (2018); Munger & Wofsy (2018)
Total NSC relative to forest biomass	3.6 ± 0.4%	2014	Furze <i>et al.</i> (2018); Munger & Wofsy (2018)
Aboveground woody biomass increment	0.16 ± 0.03 kg C m ⁻² yr ⁻¹	1994–2014	Munger & Wofsy (2018)
Belowground woody biomass increment	0.04 kg C m ⁻² yr ⁻¹	2014	Furze <i>et al.</i> (2018); Munger & Wofsy (2018)
Total woody biomass increment	0.20 kg C m ⁻² yr ⁻¹	2014	Furze <i>et al.</i> (2018); Munger & Wofsy (2018)
Annual NEE of CO ₂	-0.24 ± 0.10 kg C m ⁻² yr ⁻¹	1992–2004	Urbanski <i>et al.</i> (2007)
Growing season NEE of CO ₂	-0.49 ± 0.11 kg C m ⁻² yr ⁻¹	1992–2004	Urbanski <i>et al.</i> (2007)
Dormant season NEE of CO ₂	0.24 ± 0.05 kg C m ⁻² yr ⁻¹	1992–2004	Urbanski <i>et al.</i> (2007)
Total NSC accumulation from April to October	0.14 kg C m ⁻²	2014	Furze <i>et al.</i> (2018); Munger & Wofsy (2018)

NEE, net ecosystem exchange; NSC, nonstructural carbohydrates. Uncertainty values are ± 1 SD of the mean.

specifically, ring-porous deciduous species complete a large portion of new xylem formation using stored reserves before leaf expansion (Hinckley & Lassoie, 1981; Bréda & Granier, 1996). Thus, differences in the amount of NSC stored between species are expected based on these traits.

Throughout the year, whole-tree sugar pools were often larger than starch pools. However, deciduous species had substantial starch reserves by October. Starch storage dominating the onset of the dormant season is in agreement with previous work that quantified whole-tree pools for red oak (Richardson *et al.*, 2015). Most studies, however, look at concentrations in individual organs rather than whole-tree pools and have reported that starch concentrations were higher than sugar concentrations throughout the growing season, particularly in the branch sapwood (Hoch *et al.*, 2003) and outer stem sapwood (Hoch *et al.*, 2003; Richardson *et al.*, 2013) of several temperate tree species. When examining the concentrations of individual organs, our results are in agreement with these studies. In the growing season, starch concentrations generally dominated the coarse roots and branches, and to a lesser extent, the outer 2 cm stemwood.

However, at the whole-tree level, our results disagree and show support for sugar as the larger pool. This discrepancy is due to the inclusion of stemwood xylem to the pith in our whole-tree pool estimates which increased sugars, but not starch. When taking the entire stemwood into consideration rather than just the outer sapwood like in previous studies, sugar concentrations generally dominated not only the growing season, but also the entire year. As stemwood is the largest biomass fraction, higher stemwood sugar concentrations contributed to larger overall sugar storage than starch storage at the whole-tree level. Additionally, if we had ignored the radially varying concentrations of total NSCs and used those in the outer 2 cm stemwood and outer 1 cm root as proxies for whole-stem and root storage, then mean annual whole-tree total NSC storage would have been overestimated by 75% for our sample of 24 trees.

Seasonal patterns of whole-tree pools

Seasonal dynamics of whole-tree total NSC pools were in agreement with the conventional theory of storage dynamics in which NSC reserves increase throughout the growing season and decrease throughout the dormant season. Interestingly, this seasonal pattern was not resolved when looking at the dynamics of individual organs, sugars, or starch alone; only when these components were combined did we find that whole-tree storage dynamics aligned with the expected pattern despite seasonal interconversion between sugars and starch and within-tree transport between organs.

In general, whole-tree total NSC pools peaked in October for the deciduous species and in June for evergreen white pine, and then declined onward. The difference in timing of peak accumulation and depletion may be explained by growth characteristics. As white pine retains a majority of its needles throughout the dormant season, it has an advantage for C gain earlier in the

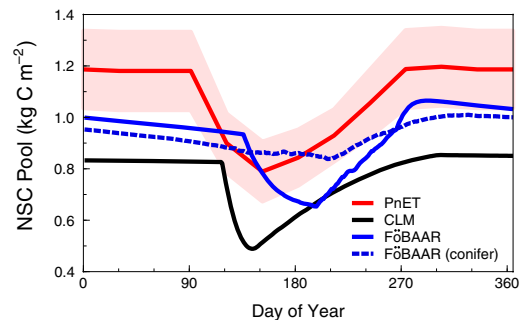


Fig. 6 Seasonal variation in the total size of the ecosystem-level nonstructural carbohydrate (NSC) storage pool (kg C m^{-2}), using two ecosystem models (PnET, Aber *et al.*, 1996; and FöBAAR, Keenan *et al.*, 2012) and a land surface model (CLM, Levis *et al.*, 2004). Model runs are assuming forest composition is 100% deciduous broadleaf tree species, except for dotted blue line which shows FöBAAR run assuming forest composition is 100% evergreen conifer species. Plotted values indicate means calculated across 15-yr model run (1991–2004), using environmental data from Harvard Forest to drive the model. For PnET, uncertainty range illustrates interannual variation (± 1 SD) around the mean.

growing season before new structural growth, leading to maximal NSC pools in June, and continued activity later into the autumn (Jurik *et al.*, 1988). However, later bud break in evergreen conifers (O’Keefe, 2015), lower photosynthetic rates (Reich *et al.*, 1995) and shoot apex development (Owston, 1969) along with xylem formation/thickening (Murmanis & Sachs, 1969) that both initiate later and continue well into the autumn may all contribute to the post-June decline. Additionally, the decline may indicate excess C being allocated to root exudation (Abramoff & Finzi, 2016).

Even though NSCs cannot be translated into growth 1:1, for instance, due to metabolic losses, we found that the requirements for annual biomass production were in line with the magnitude of whole-tree total NSC pool depletion. For the deciduous species, the annual production of foliage, branches, stemwood, and roots required 4.4–7.9 kg C, leading to an initial 1.8–3.0 kg C decline in the whole-tree total NSC pool by April/June. By contrast, white pine’s annual growth required 6.3 kg C, with an associated 2.2 kg C decline between June and October. It is often assumed that deciduous species will show a larger seasonal fluctuation in reserves than evergreen due to their reliance on stored NSCs for leaf out and xylem formation in the spring, (Kramer & Kozlowski, 1979; Piispää & Saranpää, 2001). While our results suggest that evergreen species may be relying less on stored NSCs for new growth, seasonal fluctuations in whole-tree total NSC pools were surprisingly similar. The mean minimum NSC storage in April was $\approx 75\%$ of the maximum in October for each deciduous species and 70% of the maximum in June for evergreen white pine. Thus, larger pool size did not correlate with more pronounced seasonal fluctuation, and our results agree with previous reports that showed seasonal fluctuations were not always

greater for deciduous species compared with evergreen (compiled in Martínez-Vilalta *et al.*, 2016).

Storage dynamics at the organ level

We observed substantial differences in the amount of NSCs stored between belowground and aboveground organs. Branches were the largest reservoir of total NSCs and often sugars, and were also an important store of starch, accounting for *c.* 30–40% of total NSCs and 55–75% of starch stored throughout the whole-tree at times of maximal NSC storage. Moreover, roots are thought to specialize as storage organs more so than any other organ (Loescher *et al.*, 1990; Kozłowski, 1992), so we hypothesized that the largest starch pools would be found in the roots serving a longer term storage function. Interestingly, our results show that branches had a comparable starch pool throughout the year. However, organ-level storage differed between species. For instance, red oak had a particularly large starch pool in the roots (mean annual 8 kg; effective mean concentration 44.0 mg g^{-1}) compared with that of white pine (1 kg; 8.0 mg g^{-1}). In general, deciduous species stored NSCs across organs, while white pine primarily stored its reserves aboveground.

Furthermore, the functional roles of sugars and starch were reflected in the seasonal patterns of each organ. Seasonal patterns of sugar pools were more similar between organs than starch pools. In general, sugar pools were higher in the dormant season than in the growing season for all organs, supporting an osmoprotective role for sugars throughout the tree in the wintertime (Ögren, 1997). Notably, while branch biomass represented *c.* 25% of aboveground biomass, sugar pools in the branches (mean 7.5 kg; effective mean concentration 53.0 mg g^{-1}) were equal to or larger than those in stemwood (7.5 kg; 17.0 mg g^{-1}) during cold months, suggesting that high sugar concentrations in the branches help to combat cold temperatures experienced in the canopy. By contrast, starch pools in aboveground organs generally increased over the growing season, providing evidence for starch's role in maintaining photosynthesis and phloem transport throughout the growing season (Paul & Foyer, 2001). Newly assimilated C is exported as sucrose and converted to starch for longer term storage to prevent inhibition of further transport, which would lead to the downregulation of photosynthesis.

As previously mentioned, roots were expected to have a high storage capacity, with reserves being used for annual growth (Loescher *et al.*, 1990). Yet, total NSC pools in the roots of deciduous species remained fairly stable throughout the year, and accounted for 25–35% of whole-tree total NSC reserves. In this way, roots may serve as a stable, longer term storage pool that is only drawn upon in catastrophic situations (i.e. loss of aboveground biomass), which would explain the older C previously reported in roots (Carbone *et al.*, 2013; Richardson *et al.*, 2015).

By contrast, early growing season declines were evident in the branches. Specifically, sugar pools in the branches declined between February and April, which is in accordance with branches serving as the closest source organ to support leaf out

(Landhäuser & Lieffers, 2003). Our results suggest that declining branch reserves represent contributions to new leaf production rather than conversion of antifreeze sugar compounds back to starch because branch total NSC pools also declined indicating movement out of branches rather than conversion from sugars to starch within branches. For red oak, we estimated that new leaf production would require 7.6 kg C, and observed that total NSC pools in red oak branches declined by 70% (5.5 kg C) between February and April. While stored NSCs support both new foliage and wood production, elongation and thickening of foliage is to some degree supported by concurrent photosynthesis (Keel & Schädel, 2010).

As noted earlier, the seasonal fluctuation in total NSCs at the whole-tree level was *c.* 30% for each species, suggesting minimal drawdown of stored reserves throughout the year. Martínez-Vilalta *et al.* (2016) reported similar patterns and a suite of physiological and evolutionary reasons have been proposed to explain why trees maintain large reserves if they are rarely depleted by seasonal demands (Kobe, 1997; Millard *et al.*, 2007; Adams *et al.*, 2013; Carbone *et al.*, 2013; O'Brien *et al.*, 2014). However, while total NSC reserves may not be substantially drawn down across the seasons at the whole-tree level, our results challenge this idea at the organ level. Notably, total NSCs in branches of red oak and white ash had substantial seasonal fluctuations. The total NSC pool in red oak branches declined by 70% during the winter and spring, and was replenished by autumn. A similar pattern was observed for white ash with a 50% decline.

Estimation of ecosystem-level total NSC storage

We estimated average total NSC storage across the year in a mixed temperate forest to be $1.03 \text{ kg NSCs m}^{-2}$ or 0.41 kg C m^{-2} , which falls within the $0.23\text{--}1.6 \text{ kg C m}^{-2}$ range previously reported for total NSC storage at the whole-forest level (reviewed in Dietze *et al.*, 2014). This estimate corresponds to *c.* 4% of forest biomass compared to 8% revealed in the first ecosystem-level estimate of total NSC storage in a semi-deciduous tropical forest, which was $1.6 \text{ kg NSCs m}^{-2}$ assuming a 20 kg m^{-2} woody biomass (Würth *et al.*, 2005). The majority of total NSCs were stored aboveground in both forest types. However, a direct comparison is cautioned against due to differences between the two studies such as the ratio of sapwood to heartwood in the tree species studied as well as the biomass components used for upscaled estimates of total NSC storage. In our trees, contributions to total NSC storage differed between organs: branches (40%), stemwood (25%), roots (30%), and foliage (5%).

Few studies have modelled and validated NSC pool dynamics and C allocation to various sinks at the forest stand-level, and when this validation has been done it has been with limited field measurements (Cropper & Gholz, 1993; Sampson *et al.*, 2001; Gough *et al.*, 2009). However, in this study, we combined high spatio-temporal resolution field measurements of NSCs from multiple species over the course of a year with eddy flux tower and structural growth data to assess total NSC storage in the context of whole-forest C balance at Harvard Forest. Over the course of the year, Harvard Forest exhibited net C uptake in the growing

season and release in the dormant season. The mean annual rate of net ecosystem exchange (NEE) of CO₂ was in substantial agreement with the annual total woody biomass increment, suggesting that most of the net C uptake was sequestered in long-lived, woody biomass. However, during the growing season, there was greater net C assimilation than allocation to new woody biomass production, and ecosystem-level total NSCs increased by 0.14 kg C m⁻².

Estimates of total NSC pool size and seasonal dynamics were generated for Harvard Forest (Fig. 6; Richardson *et al.*, 2012) using three process-based simulation models (PnET, Aber *et al.*, 1996; CLM, Levis *et al.*, 2004; FöBAAR, Keenan *et al.*, 2012). Model runs revealed 50% variation across models in estimates of total NSC pool size, a drawdown of the total NSC pool in spring and refilling over the summer, and similar pool size, but greatly reduced seasonal fluctuation for conifers relative to deciduous species. Notably, our results indicate that these process-based models all overpredict the amount of stored NSCs, with twice as much being stored than was estimated based on extensive field measurements. While simulation models represent C assimilation, allocation, and metabolism, they do not consider controls on sink capacity and feedbacks between these processes, yielding a 'source-driven' structure of C relations (Fatichi *et al.*, 2014), and, ultimately, simpler dynamics than are expected for complex, living plants like trees.

Our allometric scaling accounted for varying concentrations between different organs and within individual organs, particularly the radial distribution of NSCs that occurs in the stemwood; this may explain the discrepancy between our scaled-up estimates and process-based model predictions at the ecosystem level. Typically, total NSC concentrations in the outer sapwood of the stem have been measured (Fajardo *et al.*, 2013; Richardson *et al.*, 2013). If we had scaled up based on concentrations in the outer 2 cm stemwood and 1 cm root, we would have estimated 0.72 kg C m⁻² at the ecosystem level, which is closer to model-based estimates, but 75% more than the value of 0.41 kg C m⁻² which we obtained using radially varying NSC concentrations. If trees in the process-based models had full access to a total NSC pool that was two times larger than was estimated based on field measurements, then trees might appear more resilient to disturbance and stress, and modelled productivity might be less sensitive to interannual variation in weather.

Conclusions

We have constructed the most detailed assessment of NSC storage in temperate forest trees to date. We measured NSC concentrations in different organs, across multiple tree species, at a monthly time step over the course of year. We used allometric equations and forest inventory data to scale these concentrations up to the whole-tree and whole-ecosystem levels. Our results provide a picture of NSC storage in temperate forest trees in which: (1) The size of whole-tree total NSC pools differed between species. (2) Whole-tree total, sugar, and starch pools had contrasting seasonal patterns. (3) NSC storage and seasonal patterns differed between belowground and aboveground organs,

with both (2) and (3) indicating different functional roles of sugars and starch and different contributions by individual organs to the overall whole-tree C balance.

Notably, we showed that: (1) Deciduous ring-porous species had larger whole-tree total NSC pools than both deciduous diffuse-porous and evergreen conifer species. (2)(a) The seasonal patterns of whole-tree total NSC pools supported the conventional theory, but whole-tree sugar pools were higher in the dormant season than the growing season, and whole-tree starch pools peaked later in the growing season for deciduous species compared with evergreen white pine. (b) Although seasonal fluctuation in total NSCs was minimal at the whole-tree level, with comparable seasonal depletion for deciduous and evergreen species, it was substantial at the organ level, particularly in the branches. (3) Roots were not the major storage organ for starch, as branches stored comparable amounts throughout the year, and root reserves were not depleted to support new springtime growth. Furthermore, we show that commonly used, process-based ecosystem and land surface models all overpredict ecosystem-level total NSC storage. Therefore, our results improve our understanding of C dynamics at both the whole-tree and ecosystem levels and, importantly, resolve how the dynamics of individual organs contribute to the overall C balance.



Acknowledgements


This work was supported by the National Science Foundation Graduate Research Fellowship under grant no. DGE-1144152 and the Garden Club of New Jersey. ADR acknowledges additional support for research at Harvard Forest from the National Science Foundation's LTER program (DEB-1237491). This material is based upon work supported by the US Department of Energy's Office of Science, Office of Biological and Environmental Research. A special thank you is extended to Meghan Blumstein for her support throughout this project, an interuniversity undergraduate crew, including Molly Wieringa, Elizabeth Rao, and Andy Bayliss, for their tremendous work in the laboratory, and Harvard's IQSS for their statistical support services. Trevor Keenan and Andy Fox provided model output for Harvard Forest.

Author contributions

MEF, BAH, MSC and ADR planned the project. MEF and BAH conducted the field sampling with help from DMA, CDS and several generous lab members and collaborators. CDS contributed to sample preparation and methodology, MEF conducted NSC analyses and allometric scaling. MEF and ADR contributed to data analysis and interpretation of the results. MEF took the lead in writing the manuscript, with feedback and approval from co-authors.

ORCID

Mariah S. Carbone  <http://orcid.org/0000-0002-7832-7009>
Morgan E. Furze  <http://orcid.org/0000-0001-9690-6218>

Andrew D. Richardson  <http://orcid.org/0000-0002-0148-6714>

References

- Aber JD, Reich PB, Goulden ML. 1996. Extrapolating leaf CO₂ exchange to the canopy: a generalized model of forest photosynthesis compared with measurements by eddy correlation. *Oecologia* **106**: 257–265.
- Abramoff RZ, Finzi AC. 2016. Seasonality and partitioning of root allocation to rhizosphere soils in a midlatitude forest. *Ecosphere* **7**: e01547.
- Adams HD, Germino MJ, Breshears DD, Barron-Gafford GA, Guardiola-Claramonte M, Zou CB, Huxman TE. 2013. Nonstructural leaf carbohydrate dynamics of *Pinus edulis* during drought-induced tree mortality reveal role for carbon metabolism in mortality mechanism. *New Phytologist* **197**: 1142–1151.
- Ahmed R, Siqueira P, Hensley S, Bergen K. 2013. Uncertainty of forest biomass estimates in North temperate forests due to allometry: implications for remote sensing. *Remote Sensing* **5**: 3007–3036.
- Barbaroux C, Bréda N. 2002. Contrasting distribution and seasonal dynamics of carbohydrate reserves in stem wood of adult ring-porous sessile oak and diffuse-porous beech trees. *Tree Physiology* **22**: 1201–1210.
- Barbaroux C, Bréda N, Dufrene E. 2003. Distribution of above-ground and below-ground carbohydrate reserves in adult trees of two contrasting broad-leaved species (*Quercus petraea* and *Fagus sylvatica*). *New Phytologist* **157**: 605–615.
- Boose E. 2018. Fisher Meteorological Station at Harvard Forest since 2001. *Harvard Forest Data Archive: HF001*. [WWW document] URL <http://harvardforest.fas.harvard.edu:8080/exist/apps/datasets/showData.html?id=hf001> [accessed 1 July 2018].
- Bréda N, Granier A. 1996. Intra- and interannual variations of transpiration, leaf area index and radial growth of a sessile oak stand (*Quercus petraea*). *Annales des Sciences Forestières* **53**: 521–536.
- Carbone MS, Czimeczik CI, Keenan TF, Murakami PF, Pederson N, Schaberg PG, Xu X, Richardson AD. 2013. Age, allocation and availability of nonstructural carbon in mature red maple trees. *New Phytologist* **200**: 1145–1155.
- Chapin FS, Schulze ED, Mooney HA. 1990. The ecology and economics of storage in plants. *Annual Review of Ecology and Systematics* **21**: 423–447.
- Chow PS, Landhäusser SM. 2004. A method for routine measurements of total sugar and starch content in woody plant tissues. *Tree Physiology* **24**: 1129–1136.
- Cropper WP, Gholz HL. 1993. Simulation of the carbon dynamics of a Florida slash pine plantation. *Ecological Modelling* **66**: 231–249.
- Dickson RE. 1989. Carbon and nitrogen allocation in trees. *Annals of Forest Science* **46**: 631–647s.
- Dietze MC, Sala A, Carbone MS, Czimeczik CI, Mantooth JA, Richardson AD, Vargas R. 2014. Nonstructural carbon in woody plants. *Annual Review of Plant Biology* **65**: 667–687.
- Fajardo A, Piper FI, Hoch G. 2013. Similar variation in carbon storage between deciduous and evergreen treeline species across elevational gradients. *Annals of Botany* **112**: 1–9.
- Faticchi S, Leuzinger S, Körner C. 2014. Moving beyond photosynthesis: from carbon source to sink-driven vegetation modeling. *New Phytologist* **201**: 1086–1095.
- Furze ME, Huggett BA, Aubrecht DM, Stolz CD, Carbone MS, Richardson AD. 2018. Whole-tree nonstructural carbohydrate budgets in five species at Harvard Forest 2014. *Harvard Forest Data Archive: HF308*. [WWW document] URL <http://harvardforest.fas.harvard.edu:8080/exist/apps/datasets/showData.html?id=hf308> [accessed 2 July 2018].
- Gholz HL, Cropper WP. 1991. Carbohydrate dynamics in mature *Pinus elliotii* var. *elliottii* trees. *Canadian Journal of Forest Research* **21**: 1742–1747.
- Gough CM, Flower CE, Vogel CS, Dragoni D, Curtis PS. 2009. Whole-ecosystem labile carbon production in a north temperate deciduous forest. *Agricultural and Forest Meteorology* **149**: 1531–1540.
- Hartmann H, Trumbore S. 2016. Understanding the roles of nonstructural carbohydrates in forest trees—from what we can measure to what we want to know. *New Phytologist* **211**: 386–403.
- Hinckley TM, Lassoie JP. 1981. Radial growth in conifers and deciduous trees a comparison. *Mitteilungen - Vienna, Forstliche Bundesversuchsanstalt* **142**: 17–56.
- Hoch G. 2015. Carbon reserves as indicators for carbon limitation in trees. In: Lüttge U, Beyschlag W, eds. *Progress in botany, vol. 76*. Cham, Switzerland: Springer International Publishing, 321–346.
- Hoch G, Richter A, Körner C. 2003. Non-structural carbon compounds in temperate forest trees. *Plant, Cell & Environment* **26**: 1067–1081.
- Jenkins JC, Chojnacky DC, Heath LS, Birdsey RA. 2004. *Comprehensive database of diameter-based biomass regressions for North American tree species*. Northeastern Research Station, Newtown Square, PA, USA: USDA Forest Service.
- Jurik TW, Briggs GM, Gates DM. 1988. Springtime recovery of photosynthetic activity of white pine in Michigan. *Canadian Journal of Botany* **66**: 138–141.
- Keel SG, Schädel C. 2010. Expanding leaves of mature deciduous forest trees rapidly become autotrophic. *Tree Physiology* **30**: 1253–1259.
- Keenan TF, Baker I, Barr A, Ciais P, Davis K, Dietze M, Dragoni D, Gough CM, Grant R, Hollinger D *et al.* 2012. Terrestrial biosphere model performance for inter-annual variability of land-atmosphere CO₂ exchange. *Global Change Biology* **18**: 1971–1987.
- Kobe RK. 1997. Carbohydrate allocation to storage as a basis of interspecific variation in sapling survivorship and growth. *Oikos* **80**: 226–233.
- Kozłowski TT. 1992. Sources and sinks in woody plants carbohydrate. *Botanical Review* **58**: 107–222.
- Kramer PJ, Kozłowski TT. 1979. *Physiology of woody plants*. Orlando, FL, USA: Academic Press.
- Landhäusser SM, Lieffers VJ. 2003. Seasonal changes in carbohydrate reserves in mature northern *Populus tremuloides* clones. *Trees – Structure and Function* **17**: 471–476.
- Lens F, Jansen S, Robbrecht E, Smets E. 2000. Wood anatomy of the Vangueriaceae (Ixoroideae – Rubiaceae), with special emphasis on some geofrutices. *IAWA Journal* **21**: 443–455.
- Levis S, Bonan GB, Vertenstein M, Oleson KW. 2004. The Community Land Model's Dynamic Global Vegetation Model (CLM-DGVM): Technical Description and User's Guide. *NCAR Technical Note NCAR/TN-459+IA*.
- Loescher WH, McCamant T, Keller JD. 1990. Carbohydrate reserves, translocation, and storage in woody plant roots. *HortScience* **25**: 274–281.
- Martínez-Vilalta J, Sala A, Asensio D, Galiano L, Hoch G, Palacio S, Piper FI, Lloret F. 2016. Dynamics of non-structural carbohydrates in terrestrial plants: a global synthesis. *Ecological Monographs* **86**: 495–516.
- Millard P, Sommerkorn M, Grelet GA. 2007. Environmental change and carbon limitation in trees: a biochemical, ecophysiological and ecosystem appraisal. *New Phytologist* **175**: 11–28.
- Munger W, Wofsy S. 2018. Biomass Inventories at Harvard Forest EMS Tower since 1993. *Harvard Forest Data Archive: HF069*. [WWW document] URL <http://harvardforest.fas.harvard.edu:8080/exist/apps/datasets/showData.html?id=hf069> [accessed 1 May 2018].
- Murmanis L, Sachs IB. 1969. Seasonal development of secondary xylem in *Pinus strobus* L. *Wood Science and Technology* **3**: 177–193.
- O'Brien MJ, Leuzinger S, Philipson CD, Tay J, Hector A. 2014. Drought survival of tropical tree seedlings enhanced by non-structural carbohydrate levels. *Nature Climate Change* **4**: 710–714.
- Ögren E. 1997. Relationship between temperature, respiratory loss of sugar and premature dehardening in dormant Scots pine seedlings. *Tree Physiology* **17**: 47–51.
- O'Keefe J. 2015. Phenology of Woody Species at Harvard Forest since 1990. *Harvard Forest Data Archive: HF003*. [WWW document] URL <http://harvardforest.fas.harvard.edu:8080/exist/apps/datasets/showData.html?id=hf003> [accessed 1 July 2018].
- Owston PW. 1969. The shoot apex in eastern white pine: its structure, seasonal development, and variation within the crown. *Canadian Journal of Botany* **47**: 1181–1188.
- Palacio S, Maestro M, Montserratmarti G. 2007. Seasonal dynamics of non-structural carbohydrates in two species of Mediterranean sub-shrubs with different leaf phenology. *Environmental and Experimental Botany* **59**: 34–42.
- Paul MJ, Foyer CH. 2001. Sink regulation of photosynthesis. *Journal of Experimental Botany* **52**: 1383–1400.
- Piispänen R, Saranpää P. 2001. Variation of non-structural carbohydrates in silver birch (*Betula pendula* Roth) wood. *Trees* **15**: 444–451.

- Pratt RB, Jacobsen AL, Ewers FW, Davis SD. 2007. Relationships among xylem transport, biomechanics and storage in stems and roots of nine Rhamnaceae species of the California chaparral. *New Phytologist* 174: 787–798.
- Reich PB, Walters MB, Kloeppel BD, Ellsworth DS. 1995. Different photosynthesis-nitrogen relations in deciduous hardwood and evergreen coniferous tree species. *Oecologia* 104: 24–30.
- Richardson AD, Carbone MS, Huggert BA, Furze ME, Czimeczik CI, Walker JC, Xu X, Schaberg PG, Murakami P. 2015. Distribution and mixing of old and new nonstructural carbon in two temperate trees. *New Phytologist* 206: 590–597.
- Richardson AD, Carbone MS, Keenan TF, Czimeczik CI, Hollinger DY, Murakami P, Schaberg PG, Xu X. 2013. Seasonal dynamics and age of stemwood nonstructural carbohydrates in temperate forest trees. *New Phytologist* 197: 850–861.
- Richardson AD, Keenan TF, Carbone MS, Czimeczik CI, Hollinger DY, Murakami P, Schaberg PG, Xu X. 2012. Modeling nonstructural carbohydrate reserve dynamics in forest trees, Abstract B23G-0530 presented at 2012 Fall Meeting, AGU, San Francisco, CA, USA, 3–7 Dec.
- Richardson AD, O'Keefe J. 2009. Phenological differences between understory and overstory. In: Noormets A, ed. *Phenology of ecosystem processes*. New York, NY, USA: Springer, 87–117.
- Sampson DA, Johnsen KH, Ludovici KH, Albaugh TJ, Maier CA. 2001. Stand-scale correspondence in empirical and simulated labile carbohydrates in Loblolly pine. *Forest Science* 47: 60–68.
- Smith MG, Miller RE, Arndt SK, Kasel S, Bennett LT. 2017. Whole-tree distribution and temporal variation of non-structural carbohydrates in broadleaf evergreen trees. *Tree Physiology* 38: 1–12.
- Urbanski S, Barford C, Wofsy S, Kucharik C, Pyle E, Budney J, McKain K, Fitzjarrald D, Czikowsky M, Munger JW. 2007. Factors controlling CO₂ exchange on timescales from hourly to decadal at Harvard Forest. *Journal of Geophysical Research-Biogeosciences* 112: G02020.
- Würth MKR, Peláez-Riedl S, Wright SJ, Körner C. 2005. Non-structural carbohydrate pools in a tropical forest. *Oecologia* 143: 11–24.

Supporting Information

Additional Supporting Information may be found online in the Supporting Information section at the end of the article:

Fig. S1 Air temperature and precipitation data for Harvard Forest.

Fig. S2 Comparison of estimated organ biomasses between five temperate tree species.

Methods S1 NSC concentration measurements and uncertainty.

Methods S2 Allometric scaling from NSC concentrations to whole-tree pools.

Methods S3 Estimation of foliar NSC pools.

Methods S4 Estimation of ecosystem-level NSC storage.

Table S1 Diameter at breast height, height, and age for individual trees.

Table S2 Estimated biomass of each organ for individual trees.

Table S3 Tukey's HSD results from repeated measures linear mixed-effects models testing for the effect of sampling month on whole-tree total NSC, sugar, and starch pools for each species.

Table S4 Results of repeated measures linear mixed-effects models testing for the effect of organ, species, and their interaction on organ-level total NSC, sugar, and starch pools.

Table S5 Tukey's HSD results from repeated measures linear mixed-effects models testing for the effect of organ on organ-level NSC, sugar, and starch pools for each species.

Table S6 Results of repeated measures linear mixed-effects models testing for the effect of sampling month, species, and their interaction on total NSC, sugar, and starch pools in branch, stemwood, and root.

Table S7 Tukey's HSD results from repeated measures linear mixed-effects models testing for the effect of month on total NSC, sugar, and starch pools for each organ and species.

Table S8 Partitioning of sugar and starch pools among woody organs and sampling months for each species.

Please note: Wiley Blackwell are not responsible for the content or functionality of any Supporting Information supplied by the authors. Any queries (other than missing material) should be directed to the *New Phytologist* Central Office.

2

Seasonal fluctuation of nonstructural carbohydrates within tree organs reveals the metabolic availability of older stemwood reserves

In review as:

Furze, ME, Huggett, BA, Wieringa, MM, Aubrecht, DM, Carbone, MS, Walker, JC, Xu, X, Czimczik, CI, Richardson, AD. Seasonal fluctuation of nonstructural carbohydrates within tree organs reveals the metabolic availability of older stemwood reserves.

Related publication:

Richardson, AD, Carbone, MS, Huggett, BA, **Furze, ME**, Czimczik, CI, Walker, JC, Xu, X, Schaberg, PG, Murakami, P. 2015. Distribution and mixing of old and new nonstructural carbon in two temperate trees. *New Phytologist* 206: 590-597.

Abstract

Nonstructural carbohydrates (NSCs) play a critical role in plant physiology and metabolism, yet we know little about their distribution within individual organs. This leaves many open questions about whether reserves deep in the stem and roots are metabolically active and available to support functional processes. To gain insight into the availability of reserves, we measured radial patterns of NSCs in the stemwood and coarse roots for temperate tree species over the course of a year. In a subset of trees, we estimated the mean age of NSCs within and between different organs using the radiocarbon (^{14}C) bomb spike approach. NSC concentrations were highest and most seasonally dynamic in the outer stemwood. Concentrations in deeper stemwood also often varied seasonally, suggesting metabolic activity involving older reserves. By contrast, NSC concentrations in coarse roots were more stable throughout the year. Radial patterns of ^{14}C in both stemwood and coarse roots showed increasing sugar mean age from the cambium towards the pith. Our results highlight the dynamic nature of NSC pools, even in older stem rings. This seasonal variability is indicative of metabolic activity, casting doubt on the hypothesis that deeper reserves are sequestered and metabolically unavailable.

Introduction

Forest trees allocate photoassimilates to growth and metabolism, but photoassimilates can also be stored as nonstructural carbohydrates (NSCs) primarily in the form of sugars and starch (Dietze *et al.*, 2014; Hartmann & Trumbore, 2016). When stored, this reserve acts as a “food pantry” that enables stationary, long-lived trees to survive during unfavorable environmental conditions when NSC production is impaired. While there is evidence linking NSCs with stress tolerance (Myers & Kitajima, 2007; Sala *et al.*, 2012; Carbone *et al.*, 2013), we lack a detailed understanding of carbon (C) relations in trees, including the distribution and turnover of NSC reserves within both belowground and

aboveground organs. This knowledge gap hinders our ability to predict how tree species will physiologically respond to stress and has broader implications for understanding both short-term and long-term C storage and cycling at the whole-tree and ecosystem levels.

Recent work quantified whole-tree NSC reserves and showed that the amount of NSCs stored differed between organs (Smith *et al.*, 2017; Furze *et al.*, 2018a). However, the distribution and metabolic availability (as indicated by seasonal fluctuations) of NSCs within individual organs is less understood. While previous studies have characterized within-organ NSC storage by measuring the radial patterns of NSC concentrations, particularly in the stemwood (Barbaroux & Bréda, 2002; Hoch *et al.*, 2003; Gérard & Bréda, 2014; Zhang *et al.*, 2014; Richardson *et al.*, 2015; Smith *et al.*, 2017), relatively few studies have measured the radial patterns of NSC age to assess the degree to which within-organ NSC storage represents a mix of older and newer NSCs (Richardson *et al.*, 2015; Trumbore *et al.*, 2015). Quantifying such within-organ NSC dynamics in concert is essential for determining whether older reserves in deeper tissues become sequestered and metabolically unavailable.

In the stemwood, NSC concentrations tend to decrease across the younger sapwood towards the sapwood-heartwood boundary and then remain constant throughout the heartwood to the pith (Hoch *et al.*, 2003). However, high levels of NSCs have also been observed deep in the xylem (Würth *et al.*, 2005; Smith *et al.*, 2017). Furthermore, younger NSCs dominate the outermost growth rings of the stemwood, with limited “mixing in” of younger NSCs to older growth rings (Richardson *et al.*, 2015; Trumbore *et al.*, 2015). Despite these efforts, how NSCs are distributed within belowground organs like coarse roots, and, in general, how radial patterns within organs vary between species and across seasons have largely been ignored due to sampling and cost limitations. Without these data, the estimation of NSC pool sizes and turnover times will remain biased (Gaudinski *et al.*, 2009; Muhr *et al.*, 2013) and our understanding of reserve availability will remain limited.

To improve the representation of NSC storage and allocation processes in current C-cycling models and to assess the availability of reserves to support tree function, we provide a detailed accounting of the spatial and temporal variation of NSCs within belowground and aboveground organs. This study builds upon our previous work (Richardson *et al.*, 2015; Furze *et al.*, 2018a) by characterizing within-organ NSC storage in temperate trees. We collected stemwood and coarse root samples across the seasons, divided these samples into radial increments from the cambium to the pith, and measured their sugar and starch concentrations. In a subset of trees, we estimated the mean age of sugar within and between different organs. Our objective was to quantify the radial patterns in the concentration and age of NSCs across organs, species, and seasons to test the prediction that outer tissues contain dynamic, young reserves, while older reserves are sequestered in deeper tissues.

Materials and Methods

Study site

Field sampling (2014-2015) was conducted at Harvard Forest, an oak-dominated, mixed temperate forest located in Petersham, Massachusetts, USA (42.53°N, 72.17°W). We selected mature trees belonging to the following species: red oak (*Quercus rubra* L., n=6), white pine (*Pinus strobus* L., n=6), red maple (*Acer rubrum* L., n=6), paper birch (*Betula papyrifera* Marshall, n=3), white ash (*Fraxinus americana* L., n=5), and American beech (*Fagus grandifolia* Ehrh, n=3). These trees represent the dominant species in the Prospect Hill Tract of Harvard Forest, and reflect diversity in leaf habit, wood anatomy, and shade tolerance. White pine is an evergreen conifer, while the other species are deciduous broadleaf trees. Of the deciduous broadleaf species, red oak and white ash are ring-porous, and red maple, paper birch, and American beech are diffuse-porous. White ash and paper birch are shade intolerant species, while the others are of at least intermediate shade tolerance.

Field collection

Monthly samples were collected from 24 trees along Prospect Hill Rd throughout 2014. A subset of these trees (n=7), as well as 5 additional trees, were sampled for ^{14}C analyses in November 2015 (n=12); yielding 29 total trees in this study.

Each month throughout 2014, a stemwood core to the pith was collected from each of 24 trees (red oak n=6, white ash n=3, red maple n=6, paper birch n=6, and white pine n=6) with a standard 4.3-mm increment borer (Haglöf Company Group, Långsele, Sweden). The initial core was collected starting at breast height on the south or southwest face of each tree and each subsequent core was collected in a zigzag pattern (approximately 7.5 cm over, 7.5 cm up). Coarse root cores (c. \geq 5 cm diameter) were collected in January, April, June, August, and October 2014. The first root sample was taken at 20 cm along a root from the base of the tree, and subsequent cores were taken in a zigzag pattern similar to the stemwood on the same root. Samples were kept on dry ice in the field during each collection and then stored at -80°C until NSC analysis.

In November 2015, we selected 12 trees (red oak n=3, white ash n=3, red maple n=3, and American beech n=3) for radiocarbon (^{14}C) analysis of bulk sugars. Approximately half (n=7) of these trees had also been sampled in 2014 for NSC measurements. A sunlit branch (c. 1–1.5 cm diameter, multi-year 3–5 yrs old), stemwood core, coarse root core, and fine roots were collected from each tree and were kept on dry ice in the field and then stored at -80°C until ^{14}C analysis.

NSC analysis

Stemwood and coarse root cores collected throughout 2014 were subdivided into increments from the cambium (designated as 0) to the pith to determine the radial distribution of sugar and starch concentrations. Stemwood cores were divided into 6 increments: 0-1 cm, 1-2 cm, 2-3 cm, 3-4 cm, 4-8 cm, 8 cm-pith. Coarse root cores were divided into 2 increments: 0-1 cm and 1 cm-pith. Subdivisions

were freeze-dried (FreeZone 2.5, Labconco, Kansas City, MO USA, and Hybrid Vacuum Pump, Vacuubrand, Wertheim, Germany) and ground (mesh 20, Thomas Scientific Wiley Mill, Swedesboro, NJ, USA; SPEX SamplePrep 1600 MiniG, Metuchen, NJ USA). NSC analyses were conducted for all stemwood increments with the exception of the deepest heartwood (8 cm-pith). This region was sampled in January and July 2014, and due to similar NSC concentrations, they were averaged together and applied across the entire year (see Methods S1 in Furze *et al.*, 2018a).

To measure sugar concentrations (adapted from Chow & Landhäusser 2004), 10 mg of tissue was freeze-dried and extracted with 80% hot ethanol followed by colorimetric analysis with phenol-sulfuric acid. The resulting bulk sugar extract was read at 490 nm on a microplate reader (Epoch Microplate Spectrophotometer, Bio-Tek Instruments, Winooski, VT USA) or spectrophotometer (Thermo Fischer Scientific GENESYS 10S UV-Vis, Waltham, MA, USA). Sugar concentrations (expressed as mg sugar per g dry wood) were calculated from a 1:1:1 glucose-fructose-galactose (Sigma Chemicals, St. Louis, MO USA) standard curve.

To determine starch concentrations, the remaining tissue was solubilized in NaOH and then digested with an α -amylase/amyloglucosidase digestive enzyme solution. Glucose hydrolysate was determined using a PGO-color reagent solution (Sigma Chemicals, St. Louis, MO USA) and read at 525 nm. Starch concentrations (expressed as mg starch per g dry wood) were calculated based on a glucose (Sigma Chemicals, St. Louis, MO USA) standard curve. When conducting NSC analyses, we included at least one internal laboratory standard (red oak stemwood, Harvard Forest, Petersham, MA, USA) per analysis. A standardized version of the protocol we used is fully described in Landhäusser *et al.*, 2018. Additionally, the NSC concentrations presented herein were used for estimating whole-tree NSC pools using allometric equations in Furze *et al.* 2018a.

Radiocarbon (^{14}C) analysis

We used the ^{14}C ‘bomb spike’ to estimate the mean age of sugars within and between different organs sampled in November 2015. The cost of conducting ^{14}C analyses precluded the measurement of starch and additional tissues, so we focused on radial patterns of sugars in the outer 2 cm of stemwood and coarse roots where we expected sugars to be the most dynamic (Richardson *et al.*, 2013, 2015). These organs were subdivided into 4 increments starting from the cambium: 0-0.5 cm, 0.5-1 cm, 1-1.5 cm, and 1.5-2 cm. In addition to quantifying these radial patterns, the mean age of sugars was also determined in multi-year sunlit branches and bulk fine roots to compare between organs.

In the late 1950s, above-ground thermonuclear weapons testing doubled the amount of $^{14}\text{CO}_2$ in the atmosphere (Levin & Kromer, 2004), and since then this content has slowly declined over time due to dilution by ^{14}C -free CO_2 sources and exchange with land and ocean reservoirs. Because of this dilution, the C in sugars represents the ^{14}C content of the atmospheric CO_2 in the year it was fixed by photosynthesis, and thus, the ^{14}C content of a sample can be directly compared to the $^{14}\text{CO}_2$ atmospheric record to estimate the mean ^{14}C age of sugars. The resulting age estimate is the mean age of C in the sugars in the sample (or sugar mean age).

For ^{14}C analysis, sugars were extracted by hot water, combusted to CO_2 , purified on a vacuum line, converted to graphite, and then analyzed for ^{14}C content at the W.M. Keck Carbon Cycle Accelerator Mass Spectrometry facility at the University of California, Irvine (Xu *et al.*, 2007; Beverly *et al.*, 2010; Czimeczik *et al.*, 2014). The analytical uncertainty for ^{14}C is about 0.003 fraction modern for modern samples, based on long-term measurements of secondary standards. ^{14}C content was then directly compared to the northern hemisphere atmospheric $^{14}\text{CO}_2$ record (Levin *et al.*, 2008; X. Xu, unpublished) to estimate sugar mean age. The background air at Harvard Forest has been previously shown to be consistent with the atmospheric record (Richardson *et al.*, 2013; Carbone *et al.*, 2013). To confirm, we collected the annual plant jewelweed (*Impatiens capensis* Meerb) at Harvard Forest to

quantify background atmospheric $^{14}\text{CO}_2$ and the signature of current year photoassimilates at the time of sampling. Annual jewelweed samples were collected and processed for ^{14}C content each year from 2011-2015, which includes our study years 2014-2015 (Table S1).

It is important to note that the ^{14}C sugar extraction has limitations. Water is used for sugar extraction in place of C-containing solvents (i.e. ethanol) to prevent contamination of samples prior to ^{14}C analysis. However, hot water extraction yields a soluble C pool that contains some compounds beyond the expected sugars. We acknowledge this uncertainty and suggest that this method still provides a reasonable estimate for the age of sugars (Trumbore *et al.*, 2015).

The ^{14}C data for each sample are reported in Table S2. NSC data from this project are available for download and public use (Furze *et al.* 2019). The uncertainty in NSC and ^{14}C measurements is reported in Methods S1.

Statistical analyses

All statistical analyses were performed in R v.3.3.2 and analysis of variance (ANOVA) models were fit using the function `aov()`. One categorical factor or the interaction between two categorical factors was considered for each ANOVA (specified below). For significant ANOVAs, differences between pairs of means were evaluated with Tukey's honest significant difference (HSD), $\alpha = 0.05$. Monthly NSC concentrations from 2014 were categorized by season for statistical analyses (Winter = January, February, Spring = March, April, May; Summer = June, July, August; Autumn = September, October, November).

To determine if NSC concentrations varied radially from the cambium to the pith within the stemwood of five temperate species, and whether radial patterns differed between seasons, we used a two-way ANOVA to analyze total NSC concentrations among increments and seasons (Increment x Season; Fig. 1A). The same analysis was repeated for both sugar and starch concentrations (Fig. 1A).

To resolve radial patterns of NSC concentrations for each species, total NSC, sugar, and starch concentrations were assessed across stemwood increments and seasons for each individual species (Increment x Season; Fig. 1B-F). For significant interaction effects, total NSC, sugar, and starch concentrations were then assessed across stemwood increments for each individual season (Increment; See Table S3).

Similarly, to determine if NSC concentrations varied radially from the cambium to the pith within the coarse roots, and whether radial patterns differed between seasons, we used a two-way ANOVA to individually analyze total NSC, sugar, and starch concentrations among increments and seasons (Increment x Season; Fig. 2A). Radial patterns for individual species were further resolved (Increment x Season; Fig. 2B-F).

Next, we sought to compare sugar mean age within organs as well as between different organs by assessing the sugar mean age in multi-year branches, stemwood increments (S1-S4), coarse roots increments (R1-R4), and bulk fine roots. We used a two-way ANOVA to analyze sugar mean age among organ increments and species (Increment x Species; Fig. 3A).

Results

Radial patterns of NSC concentrations

In the stemwood, NSC concentrations were the highest near the cambium, declined radially across the outermost increments, and then remained fairly constant to the pith. Although, the effect of stemwood increment on total NSC, sugar, and starch concentrations depended on season (Increment x Season, all $P < 0.0001$; Fig. 1A). Sugar concentrations were generally highest in the winter and starch concentrations were highest in the autumn, particularly in the outermost increment. However, the distribution of sugars and starch across radial increments differed between species.

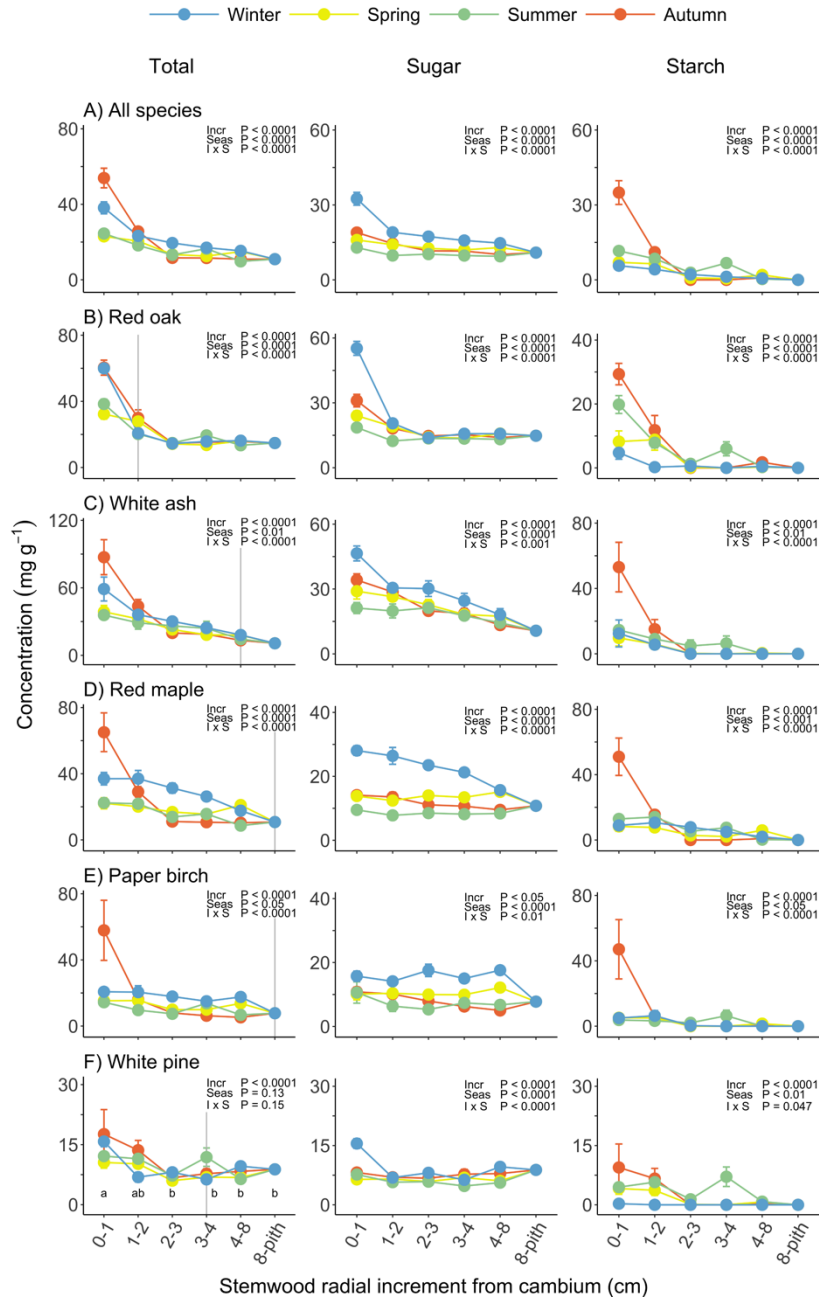


Figure 1 Radial patterns of total NSC, sugar, and starch concentrations (columns) in the stemwood of five temperate tree species (rows A-F) in 2014. Symbols indicate mean concentrations for each season. Error bars denote \pm SE of the mean. Radial increments (cm) were sampled from just inside the removed bark at the cambium (0-1) and continued to the pith (8-pith). Gray vertical lines in the first column indicate the average increment in which the sapwood-heartwood boundary was visually identified for each species (Table S4). P-values displayed are from two-way ANOVA testing for increment (Incr), season (Seas), and their interaction (I x S). For non-significant interaction effects in F, lowercase letters represent significant differences among organ increments evaluated with Tukey's HSD, $\alpha = 0.05$. For significant interaction effects in A-E, additional testing was conducted and results are provided in Table S3. Note the difference in y-axis scale between plots.

The radial patterns of sugar concentrations differed between species based on wood anatomy and leaf habit. In the deciduous ring-porous species red oak and white ash, sugar concentrations declined over the outer 2 cm of stemwood and remained constant to the pith regardless of season (Figs. 1B, 1C; Table S3). The decline was most pronounced in the winter, with sugar concentrations decreasing by approximately 52% (± 7 SE) between the outer two stemwood increments (0-1 cm and 1-2 cm). Conversely, in the deciduous diffuse-porous species red maple and paper birch, sugar concentrations were relatively stable from the cambium to the pith within each season (Figs. 1D, 1E; Table S3), with the highest concentrations in the winter. For evergreen white pine, sugar concentrations declined by approximately 55% (± 6 SE) across the outer increments in the winter like in the ring-porous species, but were otherwise stable across increments for each season similar to the diffuse-porous species (Fig. 1F; Table S3).

The radial patterns of starch concentrations in the stemwood were more consistent between species. Starch concentrations were the highest near the cambium, declined over the outer increments, and then remained constant to the pith with little or no starch present (Figs. 1B-F; Table S3). The decline was most pronounced in autumn, when starch concentrations decreased by up to 91% (± 7 SE) between the outer two stemwood increments (0-1 cm and 1-2 cm) depending on the deciduous species. Due to low starch levels beyond the outermost stemwood increments, sugars dominated deeper stemwood tissues.

The degree to which the distribution of sugars and starch were related to the sapwood-heartwood boundary (Barbaroux & Bréda, 2002) differed between species and seasons, making it difficult to identify trends. However, when examining total NSCs, it became clear that concentrations were high prior to the boundary and low thereafter in red oak, whereas concentrations reached low levels prior to the boundary in the other species (Total column, Fig. 1). Notably, sugar concentrations often varied between seasons in deeper stemwood increments, even those increments beyond the sapwood-heartwood boundary. For each tree, the approximate number of rings in each stemwood increment and the location of the sapwood-heartwood boundary are provided in Table S4.

In the coarse roots, sugar concentrations were higher in deeper tissues beyond the outer 1 cm (Tukey's HSD, $P = 0.04$) and were higher in the winter compared to other seasons (all, $P \leq 0.02$; Fig.

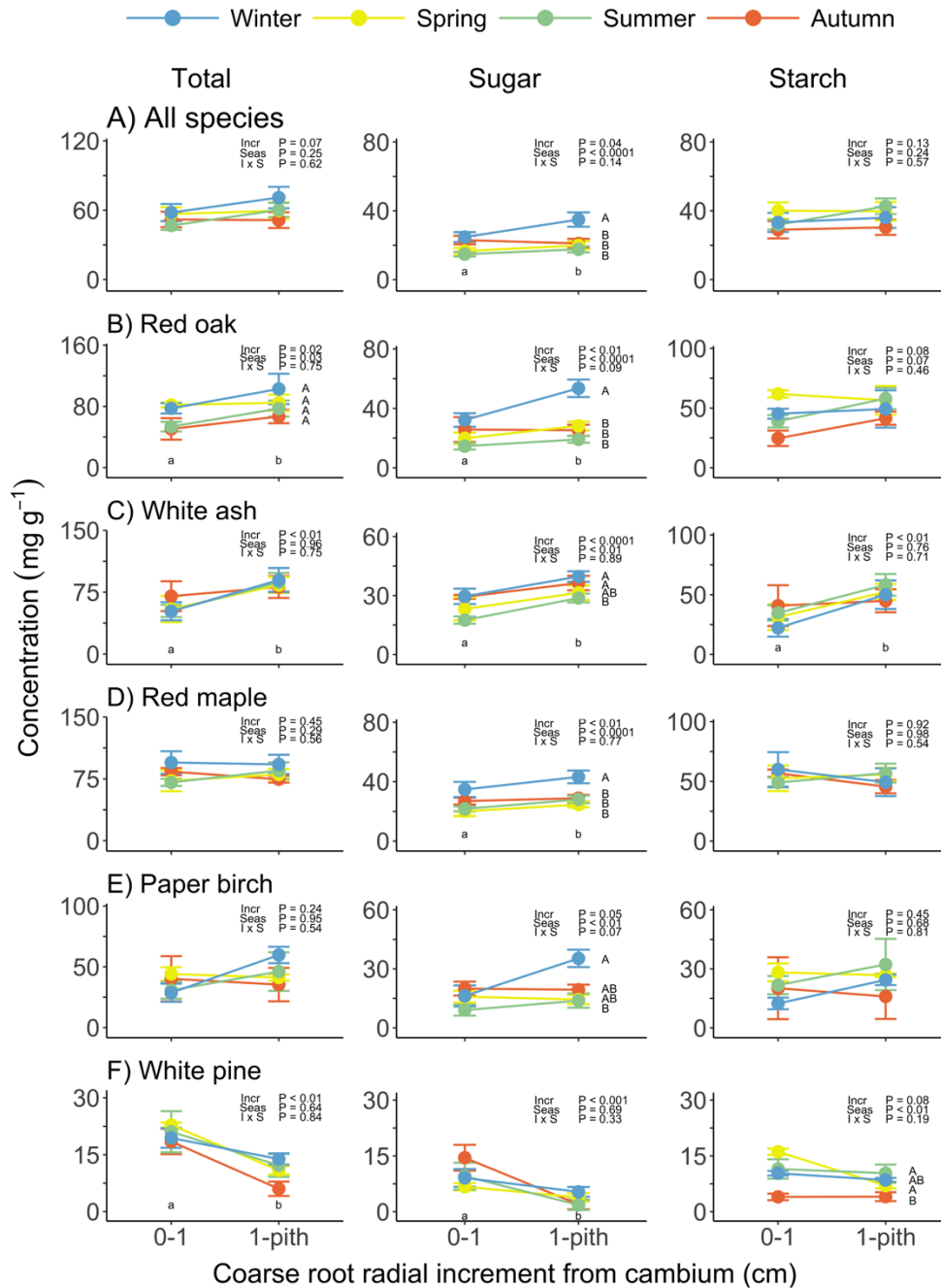


Figure 2 Radial patterns of total NSC, sugar, and starch concentrations (columns) in the coarse roots of five temperate tree species (rows A-F) in 2014. Symbols indicate mean concentrations for each season. Error bars denote \pm SE of the mean. Radial increments (cm) began just inside the removed bark at the cambium (0-1) and continued to the pith (1-pith). P-values displayed are from two-way ANOVA testing for increment (Incr), season (Seas), and their interaction (I x S). For non-significant interaction effects in A-E, lowercase letters represent significant differences among organ increments and uppercase letters represent significant differences among seasons evaluated with Tukey's HSD, $\alpha = 0.05$. Note the difference in y-axis scale between plots.

2A). In contrast, starch concentrations were generally consistent across radial increments and did not differ between seasons. However, these patterns differed between species.

Sugar concentrations tended to be highest in deeper tissues beyond the outer 1 cm for deciduous species (Figs. 2B, 2E), whereas sugar concentrations were the lowest in this region for evergreen white pine (Fig. 2F). Across species, starch concentrations did not vary by season and were consistent across radial increments in the coarse roots. White ash was the only exception, with starch concentrations lower in the outer 1 cm (Tukey's HSD, $P < 0.01$). Overall, deciduous species had higher total NSC, sugar, and starch concentrations in the coarse roots. For example, when taking into consideration the biomass of each increment, the weighted mean total NSC concentration in the coarse roots was 79.0 mg g^{-1} ($\pm 5.9 \text{ SE}$) for red oak compared to 12.2 mg g^{-1} ($\pm 1.4 \text{ SE}$) for white pine.

Radial patterns of sugar mean age, and differences between organs

The mean age of sugar varied radially within organs and also differed between organs (Fig. 3A). In the stemwood and coarse roots, the sugar mean age tended to increase radially across the outer 2 cm from the cambium towards the pith (Fig. 3A). In the outer rings near the cambium, the mean age of sugar was 1.3 yr ($\pm 0.4 \text{ SE}$) in the stemwood and 1.8 yr ($1.1 \pm \text{SE}$) in the coarse roots, whereas it was 9.2 yr ($\pm 1.1 \text{ SE}$) and 9.6 yr ($\pm 2.6 \text{ SE}$) in the deepest increment measured for each organ (1.5 to 2 cm (R4 or S4); Fig. 3A). By comparison, branch sugar mean age was in line with current/previous year photosynthetic products and fine root sugars were nearly a decade old.

While the patterns of sugar mean age within and between organs were consistent across species, sugar mean age differed between species ($P < 0.001$; Fig. 3A). Red oak and red maple had older sugars than white ash and American beech (Figs. 3B, 3E), and this difference was not due to the age of the tree from which the sugar was extracted. Tree age was not correlated with sugar mean age in any organ increment, with the exception of fine roots (Pearson's correlation, $r = -0.61$, $P = 0.04$). Notably, the oldest sugar mean age in this study was 32.5 yr, measured in deeper coarse root increments (1 to 1.5 cm (R3)/1.5 to 2 cm (R4)) of red oak.

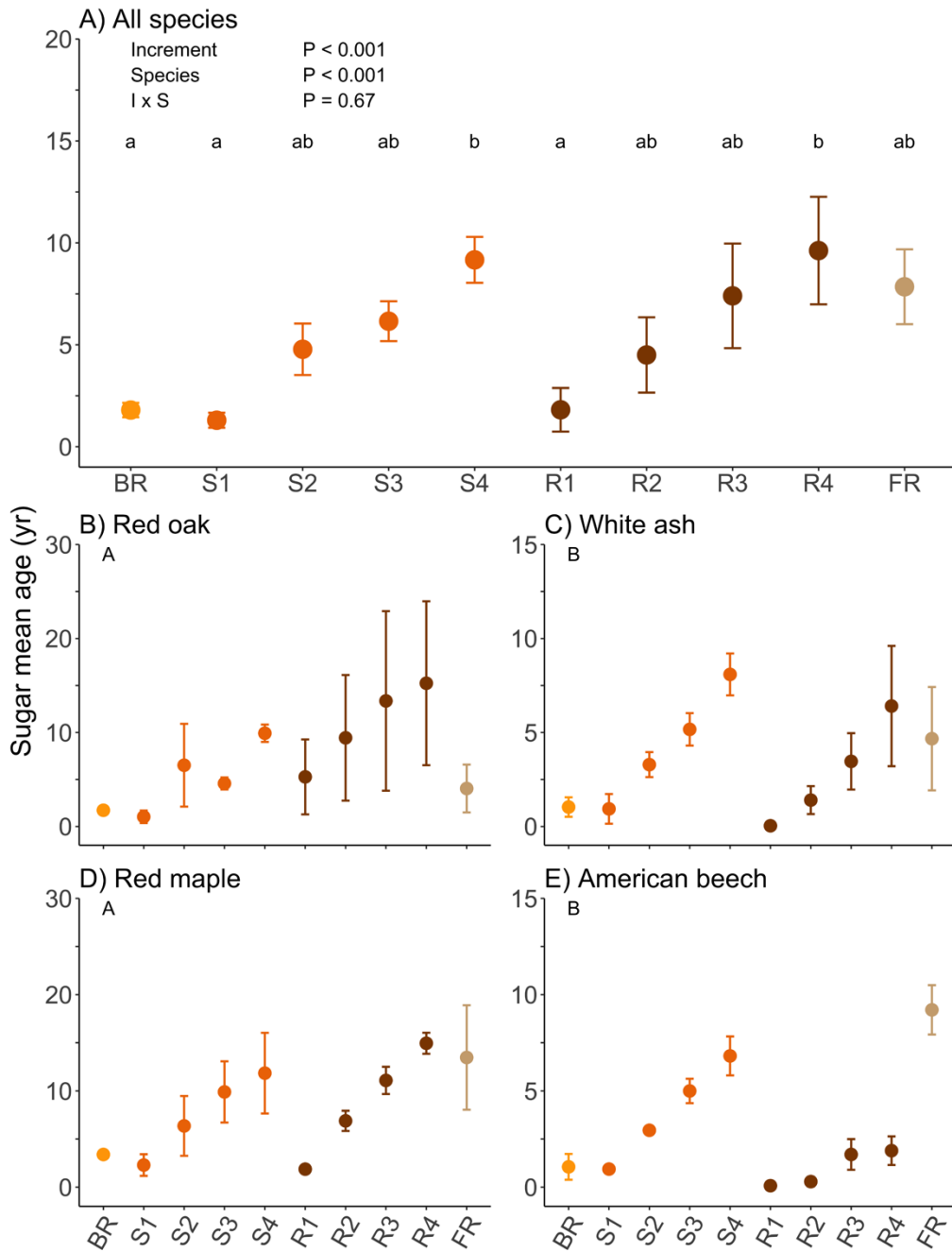


Figure 3 Mean age of sugar interpreted from radiocarbon (^{14}C) content of extracted sugars from radial increments of stemwood (S1-S4) and coarse roots (R1-R4) as well as bulk branches (BR) and fine roots (FR) of four temperate tree species (panels A-E). Symbols indicate mean sugar age. Error bars denote \pm SE of the mean. Radial measurements were taken in 0.5 cm increments for stemwood and coarse roots, with the first increments (S1/R1; 0-0.5 cm) taken just inside the removed bark at the cambium and continuing across the outer 2 cm (S4/R4; 1.5-2 cm). Lowercase letters in A represent significant differences between organ increments evaluated with Tukey's HSD, $\alpha = 0.05$. Uppercase letters in B-E represent significant differences between species evaluated with Tukey's HSD, $\alpha = 0.05$. Note the difference in y-axis scale between plots.

Discussion

By resolving the radial patterns in the concentration and age of NSCs within different organs, our results provide insight into the availability of NSC reserves to support proper tree function. Moving vertically from the canopy to the root system and moving radially from the cambium to the pith, NSC reserves become older and less dynamic, suggesting that younger NSCs in the outermost organ increments are preferentially used for growth and metabolism. While young NSC reserves appear more accessible, we provide a picture of whole-tree NSC storage in which NSC pools - belowground or aboveground, young or old, shallow or deep - are all dynamic to some degree.

The belowground NSC pool was dominated by decade-old or older reserves in deeper coarse root tissues and fine roots, which is in agreement with previous reports that show older C is stored in the root system (Carbone *et al.*, 2013; Richardson *et al.*, 2015) and used to fuel root respiration (Czimczik *et al.*, 2006; Schuur & Trumbore, 2006). Since coarse roots were not directly exposed to cold temperatures in the dormant season due to snowpack insulation, they may have relied less on the breakdown of starch into anti-freeze sugars than the stemwood (Ögren, 1997; Furze *et al.*, 2018a). This would help explain our observations of stable starch reserves across the seasons and less dynamic root reserves than aboveground organs.

The aboveground NSC pool was dominated by highly dynamic, younger reserves in the branches and outer stemwood. In the branches, younger NSCs likely resulted from fast turnover rates and/or refilling of branch reserves with current year photoassimilates following leaf out (Schädel *et al.*, 2009; Epron *et al.*, 2012). In the stemwood, NSCs were the youngest and often the most dynamic in the outermost increments, which follows from the metabolically active nature of the sapwood and its exchange of NSCs with the phloem (Frey-Wyssling & Bosshard, 1959; Ziegler, 1964; Furze *et al.*, 2018b).

We expected that NSC reserves would become sequestered in deeper stemwood tissues, especially in older rings located in the heartwood (Spicer, 2005). However, seasonal fluctuation in deeper tissues may occur in diffuse-porous species where the heartwood is often absent or negligible (Barbaroux & Bréda, 2002). Seasonal fluctuation may result from both regular sugar-starch interconversions as well as NSC depletion and refilling and serves as an indicator of metabolic activity and availability. We observed seasonal variation in deeper stemwood NSCs in diffuse-porous species. Sugar concentrations decreased by approximately 47% (± 5 SE) and 62% (± 5 SE) between the winter and summer in the 4-8 cm stemwood increment for red maple and paper birch, respectively.

By contrast, NSC concentrations were highly dynamic in the outermost rings for ring-porous species. For example, sugar concentrations decreased by approximately 66% (± 1 SE) between the winter and summer in the outer 1cm of red oak. Contrary to our expectation, seasonal variation in deeper stemwood NSCs was also observed in ring-porous species, but to a far lesser degree. For instance, the fluctuation in sugar concentration in the 4-8 cm increment was approximately one-quarter of the fluctuation observed in the outer 1 cm for red oak. This fluctuation was surprising given that the 4-8 cm increment was within the presumed inactive heartwood of ring-porous species.

The fact that NSCs were dynamic in deeper rings regardless of wood anatomy suggests that older reserves are not fully sequestered, and they are at least partially available to support metabolic functions. For example, sugar mean age in the deepest stemwood increment that we measured (1.5-2 cm) for red maple and red oak was approximately 12 yr (± 4 SE) and 10 yr (± 1 SE), respectively, and corresponded to older growth rings (c. ≥ 10 yr). Given that sugar mean age has been shown to increase with tissue age (Richardson *et al.*, 2015), we would then expect the 4-8 cm increment and beyond to contain even older sugars, possibly decades old.

Our findings contradict the idea that older NSCs become sequestered and unavailable for use (Millard *et al.*, 2007). Instead, we provide evidence that older NSCs, even in older stem rings, are available on seasonal timescales, even though younger NSCs in shallow tissues appear to be preferentially used to support growth and metabolism (Lacointe *et al.*, 1993; Richardson *et al.*, 2015). This finding would explain the contribution of older NSC reserves to stemwood and root respiration (Czimczik *et al.*, 2006; Muhr *et al.*, 2013; Trumbore *et al.*, 2015). Given that refixation of respired CO₂ in tree stems (Bloemen *et al.*, 2013; Hilman *et al.*, 2019) has the potential to make NSCs appear older than they actually are, future progress in this area should consider its influence on NSC storage and availability.

Conclusions

By using repeat within-organ sampling and radiocarbon methods, this study provides unique insight into the radial distribution of the concentration and age of NSCs within different tree organs, and how these patterns contribute to the overall whole-tree NSC pool. Specifically, we show that (1) seasonal variation in NSC concentrations was greater aboveground than belowground, (2) sugar concentrations were often higher in deeper coarse root tissues, while starch concentrations were consistent throughout coarse roots, (3) sugar and starch concentrations were the highest and most dynamic in the outer stemwood, and (4) the mean age of sugar increased radially across increments in

both the stemwood and coarse roots. Notably, we find seasonal variation of NSCs in deeper stemwood, suggesting metabolic activity of older reserves. Thus, both younger and older NSC pools are dynamic and remain at least partially available to temperate trees.

Acknowledgements

This work was supported by the National Science Foundation Graduate Research Fellowship under Grant No. DGE1144152. ADR acknowledges additional support for research at Harvard Forest from the National Science Foundation's LTER program (DEB-1237491). This material is based upon work supported by the U.S. Department of Energy, Office of Science, Office of Biological and Environmental Research.

References

- Barbaroux C, Bréda N. 2002. Contrasting distribution and seasonal dynamics of carbohydrate reserves in stem wood of adult ring-porous sessile oak and diffuse-porous beech trees. *Tree Physiology* 22: 1201–10.
- Beverly RK, Beaumont W, Taus D, Ormsby KM, von Reden KF, Santos GM, Southon JR. 2010. The Keck Carbon Cycle AMS Laboratory, University of California, Irvine: status report. *Radiocarbon* 52: 301–309.
- Bloemen J, Mcguire MA, Aubrey DP, Teskey RO, Steppe K. 2013. Transport of root-respired CO₂ via the transpiration stream affects aboveground carbon assimilation and CO₂ efflux in trees. *New Phytologist* 197: 555–565.
- Carbone MS, Czimczik CI, Keenan TF, Murakami PF, Pederson N, Schaberg PG, Xu X, Richardson AD. 2013. Age, allocation and availability of nonstructural carbon in mature red maple trees. *New Phytologist* 200: 1145–1155.
- Czimczik CI, Trumbore SE, Carbone MS, Winston GC. 2006. Changing sources of soil respiration with time since fire in a boreal forest. *Global Change Biology* 12: 957–971.
- Czimczik CI, Trumbore SE, Xu XM, Carbone MS, Richardson AD. 2014. Extraction of nonstructural carbon and cellulose from wood for radiocarbon analysis. *Bio-protocol* 4: e1169.
- Dietze MC, Sala A, Carbone MS, Czimczik CI, Mantooth JA, Richardson AD, Vargas R. 2014. Nonstructural carbon in woody plants. *Annual Review of Plant Biology* 65: 667–687.
- Epron D, Bahn M, Derrien D, Lattanzi FA, Pumpanen J, Gessler A, Högberg P, Maillard P, Dannoura M, Gérant D, *et al.* 2012. Pulse-labelling trees to study carbon allocation dynamics: a review of methods, current knowledge and future prospects. *Tree physiology* 32: 776–798.
- Frey-Wyssling A, Bosshard HH. 1959. Cytology of the ray cells in sapwood and heartwood. *Holzforchung-International Journal of the Biology, Chemistry, Physics and Technology of Wood* 13:129–137.
- Furze ME, Huggett BA, Aubrecht DM, Stolz CD, Carbone MS, Richardson AD. 2018a. Whole-tree nonstructural carbohydrate storage and seasonal dynamics in five temperate species. *New Phytologist* 221:1466-1477.

Furze ME, Trumbore S, Hartmann H. 2018b. Detours on the phloem sugar highway: stem carbon storage and remobilization. *Current Opinion in Plant Biology* 43: 89–95.

Gaudinski JB, Torn MS, Riley WJ, Swanston C, Trumbore SE, Joslin JD, Majdi H, Dawson TE, Hanson PJ. 2009. Use of stored carbon reserves in growth of temperate tree roots and leaf buds: analyses using radiocarbon measurements and modeling. *Global Change Biology* 15: 992–1014.

Gérard B, Bréda N. 2014. Radial distribution of carbohydrate reserves in the trunk of declining European beech trees (*Fagus sylvatica* L.). *Annals of Forest Science* 71: 675–682.

Hartmann H, Trumbore S. 2016. Understanding the roles of nonstructural carbohydrates in forest trees - from what we can measure to what we want to know. *New Phytologist* 211: 386–403.

Hilman B, Muhr J, Trumbore SE, Carbone MS, Yuval P, Joseph S. 2019. Comparison of CO₂ and O₂ fluxes demonstrate retention of respired CO₂ in tree stems from a range of tree species. *Biogeosciences* 16: 177-191.

Hoch G, Richter A, Korner C. 2003. Non-structural carbon compounds in temperate forest trees. *Plant, Cell & Environment* 26:1067–1081.

Holmes RL. 1983. Computer-assisted quality control in tree-ring dating and measurement. *Tree-Ring Bulletin* 43, 69–78.

Lacointe A, Kajji A, Daudet FA, Archer P, Frossard JS, Saint-Joanis B, Vandame M. 1993. Mobilization of carbon reserves in young walnut trees. *Acta Botanica Gallica* 140: 435–441.

Landhäusser SM, Chow PS, Dickman LT, Furze ME, Kuhlman I, Schmid S, Wiesenbauer J, Wild B, Gleixner G, Hartmann H, *et al.* 2018. Standardized protocols and procedures can precisely and accurately quantify non-structural carbohydrates. *Tree Physiology* 38:1764-1778.

Levin I, Hammer S, Kromer B, Meinhardt F. 2008. Radiocarbon observations in atmospheric CO₂: Determining fossil fuel CO₂ over Europe using Jungfraujoch observations as background. *Science of the Total Environment* 391: 211–216.

Levin I, Kromer B. 2004. The tropospheric ¹⁴CO₂ level in mid-latitudes of the Northern Hemisphere (1959–2003). *Radiocarbon* 46: 1261–1272.

Millard P, Sommerkorn M, Grelet GA. 2007. Environmental change and carbon limitation in trees: a biochemical, ecophysiological and ecosystem appraisal. *New Phytologist* 175: 11–28.

Muhr J, Angert A, Negrón-Juárez RI, Muñoz WA, Kraemer G, Chambers JQ, Trumbore SE. 2013. Carbon dioxide emitted from live stems of tropical trees is several years old. *Tree Physiology* 33: 743–752.

Myers JA, Kitajima K. 2007. Carbohydrate storage enhances seedling shade and stress tolerance in a neotropical forest. *Journal of Ecology* 95: 383–395.

Ögren E. 1997. Relationship between temperature, respiratory loss of sugar and premature dehardening in dormant Scots pine seedlings. *Tree Physiology* 17: 47–51.

Richardson AD, Carbone MS, Huggett BA, Furze ME, Czimeczik CI, Walker JC, Xu X, Schaberg PG, Murakami P. 2015. Distribution and mixing of old and new nonstructural carbon in two temperate trees. *New Phytologist* 206: 590–597.

Richardson AD, Carbone MS, Keenan TF, Czimeczik CI, Hollinger DY, Murakami P, Schaberg PG, Xu X. 2013. Seasonal dynamics and age of stemwood nonstructural carbohydrates in temperate forest trees. *New Phytologist* 197: 850–861.

Sala A, Woodruff DR, Meinzer FC. 2012. Carbon dynamics in trees: feast or famine? *Tree Physiology* 32: 764–775.

Schädel C, Blöchl A, Richter A, Hoch G. 2009. Short-term dynamics of nonstructural carbohydrates and hemicelluloses in young branches of temperate forest trees during bud break. *Tree Physiology* 29: 901–911.

Schuur EAG, Trumbore SE. 2006. Partitioning sources of soil respiration in boreal black spruce forest using radiocarbon. *Global Change Biology* 12: 165–176.

Smith MG, Miller RE, Arndt SK, Kasel S, Bennett LT. 2017. Whole-tree distribution and temporal variation of non-structural carbohydrates in broadleaf evergreen trees. *Tree Physiology* 38:570-581.

Spicer R. 2005. Senescence in secondary xylem: heartwood formation as an active developmental program. In: Holbrook NM, Zwieniecki MA, eds. *Vascular transport in plants*. Academic Press, 457–475.

- Stuiver M, Polach, HA. 1977. Reporting of ^{14}C data. *Radiocarbon* 19, 355–363.
- Trumbore S, Czimczik CI, Sierra CA, Muhr J, Xu X. 2015. Non-structural carbon dynamics and allocation relate to growth rate and leaf habit in California oaks. *Tree Physiology* 35: 1206–1222.
- Würth MKR, Peláez-Riedl S, Wright SJ, Körner C. 2005. Non-structural carbohydrate pools in a tropical forest. *Oecologia* 143: 11–24.
- Xu X, Khosh MS, Druffel-Rodriguez KC, Trumbore SE, Southon JE. 2010. Is the consensus value of ANU sucrose (IAEA C-6) too high? *Radiocarbon* 52, 866-874.
- Xu X, Trumbore SE, Zheng S, Southon JR, McDuffee KE, Luttgen M, Liu JC. 2007. Modifying a sealed tube zinc reduction method for preparation of AMS graphite targets: Reducing background and attaining high precision. *Nuclear Instruments and Methods in Physics Research, Section B: Beam Interactions with Materials and Atoms* 259: 320–329.
- Zhang H, Wang C, Wang X. 2014. Spatial variations in non-structural carbohydrates in stems of twelve temperate tree species. *Trees* 28: 77–89.
- Ziegler H. 1964. Storage, mobilization and distribution of reserve material in trees. In: Zimmermann M, ed. *The formation of wood in forest trees*. Academic Press, 303–320.

Supplementary Materials for Chapter 2

Table S1 Annual plant radiocarbon data. The annual plant jewelweed (*Impatiens capensis* Meerb) was collected at Harvard Forest and processed for ^{14}C content each year from 2011-2015. $\Delta^{14}\text{C}$ was measured at the W.M. Keck Carbon Cycle Accelerator Mass Spectrometry facility at UC Irvine. Values represent mean ± 1 SD of the analytical uncertainty as described in Methods S1. Fraction modern equivalent is also provided.

Year	$\Delta^{14}\text{C}$ (‰)	Fraction modern
2011	41.0 \pm 1.3	1.0488 \pm 0.0013
2012	31.8 \pm 1.3	1.0396 \pm 0.0013
2013	27.6 \pm 2.7	1.0355 \pm 0.0027
2014	23.8 \pm 2.1	1.0320 \pm 0.0021
2015	20.2 \pm 1.6	1.0283 \pm 0.0016

Table S2 Tree radiocarbon data. $\Delta^{14}\text{C}$ was measured at the W.M. Keck Carbon Cycle Accelerator Mass Spectrometry facility at UC Irvine. ^{14}C data were converted to mean age estimates using the bomb spike method as described in Methods. Values represent mean ± 1 SD of the analytical uncertainty as described in Methods S1. Fraction modern equivalent is also provided. S1= stem 0-0.5 cm, S2= stem 0.5-1, S3= stem 1-1.5 cm, S4= stem 1.5-2 cm, R1= root 0-0.5 cm, R2= root 0.5-1, R3= root 1-1.5 cm, R4= root 1.5-2 cm, FR= fine root, BR= branch, QURU=red oak, FRAM=white ash, ACRU=red maple, and FAGR=American beech.

Species	Tree	Organ	$\Delta^{14}\text{C}$ (‰)	Fraction modern	Mean age (yr)
QURU	104	S1	27.0 \pm 1.9	1.0352 \pm 0.0019	2.3
QURU	104	S2	29.1 \pm 1.6	1.0373 \pm 0.0016	2.7
QURU	104	S3	38.4 \pm 1.6	1.0467 \pm 0.0016	5.0
QURU	104	S4	64.0 \pm 2.0	1.0725 \pm 0.0020	11.6
QURU	104	R1	24.5 \pm 1.5	1.0327 \pm 0.0015	1.4
QURU	104	R2	32.3 \pm 1.8	1.0406 \pm 0.0018	3.4
QURU	104	R3	36.6 \pm 1.6	1.0449 \pm 0.0016	4.5
QURU	104	R4	53.4 \pm 1.7	1.0618 \pm 0.0017	8.8
QURU	104	FR	32.1 \pm 1.6	1.0404 \pm 0.0016	3.4
QURU	104	BR	26.0 \pm 1.5	1.0342 \pm 0.0015	2.1
QURU	107	S1	19.9 \pm 1.6	1.0281 \pm 0.0016	0.0
QURU	107	S2	24.8 \pm 1.6	1.0330 \pm 0.0016	1.5
QURU	107	S3	31.8 \pm 1.6	1.0401 \pm 0.0016	3.3
QURU	107	S4	51.3 \pm 1.8	1.0598 \pm 0.0018	8.4
QURU	107	R1	73.8 \pm 1.7	1.0824 \pm 0.0017	13.3
QURU	107	R2	128.0 \pm 2.0	1.1371 \pm 0.0020	22.8
QURU	107	R3	220.7 \pm 2.1	1.2305 \pm 0.0021	32.5
QURU	107	R4	221.4 \pm 2.1	1.2312 \pm 0.0021	32.5
QURU	107	FR	52.9 \pm 1.7	1.0614 \pm 0.0017	8.7
QURU	107	BR	25.6 \pm 1.6	1.0338 \pm 0.0016	2.0
QURU	109	S1	23.1 \pm 1.7	1.0313 \pm 0.0017	0.8
QURU	109	S2	86.7 \pm 2.0	1.0954 \pm 0.0020	15.3

Table S2 (Continued)

QURU	109	S3	39.9 ± 1.7	1.0483 ± 0.0017	5.5
QURU	109	S4	55.7 ± 1.6	1.0641 ± 0.0016	9.8
QURU	109	R1	24.2 ± 1.7	1.0324 ± 0.0017	1.2
QURU	109	R2	26.1 ± 1.7	1.0343 ± 0.0017	2.1
QURU	109	R3	31.2 ± 1.7	1.0394 ± 0.0017	3.2
QURU	109	R4	36.4 ± 1.7	1.0447 ± 0.0017	4.4
QURU	109	FR	19.2 ± 1.7	1.0274 ± 0.0017	0.0
QURU	109	BR	24.1 ± 1.7	1.0323 ± 0.0017	1.2
FRAM	108	S1	28.0 ± 1.5	1.0363 ± 0.0015	2.5
FRAM	108	S2	36.9 ± 1.5	1.0453 ± 0.0015	4.6
FRAM	108	S3	44.6 ± 1.6	1.0530 ± 0.0016	6.9
FRAM	108	S4	56.8 ± 1.4	1.0653 ± 0.0014	10.2
FRAM	108	R1	20.4 ± 1.7	1.0286 ± 0.0017	0.1
FRAM	108	R2	25.1 ± 1.3	1.0333 ± 0.0013	1.7
FRAM	108	R3	30.9 ± 1.3	1.0392 ± 0.0013	3.1
FRAM	108	R4	34.8 ± 1.3	1.0431 ± 0.0013	4.0
FRAM	108	FR	28.7 ± 1.3	1.0369 ± 0.0013	2.6
FRAM	108	BR	25.0 ± 1.6	1.0332 ± 0.0016	1.6
FRAM	150	S1	18.5 ± 1.4	1.0267 ± 0.0014	0.0
FRAM	150	S2	30.1 ± 1.3	1.0384 ± 0.0013	3.0
FRAM	150	S3	35.3 ± 1.3	1.0436 ± 0.0013	4.1
FRAM	150	S4	48.2 ± 1.4	1.0566 ± 0.0014	7.7
FRAM	150	R1	20.2 ± 1.5	1.0284 ± 0.0015	0.0
FRAM	150	R2	28.2 ± 1.3	1.0364 ± 0.0013	2.5
FRAM	150	R3	42.4 ± 1.3	1.0507 ± 0.0013	6.2
FRAM	150	R4	70.8 ± 1.4	1.0794 ± 0.0014	12.8
FRAM	150	FR	56.5 ± 1.5	1.0650 ± 0.0015	10.1
FRAM	150	BR	24.7 ± 1.3	1.0329 ± 0.0013	1.5
FRAM	167	S1	21.2 ± 1.5	1.0294 ± 0.0015	0.3
FRAM	167	S2	27.2 ± 1.6	1.0355 ± 0.0016	2.3
FRAM	167	S3	36.7 ± 2.0	1.0451 ± 0.0020	4.5
FRAM	167	S4	43.0 ± 1.6	1.0513 ± 0.0016	6.4
FRAM	167	R1	13.3 ± 1.6	1.0215 ± 0.0016	0.0
FRAM	167	R2	18.1 ± 1.3	1.0262 ± 0.0013	0.0
FRAM	167	R3	23.9 ± 1.4	1.0321 ± 0.0014	1.1
FRAM	167	R4	27.9 ± 2.1	1.0362 ± 0.0021	2.5
FRAM	167	FR	24.3 ± 1.5	1.0325 ± 0.0015	1.3
FRAM	167	BR	19.7 ± 1.4	1.0279 ± 0.0014	0.0
ACRU	102	S1	20.6 ± 2.0	1.0288 ± 0.0020	0.1
ACRU	102	S2	21.5 ± 1.6	1.0296 ± 0.0016	0.4
ACRU	102	S3	32.8 ± 1.7	1.0411 ± 0.0017	3.5
ACRU	102	S4	32.5 ± 2.1	1.0407 ± 0.0021	3.5
ACRU	102	R1	24.0 ± 1.6	1.0322 ± 0.0016	1.1
ACRU	102	R2	43.9 ± 1.7	1.0522 ± 0.0017	6.7

Table S2 (Continued)

ACRU	102	R3	62.8 ± 1.7	1.0713 ± 0.0017	11.4
ACRU	102	R4	85.2 ± 1.8	1.0939 ± 0.0018	15.0
ACRU	102	FR	72.8 ± 1.8	1.0814 ± 0.0018	13.1
ACRU	102	BR	35.2 ± 1.6	1.0435 ± 0.0016	4.1
ACRU	103	S1	34.6 ± 1.7	1.0429 ± 0.0017	3.9
ACRU	103	S2	59.3 ± 1.7	1.0678 ± 0.0017	10.7
ACRU	103	S3	74.3 ± 2.1	1.0829 ± 0.0021	13.3
ACRU	103	S4	89.3 ± 1.9	1.0980 ± 0.0019	15.8
ACRU	103	R1	27.0 ± 1.6	1.0353 ± 0.0016	2.3
ACRU	103	R2	53.3 ± 1.7	1.0618 ± 0.0017	8.8
ACRU	103	R3	74.6 ± 2.0	1.0832 ± 0.0020	13.4
ACRU	103	R4	95.0 ± 1.7	1.1038 ± 0.0017	16.8
ACRU	103	FR	130.2 ± 1.8	1.1392 ± 0.0018	23.1
ACRU	103	BR	30.8 ± 1.6	1.0391 ± 0.0016	3.1
ACRU	124	S1	29.4 ± 1.7	1.0377 ± 0.0017	2.8
ACRU	124	S2	49.5 ± 1.6	1.0579 ± 0.0016	8.0
ACRU	124	S3	71.1 ± 1.7	1.0797 ± 0.0017	12.8
ACRU	124	S4	91.6 ± 1.7	1.1004 ± 0.0017	16.3
ACRU	124	R1	26.5 ± 1.9	1.0348 ± 0.0019	2.2
ACRU	124	R2	39.2 ± 1.6	1.0475 ± 0.0016	5.2
ACRU	124	R3	51.9 ± 1.6	1.0603 ± 0.0016	8.5
ACRU	124	R4	72.5 ± 1.7	1.0811 ± 0.0017	13.0
ACRU	124	FR	35.9 ± 1.6	1.0442 ± 0.0016	4.3
ACRU	124	BR	30.2 ± 1.6	1.0385 ± 0.0016	3.0
FAGR	098	S1	23.6 ± 1.7	1.0318 ± 0.0017	1.0
FAGR	098	S2	29.8 ± 1.7	1.0381 ± 0.0017	2.9
FAGR	098	S3	36.6 ± 1.8	1.0449 ± 0.0018	4.5
FAGR	098	S4	40.2 ± 1.6	1.0485 ± 0.0016	5.5
FAGR	098	R1	18.8 ± 2.3	1.0270 ± 0.0023	0.0
FAGR	098	R2	20.5 ± 1.6	1.0286 ± 0.0016	0.1
FAGR	098	R3	27.2 ± 1.8	1.0355 ± 0.0018	2.3
FAGR	098	R4	29.0 ± 2.0	1.0372 ± 0.0020	2.7
FAGR	098	FR	64.4 ± 1.6	1.0729 ± 0.0016	11.7
FAGR	098	BR	27.1 ± 1.6	1.0353 ± 0.0016	2.3
FAGR	099	S1	24.1 ± 1.6	1.0323 ± 0.0016	1.2
FAGR	099	S2	28.5 ± 1.6	1.0367 ± 0.0016	2.6
FAGR	099	S3	35.9 ± 1.9	1.0442 ± 0.0019	4.3
FAGR	099	S4	42.0 ± 1.7	1.0504 ± 0.0017	6.1
FAGR	099	R1	20.9 ± 1.6	1.0291 ± 0.0016	0.2
FAGR	099	R2	19.6 ± 2.5	1.0278 ± 0.0025	0.0
FAGR	099	R3	20.5 ± 1.6	1.0287 ± 0.0016	0.1
FAGR	099	R4	21.6 ± 1.6	1.0298 ± 0.0016	0.4
FAGR	099	FR	46.4 ± 1.7	1.0548 ± 0.0017	7.3
FAGR	099	BR	23.3 ± 1.6	1.0315 ± 0.0016	0.9
FAGR	100	S1	22.7 ± 1.6	1.0309 ± 0.0016	0.7
FAGR	100	S2	32.0 ± 2.3	1.0403 ± 0.0023	3.4

Table S2 (Continued)

FAGR	100	S3	42.5 ± 1.7	1.0509 ± 0.0017	6.3
FAGR	100	S4	53.4 ± 1.7	1.0618 ± 0.0017	8.8
FAGR	100	R1	17.2 ± 1.6	1.0253 ± 0.0016	0.0
FAGR	100	R2	23.0 ± 1.9	1.0312 ± 0.0019	0.8
FAGR	100	R3	28.7 ± 1.6	1.0369 ± 0.0016	2.6
FAGR	100	R4	28.4 ± 1.6	1.0366 ± 0.0016	2.6
FAGR	100	FR	52.7 ± 2.1	1.0611 ± 0.0021	8.7
FAGR	100	BR	19.8 ± 1.6	1.0280 ± 0.0016	0.0

Table S3 Tukey’s HSD results from one-way ANOVA models testing for the effect of stemwood increment (cm) on total NSC, sugar, and starch concentrations for each season and species. NS= not significant, * = $P \leq 0.05$, ** = $P \leq 0.01$, *** = $P \leq 0.001$, or **** = $P \leq 0.0001$ in each white cell indicates if column month and row month are significantly different from each other or not based on the difference between their least squares means. Each light gray cell contains this difference, calculated by row increment minus column increment. If the entire grid is shaded orange, then increment was not a significant factor in the one-way ANOVA with $P \geq 0.05$ and post-hoc testing was not conducted. If the entire grid is shaded purple, then the interaction effect (I x S, Fig. 1) was not significant in two-way ANOVA testing with $P \geq 0.05$ and additional testing was not conducted below.

All species													
Winter							Spring						
Total NSC							Total NSC						
	0-1	1-2	2-3	3-4	4-8	8-p		0-1	1-2	2-3	3-4	4-8	8-p
0-1		-14.9	-18.7	-21.1	-22.8	-27.2	0-1		-2.5	-9.6	-10.5	-8.1	-12.1
1-2	****		-3.8	-6.2	-7.9	-12.3	1-2	NS		-7.1	-8.0	-5.6	-9.6
2-3	****	NS		-2.5	-4.2	-8.6	2-3	****	***		-0.9	1.5	-2.4
3-4	****	NS	NS		-1.7	-6.1	3-4	****	****	NS		2.4	-1.6
4-8	****	*	NS	NS		-4.4	4-8	****	**	NS	NS		-4.0
8-p	****	****	*	NS	NS		8-p	****	****	NS	NS	NS	
Sugar							Sugar						
	0-1	1-2	2-3	3-4	4-8	8-p		0-1	1-2	2-3	3-4	4-8	8-p
0-1		-13.4	-15.1	-16.7	-17.8	-21.6	0-1		-1.9	-3.4	-4.0	-3.0	-5.1
1-2	****		-1.7	-3.3	-4.3	-8.1	1-2	NS		-1.5	-2.1	-1.1	-3.2
2-3	****	NS		-1.6	-2.6	-6.4	2-3	NS	NS		-0.6	0.3	-1.7
3-4	****	NS	NS		-1.1	-4.9	3-4	*	NS	NS		0.9	-1.1
4-8	****	NS	NS	NS		-3.8	4-8	NS	NS	NS	NS		-2.0
8-p	****	**	*	NS	NS		8-p	***	NS	NS	NS	NS	
Starch							Starch						
	0-1	1-2	2-3	3-4	4-8	8-p		0-1	1-2	2-3	3-4	4-8	8-p
0-1		-1.5	-3.5	-4.4	-5.1	-5.7	0-1		-0.6	-6.2	-6.5	-5.0	-7.0
1-2	NS		-2.1	-3.0	-3.6	-4.2	1-2	NS		-5.6	-5.9	-4.4	-6.4
2-3	*	NS		-0.9	-1.5	-2.1	2-3	****	****		-0.3	1.2	-0.8
3-4	**	NS	NS		-0.6	-1.2	3-4	****	****	NS		1.4	-0.5
4-8	***	*	NS	NS		-0.6	4-8	***	**	NS	NS		-2.0
8-p	****	**	NS	NS	NS		8-p	****	****	NS	NS	NS	

Table S3 (Continued)

Summer							Autumn						
Total NSC							Total NSC						
	0-1	1-2	2-3	3-4	4-8	8-p		0-1	1-2	2-3	3-4	4-8	8-p
0-1		-6.3	-11.3	-8.0	-14.8	-13.6	0-1		-28.3	-42.3	-42.4	-43.0	-43.0
1-2	**		-5.0	-1.7	-8.4	-7.3	1-2	****		-14.0	-14.1	-14.7	-14.7
2-3	****	*		-3.3	-3.4	-2.3	2-3	****	***		-0.1	-0.7	-0.7
3-4	****	NS	NS		-6.7	-5.6	3-4	****	***	NS		-0.6	-0.6
4-8	****	****	NS	***		1.2	4-8	****	***	NS	NS		-0.01
8-p	****	****	NS	**	NS		8-p	****	***	NS	NS	NS	
Sugar							Sugar						
	0-1	1-2	2-3	3-4	4-8	8-p		0-1	1-2	2-3	3-4	4-8	8-p
0-1		-3.2	-2.6	-3.2	-3.5	-2.0	0-1		-4.4	-7.3	-7.4	-8.8	-8.0
1-2	*		0.56	-0.02	-0.3	1.2	1-2	**		-2.9	-3.0	-4.4	-3.6
2-3	NS	NS		-0.6	-0.9	0.6	2-3	****	NS		-0.1	-1.5	-0.7
3-4	*	NS	NS		-0.3	1.2	3-4	****	NS	NS		-1.4	-0.6
4-8	**	NS	NS	NS		1.5	4-8	****	**	NS	NS		0.8
8-p	NS	NS	NS	NS	NS		8-p	****	*	NS	NS	NS	
Starch							Starch						
	0-1	1-2	2-3	3-4	4-8	8-p		0-1	1-2	2-3	3-4	4-8	8-p
0-1		-3.1	-8.7	-4.9	-11.2	-11.6	0-1		-23.8	-35.0	-35.0	-35.0	-35.0
1-2	NS		-5.6	-1.7	-8.1	-8.5	1-2	****		-11.1	-11.1	-10.3	-11.1
2-3	****	***		3.9	-2.6	-2.9	2-3	****	**		1.7e ⁻¹⁴	0.8	-2.7e ⁻¹³
3-4	**	NS	*		-6.4	-6.7	3-4	****	**	NS		0.8	-2.9e ⁻¹³
4-8	****	****	NS	****		-0.3	4-8	****	**	NS	NS		-0.8
8-p	****	****	NS	****	NS		8-p	****	**	NS	NS	NS	
Red Oak													
Winter							Spring						
Total NSC							Total NSC						
	0-1	1-2	2-3	3-4	4-8	8-p		0-1	1-2	2-3	3-4	4-8	8-p
0-1		-39.2	-45.5	-44.2	-43.7	-45.2	0-1		-4.4	-18.1	-18.7	-16.2	-17.5
1-2	****		-6.3	-5.0	-4.5	-6.0	1-2	NS		-13.6	-14.3	-11.8	-13.1
2-3	****	*		1.2	1.7	0.3	2-3	****	***		-0.7	1.8	0.5
3-4	****	NS	NS		0.5	-0.9	3-4	****	***	NS		2.4	1.2
4-8	****	NS	NS	NS		-1.4	4-8	****	**	NS	NS		-1.3
8-p	****	*	NS	NS	NS		8-p	****	***	NS	NS	NS	
Sugar							Sugar						
	0-1	1-2	2-3	3-4	4-8	8-p		0-1	1-2	2-3	3-4	4-8	8-p
0-1		-34.7	-41.3	-39.5	-39.5	-40.4	0-1		-5.0	-9.9	-10.5	-8.3	-9.3
1-2	****		-6.6	-4.8	-4.8	-5.7	1-2	NS		-4.9	-5.4	-3.2	-4.2
2-3	****	NS		1.8	1.8	0.9	2-3	****	NS		-0.5	1.6	0.6
3-4	****	NS	NS		-0.01	-0.9	3-4	****	*	NS		2.2	1.2
4-8	****	NS	NS	NS		-0.9	4-8	****	NS	NS	NS		-1.0
8-p	****	NS	NS	NS	NS		8-p	****	NS	NS	NS	NS	

Table S3 (Continued)

Starch							Starch						
	0-1	1-2	2-3	3-4	4-8	8-p		0-1	1-2	2-3	3-4	4-8	8-p
0-1		-4.5	-4.2	-4.8	-4.3	-4.8	0-1		0.6	-8.1	-8.2	-8.0	-8.2
1-2	**		0.4	-0.2	0.3	-0.2	1-2	NS		-8.7	-8.8	-8.6	-8.8
2-3	*	NS		-0.6	-0.01	-0.6	2-3	*	*		-0.1	0.1	-0.1
3-4	**	NS	NS		0.5	-1.3e ⁻¹³	3-4	*	*	NS		0.3	6.7e ⁻¹⁵
4-8	*	NS	NS	NS		-0.5	4-8	*	*	NS	NS		-0.3
8-p	**	NS	NS	NS	NS		8-p	*	*	NS	NS	NS	
Summer							Autumn						
Total NSC							Total NSC						
	0-1	1-2	2-3	3-4	4-8	8-p		0-1	1-2	2-3	3-4	4-8	8-p
0-1		-18.2	-23.6	-19.0	-25.0	-24.0	0-1		-30.4	-45.7	-45.1	-44.7	-45.6
1-2	****		-5.4	-0.8	-6.8	-5.4	1-2	****		-15.3	-14.7	-14.3	-15.2
2-3	****	NS		4.6	-1.4	-0.02	2-3	****	**		0.6	1.0	0.1
3-4	****	NS	NS		-6.0	-4.6	3-4	****	**	NS		0.5	-0.5
4-8	****	*	NS	NS		1.4	4-8	****	**	NS	NS		-0.9
8-p	****	NS	NS	NS	NS		8-p	****	**	NS	NS	NS	
Sugar							Sugar						
	0-1	1-2	2-3	3-4	4-8	8-p		0-1	1-2	2-3	3-4	4-8	8-p
0-1		-6.2	-5.1	-5.2	-5.4	-3.8	0-1		-12.9	-16.3	-15.8	-17.1	-16.2
1-2	****		1.2	1.1	0.8	2.4	1-2	****		-3.5	-2.9	-4.2	-3.4
2-3	***	NS		-0.1	-0.4	1.3	2-3	****	NS		0.6	-0.7	0.1
3-4	***	NS	NS		-0.3	1.4	3-4	****	NS	NS		-1.3	-0.5
4-8	***	NS	NS	NS		1.6	4-8	****	NS	NS	NS		0.8
8-p	*	NS	NS	NS	NS		8-p	****	NS	NS	NS	NS	
Starch							Starch						
	0-1	1-2	2-3	3-4	4-8	8-p		0-1	1-2	2-3	3-4	4-8	8-p
0-1		-12.0	-18.5	-13.9	-19.6	-19.8	0-1		-18.0	-29.3	-29.3	-27.8	-29.3
1-2	****		-6.6	-1.9	-7.6	-7.9	1-2	****		-11.8	-11.8	-10.1	-11.8
2-3	****	NS		4.7	-1.0	-1.3	2-3	****	**		2.9e ⁻¹⁴	1.8	2.8
3-4	****	NS	NS		-5.7	-6.0	3-4	****	**	NS		-1.8e ⁻¹⁵	-1.8e ⁻¹⁵
4-8	****	*	NS	NS		-0.3	4-8	****	*	NS	NS		-1.8
8-p	****	**	NS	NS	NS		8-p	****	**	NS	NS	NS	
White ash													
Winter							Spring						
Total NSC							Total NSC						
	0-1	1-2	2-3	3-4	4-8	8-p		0-1	1-2	2-3	3-4	4-8	8-p
0-1		-22.8	-28.8	-34.4	-40.9	-48.2	0-1		-6.4	-15.8	-20.5	-20.9	-28.0
1-2	*		-6.0	-11.6	-18.1	-25.4	1-2	NS		-9.4	-14.1	-14.5	-21.6
2-3	**	NS		-5.6	-12.1	-19.4	2-3	*	NS		-4.7	-5.1	-12.2
3-4	***	NS	NS		-6.5	-13.9	3-4	***	*	NS		-0.4	-7.5
4-8	****	NS	NS	NS		-7.4	4-8	***	*	NS	NS		-7.1
8-p	****	*	NS	NS	NS		8-p	****	***	NS	NS	NS	
Sugar							Sugar						

Table S3 (Continued)

	0-1	1-2	2-3	3-4	4-8	8-p		0-1	1-2	2-3	3-4	4-8	8-p
0-1		-15.9	-16.3	-21.9	-28.4	-35.8	0-1		-2.6	-6.3	-10.8	-11.6	-18.3
1-2	**		-0.4	-6.0	-12.5	-19.8	1-2	NS		-3.8	-8.2	-9.0	-15.7
2-3	**	NS		-5.6	-12.1	-19.5	2-3	NS	NS		-4.5	-5.3	-12.0
3-4	****	NS	NS		-6.5	-13.9	3-4	*	NS	NS		-0.8	-7.5
4-8	****	*	NS	NS		-7.4	4-8	*	NS	NS	NS		-6.7
8-p	****	***	***	*	NS		8-p	****	***	**	NS	NS	
Starch							Starch						
	0-1	1-2	2-3	3-4	4-8	8-p		0-1	1-2	2-3	3-4	4-8	8-p
0-1							0-1		-3.8	-9.5	-9.7	-9.2	-9.7
1-2							1-2	NS		-5.7	-5.9	-5.5	-5.9
2-3							2-3	NS	NS		-0.2	0.2	-0.2
3-4							3-4	NS	NS	NS		0.4	-4.0e ⁻¹⁵
4-8							4-8	NS	NS	NS	NS		-0.4
8-p							8-p	NS	NS	NS	NS	NS	
Summer							Autumn						
Total NSC							Total NSC						
	0-1	1-2	2-3	3-4	4-8	8-p		0-1	1-2	2-3	3-4	4-8	8-p
0-1		-6.8	-9.6	-11.8	-21.4	-25.0	0-1		-43.5	-67.4	-68.5	-73.9	-76.5
1-2	NS		-2.8	-4.9	-14.5	-18.2	1-2	***		-23.8	-25.0	-30.4	-33.0
2-3	NS	NS		-2.2	-11.8	-15.4	2-3	****	NS		-1.1	-6.6	-9.1
3-4	NS	NS	NS		-9.6	-13.3	3-4	****	NS	NS		-5.4	-8.0
4-8	*	NS	NS	NS		-3.7	4-8	****	*	NS	NS		-2.6
8-p	**	*	NS	NS	NS		8-p	****	*	NS	NS	NS	
Sugar							Sugar						
	0-1	1-2	2-3	3-4	4-8	8-p		0-1	1-2	2-3	3-4	4-8	8-p
0-1		-1.3	0.1	-3.5	-6.8	-10.5	0-1		-5.5	-14.3	-15.4	-20.8	-23.5
1-2	NS		1.4	-2.2	-5.5	-9.2	1-2	NS		-8.8	-9.9	-15.3	-17.9
2-3	NS	NS		-3.6	-6.9	-10.6	2-3	***	*		-1.1	-6.6	-9.2
3-4	NS	NS	NS		-3.3	-7.0	3-4	****	*	NS		-5.4	-8.0
4-8	NS	NS	NS	NS		-3.7	4-8	****	****	NS	NS		-2.6
8-p	*	*	*	NS	NS		8-p	****	****	*	NS	NS	
Starch							Starch						
	0-1	1-2	2-3	3-4	4-8	8-p		0-1	1-2	2-3	3-4	4-8	8-p
0-1		-5.5	-9.7	-8.2	-14.5	-14.5	0-1		-38.0	-53.0	-53.0	-53.0	-53.0
1-2	NS		-4.2	-2.7	-9.1	-9.1	1-2	***		-15.1	-15.1	-15.1	-15.1
2-3	NS	NS		1.5	-4.8	-4.8	2-3	****	NS		2.5e ⁻¹⁴	-2.5e ⁻¹⁴	-1.8e ⁻¹⁵
3-4	NS	NS	NS		-6.3	-6.3	3-4	****	NS	NS		-5.0e ⁻¹⁴	-2.7e ⁻¹⁴
4-8	*	NS	NS	NS		9.8e ⁻¹⁵	4-8	****	NS	NS	NS		2.3e ⁻¹⁴
8-p	*	NS	NS	NS	NS		8-p	****	NS	NS	NS	NS	
Red maple													
Winter							Spring						

Table S3 (Continued)

Total NSC							Total NSC						
	0-1	1-2	2-3	3-4	4-8	8-p		0-1	1-2	2-3	3-4	4-8	8-p
0-1		0.1	-5.7	-10.8	-19.3	-26.2	0-1		-2.0	-5.3	-6.6	-1.1	-11.4
1-2	NS		-5.7	-10.8	-19.4	-26.2	1-2	NS		-3.2	-4.5	1.0	-9.3
2-3	NS	NS		-5.1	-13.7	-20.5	2-3	NS	NS		-1.3	4.2	-6.1
3-4	NS	NS	NS		-8.6	-15.4	3-4	NS	NS	NS		5.5	-4.8
4-8	***	***	*	NS		-6.9	4-8	NS	NS	NS	NS		-10.3
8-p	****	****	***	**	NS		8-p	**	*	NS	NS	*	
Sugar							Sugar						
	0-1	1-2	2-3	3-4	4-8	8-p		0-1	1-2	2-3	3-4	4-8	8-p
0-1		-1.7	-4.6	-6.8	-12.4	-17.3	0-1						
1-2	NS		-2.9	-5.2	-10.7	-15.6	1-2						
2-3	NS	NS		-2.2	-7.8	-12.7	2-3						
3-4	*	NS	NS		-5.6	-10.5	3-4						
4-8	****	****	**	NS		-4.9	4-8						
8-p	****	****	****	****	NS		8-p						
Starch							Starch						
	0-1	1-2	2-3	3-4	4-8	8-p		0-1	1-2	2-3	3-4	4-8	8-p
0-1		1.7	-1.1	-4.0	-7.0	-8.9	0-1		-0.6	-5.4	-6.2	-2.4	-8.3
1-2	NS		-2.8	-5.7	-8.7	-10.6	1-2	NS		-4.8	-5.6	-1.8	-7.7
2-3	NS	NS		-2.9	-5.9	-7.8	2-3	NS	NS		-0.7	3.1	-2.8
3-4	NS	NS	NS		-3.0	-5.0	3-4	NS	NS	NS		3.8	-2.1
4-8	NS	NS	NS	NS		-2.0	4-8	NS	NS	NS	NS		-5.9
8-p	NS	*	NS	NS	NS		8-p	*	NS	NS	NS	NS	
Summer							Autumn						
Total NSC							Total NSC						
	0-1	1-2	2-3	3-4	4-8	8-p		0-1	1-2	2-3	3-4	4-8	8-p
0-1		-0.5	-8.5	-6.7	-13.8	-11.6	0-1		-36.0	-54.0	-54.4	-54.7	-54.3
1-2	NS		-8.0	-6.2	-13.2	-11.1	1-2	****		-18.0	-18.4	-18.7	-18.3
2-3	*	*		1.8	-5.3	-3.1	2-3	****	NS		-0.4	-0.7	-0.3
3-4	NS	NS	NS		-7.1	-4.9	3-4	****	NS	NS		-0.3	0.1
4-8	****	****	NS	NS		2.2	4-8	****	NS	NS	NS		0.4
8-p	***	***	NS	NS	NS		8-p	****	NS	NS	NS	NS	
Sugar							Sugar						
	0-1	1-2	2-3	3-4	4-8	8-p		0-1	1-2	2-3	3-4	4-8	8-p
0-1		-1.7	-1.0	-1.3	-1.1	1.3	0-1		-0.6	-3.1	-3.5	-4.6	-3.3
1-2	NS		0.7	0.4	0.6	3.0	1-2	NS		-2.5	-2.9	-4.0	-2.8
2-3	NS	NS		-0.3	-0.1	2.3	2-3	NS	NS		-0.4	-1.6	-0.3
3-4	NS	NS	NS		0.2	2.6	3-4	NS	NS	NS		-1.2	0.1
4-8	NS	NS	NS	NS		2.4	4-8	*	NS	NS	NS		1.3
8-p	NS	*	NS	NS	NS		8-p	NS	NS	NS	NS	NS	
Starch							Starch						
	0-1	1-2	2-3	3-4	4-8	8-p		0-1	1-2	2-3	3-4	4-8	8-p
0-1		1.1	-7.5	-5.4	-12.7	-12.9	0-1		-35.4	-51.0	-51.0	-50.1	-51.0

Table S3 (Continued)

1-2	NS		-8.7	-6.5	-13.8	-14.0	1-2	****		-15.5	-15.5	-14.7	-15.5
2-3	NS	*		2.1	-5.1	-5.4	2-3	****	NS		-2.1e ⁻¹⁴	0.8	-7.1e ⁻¹⁵
3-4	NS	NS	NS		-7.3	-7.5	3-4	****	NS	NS		0.8	1.4e ⁻¹⁴
4-8	***	****	NS	NS		-0.2	4-8	****	NS	NS	NS		-0.8
8-p	****	****	NS	NS	NS		8-p	****	NS	NS	NS	NS	
Paper birch													
Winter							Spring						
Total NSC							Total NSC						
	0-1	1-2	2-3	3-4	4-8	8-p		0-1	1-2	2-3	3-4	4-8	8-p
0-1		-0.2	-2.9	-5.8	-3.2	-13.0	0-1		0.1	-5.3	-5.4	-1.6	-7.5
1-2	NS		-2.7	-5.5	-2.9	-12.8	1-2	NS		-5.4	-5.5	-1.7	-7.6
2-3	NS	NS		-2.9	-0.3	-10.1	2-3	NS	NS		-0.04	3.7	-2.2
3-4	NS	NS	NS		-2.6	-7.2	3-4	NS	NS	NS		3.8	-2.2
4-8	NS	NS	NS	NS		-9.8	4-8	NS	NS	NS	NS		-5.9
8-p	**	**	*	NS	*		8-p	NS	NS	NS	NS	NS	
Sugar							Sugar						
	0-1	1-2	2-3	3-4	4-8	8-p		0-1	1-2	2-3	3-4	4-8	8-p
0-1		-1.6	1.8	-0.8	1.9	-8.0	0-1						
1-2	NS		3.4	0.9	3.5	-6.4	1-2						
2-3	NS	NS		-2.6	0.1	-9.8	2-3						
3-4	NS	NS	NS		2.6	-7.2	3-4						
4-8	NS	NS	NS	NS		-9.8	4-8						
8-p	**	*	***	**	***		8-p						
Starch							Starch						
	0-1	1-2	2-3	3-4	4-8	8-p		0-1	1-2	2-3	3-4	4-8	8-p
0-1		1.4	-4.7	-5.0	-5.0	-5.0	0-1		-0.2	-5.2	-5.2	-3.6	-5.2
1-2	NS		-6.1	-6.4	-6.4	-6.4	1-2	NS		-5.0	-5.0	-3.5	-5.0
2-3	NS	NS		-0.3	-0.3	-0.3	2-3	NS	NS		7.8e ⁻¹⁵	1.6	3.1e ⁻¹⁵
3-4	NS	NS	NS		-4.7e ⁻¹⁵	2.0e ⁻¹⁵	3-4	NS	NS	NS		1.6	-4.7e ⁻¹⁵
4-8	NS	NS	NS	NS		6.7e ⁻¹⁵	4-8	NS	NS	NS	NS		-1.6
8-p	NS	NS	NS	NS	NS		8-p	NS	NS	NS	NS	NS	
Summer							Autumn						
Total NSC							Total NSC						
	0-1	1-2	2-3	3-4	4-8	8-p		0-1	1-2	2-3	3-4	4-8	8-p
0-1		-4.8	-7.0	-0.7	-7.7	-6.6	0-1		-41.9	-49.9	-51.6	-52.6	-50.1
1-2	NS		-2.2	4.1	-2.9	-1.9	1-2	**		-8.1	-9.8	-10.7	-8.2
2-3	NS	NS		6.3	-0.7	0.4	2-3	***	NS		-1.7	-2.7	-0.2
3-4	NS	NS	NS		-7.0	-6.0	3-4	***	NS	NS		-1.0	1.5
4-8	NS	NS	NS	NS		1.0	4-8	***	NS	NS	NS		2.5
8-p	NS	NS	NS	NS	NS		8-p	***	NS	NS	NS	NS	
Sugar							Sugar						
	0-1	1-2	2-3	3-4	4-8	8-p		0-1	1-2	2-3	3-4	4-8	8-p
0-1							0-1		-0.7	-2.9	-4.6	-5.8	-3.1
1-2							1-2	NS		-2.2	-3.9	-5.1	-2.3

Table S3 (Continued)

2-3							2-3	NS	NS		-1.7	-2.9	-0.2
3-4							3-4	NS	NS	NS		-1.2	1.5
4-8							4-8	NS	NS	NS	NS		2.8
8-p							8-p	*	NS	NS	NS	NS	
Starch							Starch						
	0-1	1-2	2-3	3-4	4-8	8-p		0-1	1-2	2-3	3-4	4-8	8-p
0-1							0-1		-41.2	-47.0	-47.0	-46.8	-47.0
1-2							1-2	**		-5.9	-5.9	-5.6	-5.9
2-3							2-3	***	NS		-2.0e ⁻¹⁴	0.3	-2.0e ⁻¹⁴
3-4							3-4	***	NS	NS		0.3	0.0
4-8							4-8	***	NS	NS	NS		-0.3
8-p							8-p	***	NS	NS	NS	NS	
White pine													
Winter							Spring						
Total NSC							Total NSC						
	0-1	1-2	2-3	3-4	4-8	8-p		0-1	1-2	2-3	3-4	4-8	8-p
0-1							0-1						
1-2							1-2						
2-3							2-3						
3-4							3-4						
4-8							4-8						
8-p							8-p						
Sugar							Sugar						
	0-1	1-2	2-3	3-4	4-8	8-p		0-1	1-2	2-3	3-4	4-8	8-p
0-1		-8.6	-7.4	-9.2	-5.9	-6.7	0-1		0.1	-0.5	0.5	-0.4	2.4
1-2	****		1.2	-0.6	2.7	2.0	1-2	NS		-0.6	0.4	-0.5	2.3
2-3	****	NS		-1.8	1.5	0.7	2-3	NS	NS		1.0	0.2	2.9
3-4	****	NS	NS		3.3	2.5	3-4	NS	NS	NS		-0.8	2.0
4-8	***	NS	NS	NS		-0.8	4-8	NS	NS	NS	NS		2.8
8-p	****	NS	NS	NS	NS		8-p	NS	NS	*	NS	*	
Starch							Starch						
	0-1	1-2	2-3	3-4	4-8	8-p		0-1	1-2	2-3	3-4	4-8	8-p
0-1							0-1		-0.4	-4.0	-4.1	-3.4	-4.1
1-2							1-2	NS		-3.6	-3.7	-2.9	-3.7
2-3							2-3	*	*		-0.1	0.6	-0.1
3-4							3-4	**	*	NS		0.7	5.3e ⁻¹⁵
4-8							4-8	NS	NS	NS	NS		-0.7
8-p							8-p	**	*	NS	NS	NS	
Summer							Autumn						
Total NSC							Total NSC						
	0-1	1-2	2-3	3-4	4-8	8-p		0-1	1-2	2-3	3-4	4-8	8-p
0-1							0-1						
1-2							1-2						

Table S3 (Continued)

2-3							2-3						
3-4							3-4						
4-8							4-8						
8-p							8-p						
Sugar							Sugar						
	0-1	1-2	2-3	3-4	4-8	8-p		0-1	1-2	2-3	3-4	4-8	8-p
0-1		-1.9	-1.8	-2.9	-2.1	1.2	0-1						
1-2	NS		0.1	-1.0	-0.1	3.1	1-2						
2-3	NS	NS		-1.1	-0.3	3.0	2-3						
3-4	*	NS	NS		0.8	4.1	3-4						
4-8	NS	NS	NS	NS		3.2	4-8						
8-p	NS	**	*	***	**		8-p						
Starch							Starch						
	0-1	1-2	2-3	3-4	4-8	8-p		0-1	1-2	2-3	3-4	4-8	8-p
0-1		1.3	-3.1	2.6	-3.7	-4.5	0-1		-2.8	-9.5	-9.5	-9.0	-9.5
1-2	NS		-4.3	1.4	-4.9	-5.7	1-2	NS		-6.6	-6.6	-6.2	-6.6
2-3	NS	NS		5.7	-0.6	-1.4	2-3	NS	NS		-9.3e ⁻¹⁵	0.4	1.1e ⁻¹⁴
3-4	NS	NS	*		-6.3	-7.1	3-4	NS	NS	NS		0.4	2.0e ⁻¹⁴
4-8	NS	NS	NS	**		-0.8	4-8	NS	NS	NS	NS		-0.4
8-p	NS	*	NS	***	NS		8-p	NS	NS	NS	NS	NS	

Table S4 Tree and stemwood characteristics. Diameter at breast height, height, age, start of heartwood year, and approximate number of rings in each stemwood increment for individual trees (n=24) sampled throughout 2014. For each tree, a stemwood core for dendrochronology was collected 3 inches below the initial core collected for NSC analysis in January 2014. A second stemwood core was collected perpendicularly to this core in June 2015. To determine ring width measurements and tree ages, we mounted, dried, and sanded these cores. We measured ring widths with a resolution of 0.001 mm and accuracy of 0.010 mm m⁻¹ using a sliding stage and linear encoder (TA Tree Ring System, Velmex Inc., Bloomfield, NY, USA). The computer program COFECHA was used to cross-date cores (Holmes, 1983) and estimate tree ages. The number of rings in each stemwood increment was estimated by ring widths from January 2014 cores. Additionally, the sapwood-heartwood boundary was identified based on wood color and the heartwood start year is indicated below. The corresponding number of rings is in bold to indicate the increment in which the heartwood started for each tree; QURU=red oak, FRAM=white ash, ACRU=red maple, BEPA=paper birch, and PIST=white pine. Note: Estimated ages for QURU 115, 117, and 118 were misreported in Furze *et al.*, 2018 Table S1 and were corrected above. Further, for Fig. 2 in the main text – to determine placement of gray vertical bars which represent the average increment in which the sapwood-heartwood boundary was visually identified, we calculated the mean (\pm SD) cumulative ring width (cm) at the heartwood start year for each species: red oak 1.7 cm (\pm 0.4, n=6), white ash 7.6 cm (\pm 1.2, n=3), red maple 9.0 cm (\pm 3.1, n=5), paper birch 9.8 cm (\pm 1.0, n=2), and white pine 3.5 cm (\pm 1.4, n=6). The sapwood-heartwood boundary could not be identified for two trees as denoted by NA.

Species	Tree	DBH (cm)	Ht (m)	Age (yr)	Heartwood start (yr)	0-1	1-2	2-3	3-4	4-8	8+
FRAM	101	33.0	23.4	111	1937	21	15	6	9	34	27
ACRU	102	39.5	22.0	61	NA	5	5	5	4	16	24
ACRU	103	26.0	21.6	65	1974	8	11	4	4	13	20
QURU	104	43.0	23.2	96	2005	4	4	5	5	18	58

Table S4 (Continued)

ACRU	105	29.0	20.7	86	1930	10	10	7	5	14	39
BEPA	106	26.5	19.3	74	1956	16	7	10	1	19	19
QURU	107	43.0	22.6	83	2007	5	5	5	5	15	42
FRAM	108	39.5	19.5	91	1966	7	6	7	7	24	38
QURU	109	46.0	18.6	108	2000	6	6	4	5	17	68
BEPA	110	40.5	19.5	104	NA	19	13	7	4	17	42
PIST	111	38.0	23.2	65	1992	6	4	6	4	16	27
ACRU	112	33.0	21.0	72	1980	9	5	4	4	15	35
BEPA	113	30.5	20.1	67	1965	15	7	5	4	11	21
PIST	114	34.5	20.1	66	1994	11	7	6	4	22	13
QURU	115	30.0	20.7	69	2007	5	6	6	5	20	26
PIST	116	31.0	19.8	75	1984	24	7	3	5	17	9
QURU	117	29.0	19.8	72	2004	5	6	8	5	19	22
QURU	118	34.5	21.9	82	2004	6	7	6	6	16	35
PIST	119	50.0	20.3	67	1994	4	4	5	5	11	40
ACRU	120	34.0	21.7	97	1958	16	8	10	5	33	23
PIST	121	41.0	20.9	80	1993	7	7	6	6	18	27
PIST	122	44.5	21.3	87	1989	6	6	6	2	18	44
FRAM	123	28.0	18.7	75	1956	14	10	7	5	15	21
ACRU	124	30.0	19.8	68	1955	8	10	7	6	15	20

Methods S1 Uncertainty in NSC and radiocarbon measurements

For NSC concentration measurements, an internal laboratory standard (red oak stemwood, Harvard Forest, Petersham, MA, USA) was run per NSC analysis to assess uncertainty. Measured sugar and starch concentrations for the standard were within $\pm 10\%$ of the mean (\pm SD) (sugar, 35.9 ± 3.8 mg g⁻¹; starch, 24.5 ± 2.1 mg g⁻¹).

For radiocarbon measurements, we assessed uncertainty in a few ways. First, there is an analytical uncertainty (1 SD) determined for each sample run on the AMS. This is derived based on counting statistics and the analytical reproducibility of the primary standards (Oxalic acid standard OXI) run with each wheel (Stuiver *et al.*, 1977). For the samples analyzed in this study, the mean uncertainty in measured $\Delta^{14}\text{C}$ was 1.7 ‰ (\pm 0.2 SD, n=120).

Second, a standard was run with each wheel on the AMS. We measured a mean $\Delta^{14}\text{C}$ value of 486.7 ‰ (\pm 2.4 SD, n=5) for ANU sucrose (IAEA C-6), which corresponds to 1.4985 ± 0.0024 in

Fraction Modern notation. This is in agreement with the long-term mean value measured at UC Irvine of 1.5016 (± 0.0002 SE) (Xu *et al.*, 2010).

Third, we conducted a second extraction for a handful of our study samples (n=7) and ran these separately on the AMS. The standard deviation of the mean $\Delta^{14}\text{C}$ value for each replicate pair (n=7) ranged from 0.2 to 7.9 ‰, depending on the tissue.

3

Carbon isotopic tracing of sugars throughout whole-trees exposed to climate warming

In review as:

Furze, ME, Drake, JE, Wiesenbauer, J, Richter, A, Pendall, E. Carbon isotopic tracing of sugars throughout whole-trees exposed to climate warming.

Related publication:

Drake, JE, **Furze, ME**, Tjoelker, MG, Carrillo, Y, Barton, CVM., Pendall, E. 2019. Climate warming and tree carbon use efficiency in a whole-tree $^{13}\text{CO}_2$ tracer study. *New Phytologist*.

Abstract

Trees allocate C from sources to sinks by way of a series of processes involving carbohydrate transport and utilization. Yet, it is unclear how these dynamics will respond to a warmer world. Here, we conducted a warming and pulse-chase experiment on *Eucalyptus parramattensis* growing in a whole-tree chamber system to test whether warming impacts carbon allocation by increasing the speed of carbohydrate dynamics. We pulse-labeled whole trees with ^{13}C -CO₂ to follow recently fixed C through different organs by using compound-specific isotope analysis of sugars. We then compared the concentrations and mean residence times of individual sugars between ambient and warmed (+3°C) treatments. Trees dynamically allocated ^{13}C -labeled sugars throughout the aboveground-belowground continuum. We did not, however, find a significant treatment effect on C dynamics, as sugar concentrations and mean residence times were not altered by warming. From the canopy to the root system, ^{13}C enrichment of sugars decreased and mean residence times increased, reflecting dilution and mixing of recent photoassimilates with older reserves along the transport pathway. Our results suggest that a locally endemic Eucalypt was seemingly able to adjust its physiology to warming representative of future temperature predictions for Australia.

Introduction

Carbon (C) dynamics in trees result from the complex integration of multiple sinks competing for photoassimilates supplied by sources (Kozłowski, 1992). As the C requirements of different organs and processes vary temporally due to normal functioning or unexpected stress, trees must adjust C allocation to survive. In general, photoassimilates produced during photosynthesis in the leaves are exported into the phloem and allocated throughout the tree. The transport of photoassimilates from sources to sinks via the phloem is driven by a hydrostatic pressure gradient which is controlled in part by the utilization of carbohydrates in sink organs (Knoblauch et al., 2016;

Münch, 1930). Thus, along the long-distance transport pathway, photoassimilates are frequently exchanged with older reserves (i.e. nonstructural carbohydrates) and released into sinks to serve as C skeletons for growth, metabolism, and storage (Furze, Trumbore, & Hartmann, 2018).

Environmental conditions have the potential to alter whole-tree C dynamics by influencing the activity of sources and sinks, with implications for ecosystem-level C budgets. For instance, temperature is likely to affect the rate of chemical reactions involved in carbohydrate transport and utilization and in turn influence the distribution of carbohydrates throughout the tree. Elevated temperatures may increase sink strength (i.e. increased growth, respiration, root exudation), leading to faster turnover rates of reserves in organs and faster transfer of sugars along the transport pathway (Dannoura et al., 2011; Plain et al., 2009). Given that unprecedented temperature increases are expected across the globe, it is important to understand how within-tree C dynamics will respond to higher temperatures.

While some tree species adjust their physiology to changes in temperature (Reich et al., 2016), there is uncertainty surrounding the capacity for acclimation (Atkin & Tjoelker, 2003). Many studies have quantified physiological acclimation of photosynthesis and respiration to experimental warming (Aspinwall et al., 2016; Drake et al., 2016; Slot & Kitajima, 2015; Yamori, Hikosaka, & Way, 2014), but relatively few studies have quantified how experimental warming alters within-tree C dynamics associated with carbohydrate transport (Epron et al., 2012). That is, while previous studies have quantified physiological acclimation at the point of C uptake via photosynthesis and C release via respiration, the dynamics of internal carbohydrate transport that connect these end points of metabolism remains poorly studied. In the absence of a physiological change, warming is expected to increase carbohydrate transport and utilization, leading to a reduction in the concentrations and mean residence times of sugars throughout the trees.

Pulse-labeling with stable C isotopes has proven to be a valuable tool for understanding C dynamics as it allows labeled carbon dioxide (CO₂) to be traced throughout plants (reviewed in Epron *et al.* 2012). In particular, ¹³C-CO₂ pulse-chase experiments have been widely used to assess the temporal dynamics of labeled photoassimilates in trees growing in both natural (Kagawa, Sugimoto, & Maximov, 2006b) and perturbed conditions such as drought, increased temperature, and elevated CO₂ (Blessing, Werner, Siegwolf, & Buchmann, 2015; Hesse, Goisser, Hartmann, & Grams, 2018; Streit *et al.*, 2013). However, previous studies have often used potted saplings or small trees (Barthel *et al.*, 2011; Endrulat, Saurer, Buchmann, & Brunner, 2010; Vizoso *et al.*, 2008), and individual branches or the crown (Epron *et al.*, 2011; Kagawa, Sugimoto, & Maximov, 2006a; Plain *et al.*, 2009). Few ¹³C labeling experiments have been conducted on large whole-trees in the field (Epron *et al.*, 2015; Kuptz, Fleischmann, Matyssek, & Grams, 2011; Warren *et al.*, 2012). To our knowledge, only a single ¹³C labeling experiment has been combined with long-term warming and this work was conducted on potted saplings (Blessing *et al.*, 2015). Many aspects of tree morphology and physiology change as trees transition from small seedlings to large mature trees, including wood quantity, leaf mass fraction, and growth rates (Duursma & Falster, 2016; Poorter *et al.*, 2012). Thus, how rising temperatures may affect the dynamics of carbohydrate transport and metabolism in large field-grown trees deserves attention.

Furthermore, processes involving C vary spatially within a tree, seasonally throughout the year, and on timescales ranging from minutes to decades, and different sugars serve specialized functions and may differentially respond to environmental change. For example, while sucrose and raffinose function as the main transport sugars, glucose and fructose play a large role in metabolism and osmoregulation (reviewed in Hartmann & Trumbore 2016). The fate of the ¹³C label can be tracked in the C of individual sugars using compound-specific isotope analysis (Richter *et al.*, 2009). Thus, coupling compound-specific ¹³C analysis of individual sugars with pulse-labeling (Keel *et al.*, 2012;

Streit et al., 2013) allows higher resolution of whole-tree C dynamics as they together capture the diverse exchanges between older reserves and newly fixed ^{13}C -labeled photoassimilates,

We conducted a warming and *in situ* ^{13}C -CO₂ pulse-chase experiment on whole-trees (Fig. 1). Following pulse-labeling, leaves, phloem, and roots were collected for the measurement of sugar concentrations as well as the carbon isotope composition ($\delta^{13}\text{C}$) of sugars and bulk tissues using compound-specific isotope analysis. We hypothesized that warming would increase sink activity, resulting in reduced mean residence times and reduced concentrations of sugars across organs. Our results provide insight into the physiological and environmental controls on whole-tree C source-sink relations, which has implications for tree and ecosystem function under global change.

Materials and Methods

Study site

Our warming and ^{13}C -CO₂ pulse-chase experiment was conducted in a system of twelve whole-tree chambers (WTC) located in Richmond, New South Wales, Australia (33°36'40"S, 150°44'26.5"E). This site has a mean annual temperature of 17°C and mean annual precipitation of 720 mm. We selected six cylindrical chambers (~53 m³) for this study, each enclosing a single tree of the locally endemic woodland tree species *Eucalyptus parramattensis* (Parramatta red gum). The WTCs monitored and controlled environmental parameters such as air temperature, vapor pressure deficit, and atmosphere CO₂ concentration, and were subdivided with a suspended plastic floor sealed around the tree stem at 45-cm height to prevent the mixing of belowground and aboveground gas fluxes. The design and function of the WTCs has been previously described (Barton *et al.*, 2010; Drake *et al.*, 2016), including for this specific experiment with *E. parramattensis* (Drake *et al.*, 2019).

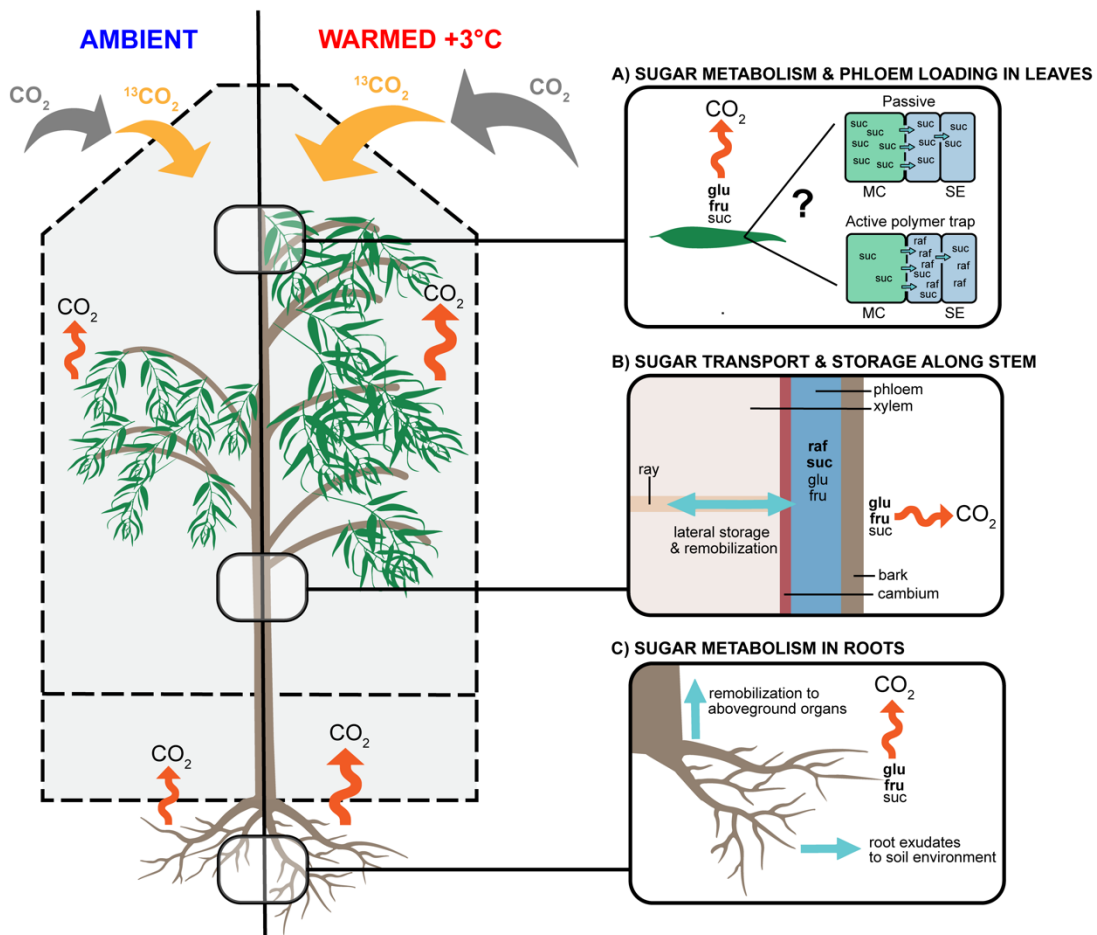


Figure 1 Comparison between *E. parramattensis* in whole-tree chambers growing under ambient and warmed (+3°C) treatments. Left: Trees grown in ambient conditions were smaller than those in warmed conditions and assimilated less ^{13}C -labeled CO_2 (yellow arrows). After the 4 h labeling period, unlabeled CO_2 (gray arrows) was taken up and began to dilute the labeled C pool. We hypothesized that warming would increase sink activity compared to ambient conditions (i.e. respiration; orange wavy arrows), resulting in reduced concentrations and reduced mean residence times of soluble sugars throughout trees. Right: Zoom-in overview of carbohydrate transport and utilization. A) At the leaf level, sugars are quickly exported or respired. Glucose and fructose function as metabolites, while sucrose and raffinose serve as transport sugars and are loaded into the phloem and shuttled throughout the tree. There are three phloem loading mechanisms, two symplastic strategies (shown) and one apoplastic strategy (not shown). B) Along the stem, sugars are used for biomass production, but they are also respired or stored. Older stem reserves are remobilized back into the phloem. Because the phloem is leaky, sugars are leaked out of and retrieved back into the phloem along the vertical long-distance transport pathway, leading to dilution of the ^{13}C label from the canopy to the roots. C) Once at the roots, sugars are used for biomass production, stored, respired, or exuded to the soil environment. Older reserves are remobilized and transported back up to aboveground organs. Abbreviations: glu=glucose, fru=fructose, suc=sucrose, raf=raffinose, MC=mesophyll cell, and SE=sieve element. Bolded sugars indicate dominant ones involved in the process depicted.

Warming and ^{13}C -CO₂ pulse-chase experiment

Potted seedlings that were germinated from seeds obtained from Harvest Seeds and Native Plants (Terry Hills, NSW, Australia) were placed into each WTC on October 28, 2015 and the experimental warming treatment was initiated. On December 23, 2015, one seedling was planted into the soil within each WTC. The long-term experimental warming treatment was previously described in Drake et al. (2018, 2019). In brief, WTCs were evenly divided between ambient and warmed treatments (n=6 trees per treatment). Ambient WTCs tracked relative humidity and air temperature of the study site, while warmed WTCs tracked ambient relative humidity and air temperature +3°C. An increase of 3°C is projected for Australia by 2100 (*Australian Bureau of Meteorology State of the Climate Report*, 2016; IPCC, 2014). Additionally, WTCs were irrigated every two weeks with half of the mean monthly rainfall measured over the past 30 years.

Nine months after the warming treatment was initiated, six of the twelve WTCs were chosen for isotopic labeling (n=3 for each treatment), and two additional WTCs were included as unlabeled controls. At the time of labeling, warmed trees (height 6.9 m \pm 0.2 SD) were larger than ambient trees (height 5.6 m \pm 0.5 SD). On the afternoon of August 5, 2016, the air intake and outlet of the WTCs were sealed to create a well-mixed closed volume and approximately 1 liter of 98% atom percent ^{13}C -CO₂ was injected twice into the aboveground division of each WTC. The $\delta^{13}\text{C}$ value of WTC air was monitored throughout the labeling event and the second injection resulted in isotopic compositions between +7,000 to +10,000 ‰. After four hours, the WTCs were vented with outside air.

Sampling

During the pulse-chase period, various organs were sampled for the measurement of sugar concentrations as well as the $\delta^{13}\text{C}$ of sugars and bulk tissues. Leaves were sampled 4, 17, 26, 49, and 438 hours after labeling, phloem was sampled 23, 47, and 167 hours after labeling, and roots were

sampled 22, 47, 164, 621 hours after labeling. Sampling times were chosen to best capture the expected fast turnover of recent photoassimilates in leaves compared to other organs (Epron et al., 2012). Samples were also collected from two unlabeled WTCs throughout the pulse-chase period, as well as from experimental WTCs prior to labeling, to represent the natural C isotope abundance under ambient and warmed conditions.

At each respective sampling time point, two sunlit leaves were collected from the upper one-third of the canopy. Phloem samples were collected at approximately 12:00. A 6 mm x 18 mm cut was initially made using a chisel 1 m from the ground and each subsequent phloem sample was collected in a zigzag pattern (approximately 4 cm over, 10 cm up). The bark was peeled off and discarded, and the chisel was washed with deionized water between trees. Fine roots (<2 mm diameter) were obtained using a hand trowel (0-15 cm depth) and washed with deionized water. All samples were stored at -80°C prior to being freeze-dried and ground for laboratory analyses.

In addition to the measurements that were collected during the pulse-chase period and presented herein (sugar concentrations and $\delta^{13}\text{C}$ of sugars and bulk tissues), we also chased the pulse in the respiration of leaves, whole-crowns, roots, and soil to quantify the respiratory partitioning of gross primary production and carbon use efficiency (Drake et al., 2019). The $\delta^{13}\text{C}$ values of leaf and root respiration during the pulse-labeling period were compared to the $\delta^{13}\text{C}$ values of leaf and root sucrose from similar sampling time points to show that sugars were the dominant substrate for respiration (Fig. S1; Methods S1). Beginning on November 23, 2016, the trees were fully harvested and total dry biomass was estimated.

Compound-specific and bulk measurement of $\delta^{13}\text{C}$ values, and sugar concentrations

To determine the $\delta^{13}\text{C}$ and concentration of soluble sugars (raffinose, sucrose, fructose, glucose), compound-specific isotope analysis was conducted on sugar extracts. Sugars were extracted

with 1.0 ml of deionized water per 30 mg of freeze-dried and ground plant material at 85°C for 30 min. After centrifugation, the supernatant was passed over two ion-exchange cartridges (OnGuard II H and OnGuard II A, 1cc cartridges; Dionex Corporation, Sunnyvale, CA, USA) to remove ionic compounds and the resulting neutral fraction was collected and analyzed for sugars. Compound-specific isotope signatures were measured using a high-performance liquid chromatography system linked to a Delta V Advantage IRMS via a LC IsoLink (both Thermo Electron, Vienna Austria). Sugars were separated on a Nucleogel Pb column (7.8 mm x 300 mm; Machery-Nagel, Germany) with 0.35 mL min⁻¹ ultrapure water as eluent at 80 °C. Sodium persulfate (0.5 M) and phosphoric acid (1.7 M) were used at flow rates of 0.05 ml min⁻¹ each for the online digestion of the sugars at 100 °C in the Isolink device. All samples were also analyzed for δ¹³C of bulk tissue by elemental analyzer-isotope ratio mass spectroscopy (EA-IRMS; Costech 4010 Elemental Analyzer, Thermo Finnigan Delta Plus XP, Bremen, Germany).

To assess the amount of ¹³C added by pulse-labeling, the δ¹³C of labeled samples was first converted to atom percent ¹³C:

$$AP = \frac{100}{\frac{1}{\left(\frac{\delta^{13}C}{1000} + 1\right) \times ARC} + 1} \quad \text{Eqn 1}$$

where AP is the isotopic composition in atom percent, $\delta^{13}C$ is the measured isotopic composition in per mil (‰), and ARC is the absolute ¹³C/¹²C ratio of Vienna PeeDee Belemnite (VPDB; 0.0111802). An identical set of samples was collected prior to labeling and the atom percent ¹³C values of unlabeled samples were subtracted from those of labeled samples to determine ¹³C excess:

$$^{13}C \text{ excess} = AP_{\text{labeled}} - AP_{\text{unlabeled}} \quad \text{Eqn 2}$$

Estimation of mean residence times based on an exponential decay function

Mean residence time (MRT) of C in individual sugars and bulk tissues was determined by an exponential decay function fitted to the ^{13}C excess data using the nls function in R:

$$N(t) = N_0 * e^{-\lambda t} \quad \text{Eqn 3}$$

where t is the time (in hours) after the peak in ^{13}C excess, N_0 is the peak amount of ^{13}C , and λ is the decay constant. We then calculated the MRT as $1/\lambda$. Curves were fitted by organ and sugar type for each tree after the maximum in ^{13}C excess had been reached. If less than three data points remained, then a curve was not fitted. Goodness of fit was assessed for each curve by comparing predicted values to measured values using Pearson's correlation, $\alpha = 0.05$ (all $r \geq 0.93$, $P \leq 0.03$).

Statistical analyses

Statistical analyses were performed in R version 3.3.2. Linear mixed-effects (lme) models were fit by maximum likelihood using the lme() function. These models contain fixed effects (specified in parentheses below), individual tree as a random effect, and an interaction term to account for tree biomass (biomass x treatment). General linear models were fit using the lm() function with one categorical factor (treatment) and also accounted for tree biomass. For significant models, differences between pairs of means were evaluated with Tukey's HSD, $\alpha = 0.05$.

To test for differences in sugar concentrations between trees growing in ambient versus warmed WTCs following pulse-labeling, we used a lme model to analyze sugar concentration among sampling times and treatments for each organ and sugar type (sampling time x treatment). Furthermore, to test for differences in the temporal dynamics of $\delta^{13}\text{C}$ between trees growing in ambient and warmed WTCs, we used a lme model to analyze $\delta^{13}\text{C}$ values among sampling times and treatments for each organ and sugar type or bulk tissue type (sampling time x treatment). To compare MRTs of C in individual sugars and bulk tissues between trees growing in ambient versus warmed

WTCs following pulse-labeling, we used a general linear model to analyze MRTs among treatments for each organ and sugar type (treatment x biomass).

Results

Concentrations of individual sugars

Warming did not alter sugar concentrations, as individual sugar concentrations in the leaves, phloem, and roots did not significantly differ between ambient and warmed treatments (Table 1; all $P \geq 0.14$). Averaged across treatments and sampling times following pulse-labeling, leaves had the

Table 1 Mean concentrations of sugars extracted from leaves, phloem, and roots of *E. parramattensis* growing under ambient and warmed treatments. Concentration is the mean \pm SE for three trees per treatment across sampling times following pulse-labeling in August 2016. In some cases, sugar concentrations from fewer than three trees were available for a given sampling time. No significant treatment effects were found in linear mixed-effects model testing (all $P \geq 0.14$).

Tissue	Compound	Ambient		Warmed	
		Conc (mg g ⁻¹)	SE	Conc (mg g ⁻¹)	SE
Leaves	sucrose	33.8	4.3	26.2	2.4
	glucose	5.9	0.4	4.4	0.3
	fructose	15.3	0.8	11.8	0.5
	raffinose	6.1	0.1	5.6	0.2
Phloem	sucrose	20.4	2.9	22.7	1.4
	glucose	1.9	0.9	0.9	0.2
	fructose	2.8	0.4	1.8	0.2
	raffinose	7.6	0.6	9.0	0.7
Roots	sucrose	10.3	1.5	11.0	1.8
	glucose	2.8	0.4	2.3	0.2
	fructose	8.1	1.5	4.8	0.5
	raffinose	1.5	0.1	1.5	0.2

highest total sugar concentrations (55 mg g⁻¹ \pm 3 SE) followed by phloem (33 mg g⁻¹ \pm 2 SE) and roots (21 mg g⁻¹ \pm 2 SE). Sucrose comprised the largest fraction of total sugar concentrations, accounting for approximately 53% (\pm 2 SE) in leaves, 65% (\pm 2 SE) in phloem, and 52% (\pm 3 SE) in roots. In the leaves and roots, fructose was the second largest fraction, accounting for nearly 30%. Interestingly, raffinose made up 26% (\pm 2 SE) of the sugars in the phloem but only 10% (\pm 0.5 SE) and 8% (\pm 0.6

SE) in leaves and roots, respectively. The presence of raffinose in the phloem suggests an active polymer trap mechanism for phloem loading in *E. parramattensis* (Fig. 1a).

Temporal dynamics of $\delta^{13}\text{C}$ throughout whole-trees

Overall, trees dynamically allocated ^{13}C -labeled sugars throughout the aboveground-belowground continuum. Following pulse-labeling, ^{13}C enrichment was highest in the individual sugars and bulk tissue of leaves and decreased when moving vertically down the tree from the leaves to the phloem to the roots. Across organs, peak $\delta^{13}\text{C}$ values were generally followed by an exponential decrease, but the time for depletion of the pools back to pre-labeling values increased when moving vertically down the tree. Importantly, the temporal dynamics of $\delta^{13}\text{C}$ did not significantly differ

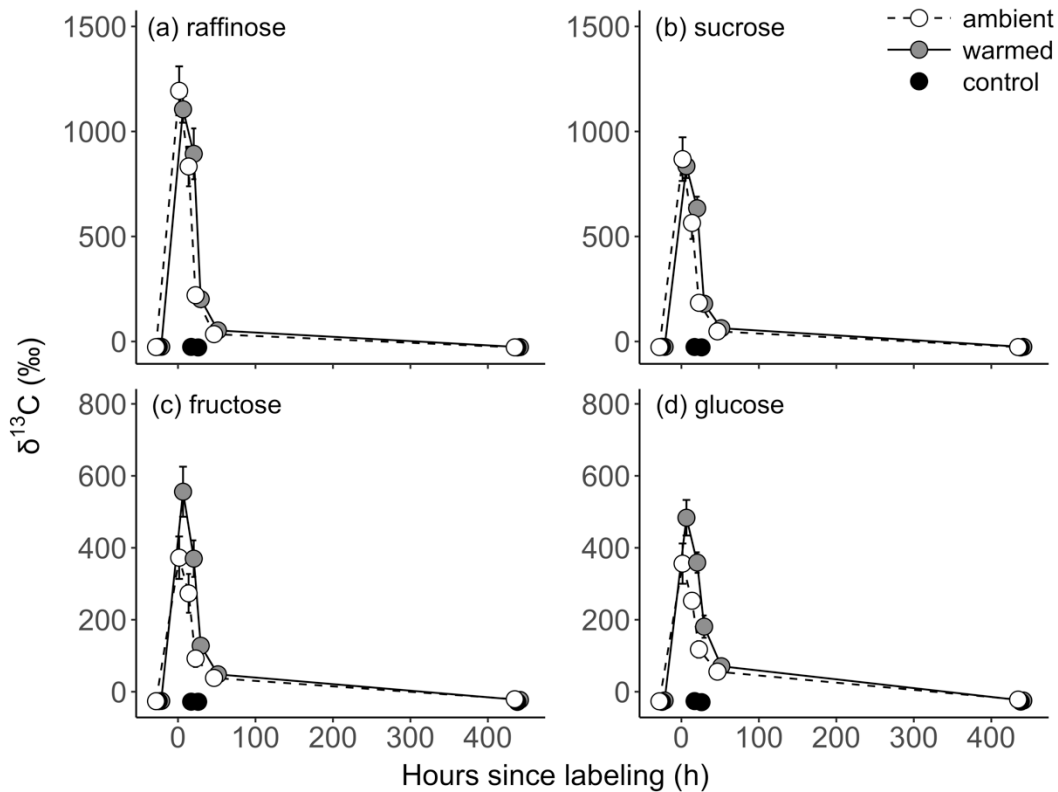


Figure 2 Temporal dynamics of the ^{13}C label in leaf (a) raffinose, (b) sucrose, (c) fructose, and (d) glucose for different treatments (ambient: white, warmed: gray, and control: black). Error bars denote \pm SE of the mean. Mean for three trees per treatment and two control trees at each sampling time. In some cases, the error is smaller than the size of the symbol. Note the difference in y-axis scale between plots.

between ambient and warmed treatments (all $P \geq 0.09$; Figs. 2-5).

At the canopy-level, $\delta^{13}\text{C}$ values of leaf sugars peaked in the first leaf sampling, which was 4 hours after pulse-labeling (Fig. 2). Raffinose ($1150 \text{ ‰} \pm 62 \text{ SE}$) and sucrose ($852 \text{ ‰} \pm 53 \text{ SE}$) were the most highly labeled sugars in the leaves, with $\delta^{13}\text{C}$ values that were nearly 2 times larger than that of fructose and glucose. In line with expected fast MRTs of C in leaf sugars, the ^{13}C label decreased rapidly and was already near natural abundance values 2 days post-labeling.

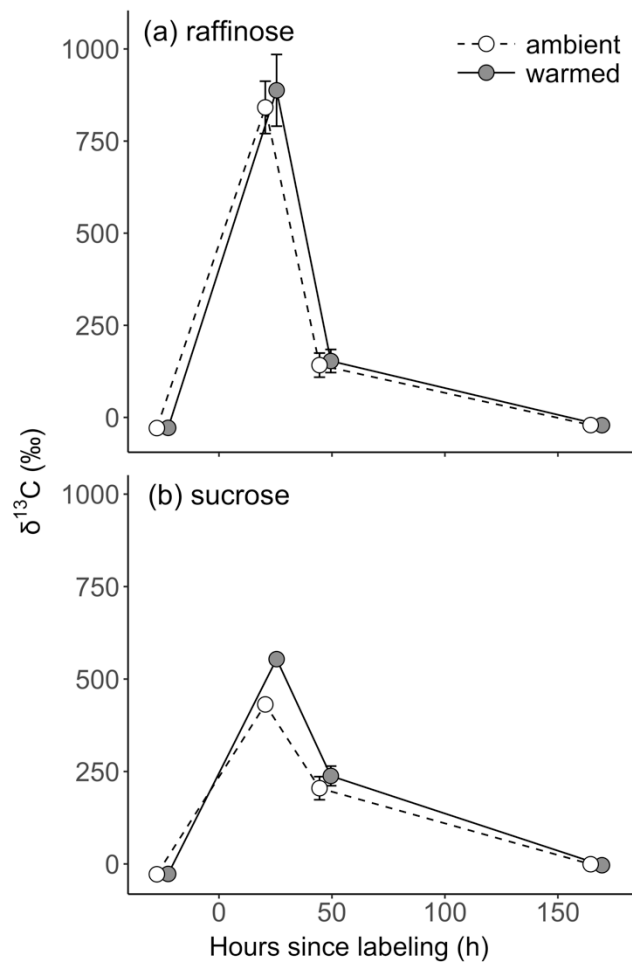


Figure 3 Temporal dynamics of the ^{13}C label in phloem (a) raffinose and (b) sucrose for different treatments (ambient: white, warmed: gray). Error bars denote \pm SE of the mean. Mean for three trees per treatment at each sampling time. In some cases, the error is smaller than the size of the symbol.

Similarly, $\delta^{13}\text{C}$ values of phloem sugars peaked in the first phloem sampling nearly 24 hours after pulse-labeling, but were generally lower than the values observed in the leaves (Fig. 3). In both

the leaves and the phloem, raffinose was the most highly labeled sugar. Phloem raffinose ($865 \text{ ‰} \pm 55 \text{ SE}$) was twice as enriched as sucrose ($493 \text{ ‰} \pm 28 \text{ SE}$). Whereas the ^{13}C label in sugars quickly decreased in the leaves, depletion back to natural abundance values was 3.5 times slower in the phloem.

In the roots, peak $\delta^{13}\text{C}$ values were also generally observed during the first root sampling, ranging between 22-47 hours, and $\delta^{13}\text{C}$ values were generally lower than the values observed in both the leaves and phloem (Fig. 4). Raffinose was also the most highly labeled sugar in the roots. While the maximum $\delta^{13}\text{C}$ of root raffinose ($926 \text{ ‰} \pm 86 \text{ SE}$) was in line with that observed in the leaves and phloem, enrichment of the other root sugars was substantially less than in aboveground organs. For example, the maximum $\delta^{13}\text{C}$ of sucrose decreased each time by approximately 50% when moving sequentially from the leaves to the phloem to the roots (Figs. 2b, 3b, 4b).

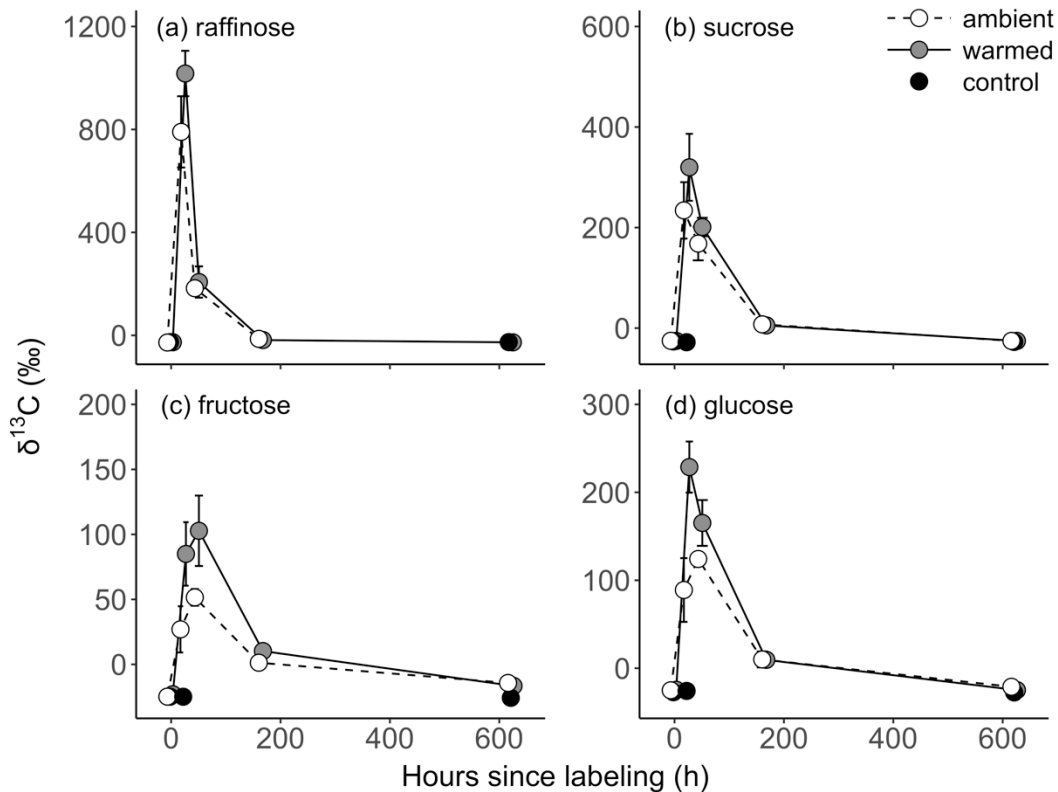


Figure 4 Temporal dynamics of the ^{13}C label in root (a) raffinose, (b) sucrose, (c) fructose, and (d) glucose for different treatments (ambient: white, warmed: gray, and control: black). Error bars denote \pm SE of the mean. Mean for three trees per treatment and two control trees at each sampling time. $\delta^{13}\text{C}$ values from fewer trees were available for certain sampling times and treatments in (a) and (d). In some cases, the error is smaller than the size of the symbol. Note the difference in y-axis scale between plots.

Despite higher enrichment of individual sugars than bulk tissues, our bulk tissue $\delta^{13}\text{C}$ results suggest that turnover rates in leaves were remarkably rapid compared to the phloem and roots, and newly fixed photoassimilates were contributing less to biomass synthesis in the leaves (Fig. 5). In agreement with leaf sugars, the ^{13}C label in bulk leaf tissue peaked 4 hours after pulse-labeling and quickly returned close to pre-labeling $\delta^{13}\text{C}$ values within 2 days. The $\delta^{13}\text{C}$ dynamics of bulk phloem and phloem sugars were also in agreement with each other. However, in both aboveground organs, a bit of remnant ^{13}C label was still present at the last sampling time point (Figs. 5a, 5b). In contrast, a substantial amount of ^{13}C label remained in the roots. While the ^{13}C label in root sugars depleted after 1 week, the ^{13}C label in bulk root tissue remained elevated for nearly 1 month, and did not begin to decrease within the timeframe of our study (Fig. 5c). Thus, we were unable to calculate MRTs for bulk root tissue.

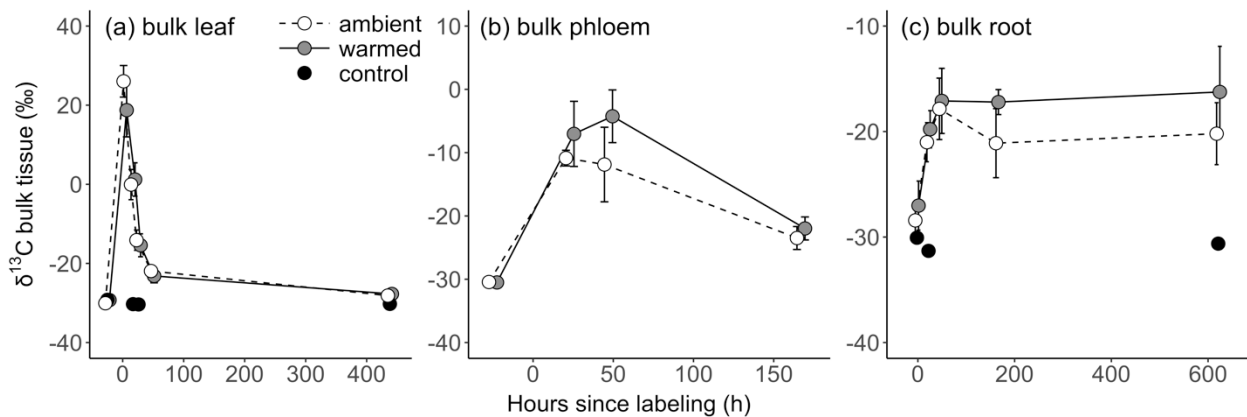


Figure 5 Temporal dynamics of the ^{13}C label in bulk tissue of (a) leaves, (b) phloem, and (c) roots for different treatments (ambient: white, warmed: gray, and control: black). Error bars denote \pm SE of the mean. Mean for three trees per treatment and two control trees at each sampling time. $\delta^{13}\text{C}$ values from two ambient trees and one control tree were available for the first sampling time in (c). In some cases, the error is smaller than the size of the symbol. Note the difference in y-axis scale between plots.

MRTs of C in individual sugars and bulk tissues

Following ^{13}C - CO_2 application, $\delta^{13}\text{C}$ values of sugars spiked and then declined exponentially, such that equation (3) could be used to estimate MRTs. Warming did not alter the speed of C dynamics, as the MRTs of C in individual sugars in the leaves, phloem, and roots did not significantly

differ between ambient and warmed treatments (Table 2; all $P \geq 0.37$). Averaged across treatments following pulse-labeling, sucrose and raffinose had the fastest MRTs for each organ. However, MRTs differed between organs. Our results generally showed increased MRTs of C in sugars moving from the canopy to the root system. For instance, the turnover rate of C in sucrose was faster in the leaves ($21 \text{ h} \pm 1 \text{ SE}$) than in the phloem ($35 \text{ h} \pm 4 \text{ SE}$) and roots ($65 \text{ h} \pm 8 \text{ SE}$).

Similarly, warming did not alter the MRT of C in bulk leaf tissue ($P = 0.46$; Table 2). Averaged across treatments following pulse-labeling, the MRT of newly fixed C in bulk leaf tissue was $20 \text{ h} (\pm 1 \text{ SE})$. This turnover rate was in line with rates for individual leaf sugars. For phloem and roots, there were not enough data points to fit curves, thus, MRTs of C in bulk phloem and root tissues could not be resolved. However, important differences in the temporal dynamics of the ^{13}C label in these bulk tissues were discussed in the previous section.

Table 2 Mean residence time (MRT) of C in different compounds/fractions of *E. parramattensis* growing under ambient and warmed treatments. MRT is the mean \pm SE of three trees per treatment following pulse-labeling in August 2016. MRTs were estimated by fitting an exponential decay function to the observed decline in atom percent ^{13}C excess after pulse-labeling. In some cases, MRTs could only be estimated for one or two trees due to less than three data points for curve fitting ((SE not applicable (NA)). No significant treatment effects were found (all $P \geq 0.37$).

Tissue	Compound	Ambient		Warmed	
		MRT (h)	SE	MRT (h)	SE
Leaves	sucrose	20	1	22	3
	glucose	28	2	29	4
	fructose	24	1	22	1
	raffinose	19	0	18	1
	<i>bulk</i>	19	2	22	1
Phloem	sucrose	37	7	32	5
	raffinose	15	1	15	1
Roots	sucrose	65	5	66	17
	glucose	88	6	81	5
	fructose	158	75	104	30
	raffinose	19	NA	18	2

Discussion

Experimental warming did not alter C dynamics

Warming was expected to increase carbohydrate transport and utilization, leading to a reduction in the concentrations and MRTs of sugars throughout the trees. However, we observed concentrations and MRTs of sugars that were not reduced under warming. These results suggest that 1) warming of +3°C was insufficient to stimulate phloem transport and carbohydrate utilization, 2) other resources (i.e. water, light, nutrients) limited stimulation, or 3) the trees physiologically adjusted to the 9-month long warming treatment. Previous warming experiments with other *Eucalyptus* species, including a previous experiment in these chambers, lend support for 3) due to their documented strong and nearly homeostatic acclimation of autotrophic respiration to warming (Aspinwall et al., 2016; Drake et al., 2015, 2016).

In this study, complementary measurements taken during the pulse-chase period also showed homeostatic respiratory acclimation of foliar and whole-crown respiration rates, and revealed that experimental warming had no impact on respiratory partitioning (Drake et al., 2019). This provides further support for our results which suggest that *E. parramattensis* was able to adjust its physiology to +3°C as indicated by similar C dynamics between ambient and warmed treatments. Despite the fact that carbon dynamics were not altered under experimental warming, our findings provide insight into the dynamic allocation of ¹³C-labeled sugars throughout large, field-grown trees.

Tracing ¹³C-labeled sugars throughout whole-trees

In general, pulse-labeling of whole-trees revealed that ¹³C enrichment decreased and MRTs increased moving from the leaves to the phloem to the roots. Trees in our study were taller than 5 m and it took ¹³C-labeled sugars approximately 22 hours to travel from the leaves to the roots, implying a transport velocity of $0.28 \pm 0.04 \text{ m h}^{-1}$ which is within the 0.20 to 0.82 m h^{-1} range previously reported

for Eucalypts (Epron et al., 2015). This velocity is likely an underestimate given that the ^{13}C label was detected in the roots at the first root sampling and its initial presence may have occurred earlier. However, a decrease in the ^{13}C label and increased MRTs when traveling from the canopy to the root system indicates dilution and mixing of ^{13}C -labeled sugars with older unlabeled reserves along the long-distance transport pathway (Furze et al., 2018).

In the leaves, pulse-labeling resulted in maximum $\delta^{13}\text{C}$ values of + 1150 ‰. Leaf sugars in our study represented newly fixed photoassimilates, and a fast decrease in $\delta^{13}\text{C}$ values for both leaf sugars and bulk tissue indicated that the sugars were rapidly exported from the leaves, used as substrates for respiration, and/or rapidly diluted by subsequent photoassimilates. In particular, sucrose and raffinose were the most highly labeled sugars and had the fastest turnover rates not only in the leaves, but also across all organs. In previous work, sucrose was identified as having the lowest dilution with older reserves (Streit et al., 2013), and our results suggest that both sucrose and raffinose had lower dilution with older reserves than other sugars, reflecting their role as transport sugars (Hartmann & Trumbore, 2016). In addition, high enrichment in these sugars likely reflects not only transport, but also storage in vacuoles.

Although the $\delta^{13}\text{C}$ of starch was not quantified in our study, if ^{13}C -labeled starch accumulated in the leaves and was subsequently hydrolyzed into sugars for distribution throughout the trees, these dynamics were accounted for in our $\delta^{13}\text{C}$ sugar measurements. While the remnant ^{13}C label present in bulk leaf tissue at the last sampling time point may represent starch storage or incorporation into leaf biomass, our results suggest that the majority of the ^{13}C -label was quickly exported or respired from the leaves in sugars. As previous labeling studies have indicated a close association between starch and sucrose based on similar MRTs for these compounds (Streit et al., 2013), any buildup of ^{13}C -labeled starch in the leaves would likely be transient in nature.

In contrast to aboveground organs, sugars in the root system were the least enriched and had the slowest turnover rates due to mixing with older reserves along the transport pathway. However, while the peak in $\delta^{13}\text{C}$ of root sugars returned to natural abundance after 1 week, the ^{13}C label remained in the bulk root tissue and did not deplete within the month-long timeframe of our study. Elevated and persistent $\delta^{13}\text{C}$ values in bulk root tissue may highlight starch's role as a long term storage compound in the root system compared to its more transient role in leaves (Barthel et al., 2011; Blessing et al., 2015; Smith & Stitt, 2007). Additionally, persistent enrichment in bulk root tissue may reflect the allocation of newly fixed photoassimilates to root biomass during the pulse-chase period.

Phloem loading strategy may influence C dynamics

The whole-tree distribution of photoassimilates discussed above begins in the leaves where sucrose is exported from photosynthetic mesophyll cells into the minor vein phloem. While the mechanism of phloem loading has only been characterized for a few plant species, most trees are thought to be passive loaders (Rennie & Turgeon, 2009; Savage et al., 2017). However, previous work provided evidence for an active polymer trap mechanism in *E. globulus* trees due to the presence of raffinose in phloem sap (Merchant et al., 2010); we also found this in our study species *E. parramattensis*. During polymer trapping, sucrose in the leaf mesophyll diffuses into specialized companion cells in the minor vein. There, sucrose is converted into larger oligosaccharides like raffinose and stachyose that cannot back diffuse, and thus, these compounds accumulate in the phloem.

The impact of environmental factors on phloem physiology, including phloem loading at the leaf-level and phloem physiology along the transport pathway, in field-grown trees is not well understood (Ayre, 2011; Van Bel, 2003; Xu, Chen, Ren, Chen, & Liesche, 2018), but loading strategy has potential implications for whole-tree C relations. Given that polymer trapping is an active phloem loading mechanism (Turgeon, 2010), we hypothesize that it may enable polymer trapping species to

have tighter regulation of C export at the leaf mesophyll-phloem interface, and in turn make C allocation less sensitive to changes in environmental factors like temperature, light, and CO₂. Additionally, because phloem loading strategy is known to be conserved at the family and sub-family levels (Gamalei, 1989; Turgeon, Medville, & Nixon, 2001), other Eucalypt species may follow suit and respond similarly to environmental perturbations. While our results provide evidence for this mechanism in *E. parramattensis*, future studies should couple the exposure of leaves to exogenous labeled sugars with spatially explicit isotope analysis (such as autoradiography or SIMS) to confirm phloem loading strategy (Rennie & Turgeon, 2009).

Conclusions

Combining long-term experimental warming along with ¹³C-CO₂ pulse-labeling and compound-specific isotope analysis to trace recently assimilated sugars from the leaves to the roots of large whole-trees in the field, provided insights into the C source-sink relations of *E. parramattensis*, but did not reveal an effect of temperature on these dynamics. While ¹³C-labeled sugars were dynamically allocated throughout the trees, less enrichment and slower MRTs belowground compared to aboveground organs indicated that the ¹³C-labeled sugars were diluted by older reserves as well as with distance from the source along the transport pathway. Further, the presence of raffinose in the phloem provided evidence for a polymer trap mechanism for phloem loading, which may contribute to Eucalypt species' ability to counter stressors associated with global change. Thus, our results improve our understanding of C dynamics at the whole-tree level, and, importantly, provide insight into the physiological and environmental controls on within-tree C relations.

Acknowledgements

This work was supported by the National Science Foundation's Inter-University Training for Continental Scale Ecology program (Grant No. 1137336), the National Science Foundation's Graduate Research Fellowship program (Grant No. DGE1144152), and the National Science Foundation's Graduate Research Opportunities Worldwide program. We thank Mark Tjoelker and Craig Barton for their coordination and maintenance of the WTC study as well as Angelica Vårhammer, Dushan Kumarathunge, and Anne Griebel for their help with sample collection. We also thank undergraduates Molly Wieringa and Elizabeth Rao for their help with data entry and sample preparation, Jessica Gersony and Missy Holbrook for their knowledge on phloem physiology, the Richardson laboratory for use of their laboratory space and equipment, and the University of Wyoming Stable Isotope Facility for conducting bulk stable isotope analysis. Additionally, MEF, JED, and EP thank the Hawkesbury Institute for the Environment's Research-in-Residence program and the University of Utah's IsoCamp for their generous support of this work. The WTC experiment was made possible through a collaboration with Sune Linder and the Swedish University of Agricultural Sciences, who designed, built, and provided the whole tree chambers. The WTC experiment was supported by the Australian Research Council (Discovery, DP140103415), a New South Wales government Climate Action Grant (NSW T07/CAG/016), the Hawkesbury Institute for the Environment, and Western Sydney University.

References

- Aspinwall MJ, Drake JE, Company C, Vårhammar A, Ghannoum O, Tissue DT, Reich PB, Tjoelker MG. 2016. Convergent acclimation of leaf photosynthesis and respiration to prevailing ambient temperatures under current and warmer climates in *Eucalyptus tereticornis*. *New Phytologist* 212: 354–367.
- Atkin OK, Tjoelker MG. 2003. Thermal acclimation and the dynamic response of plant respiration to temperature. *Trends in Plant Science* 8: 343–351.
- Australian Bureau of Meteorology State of the Climate Report. 2016.
- Ayre BG. 2011. Membrane-transport systems for sucrose in relation to whole-plant carbon partitioning. *Molecular Plant* 4: 377–394.
- Barthel M, Hammerle A, Sturm P, Baur T, Gentsch L, Knohl A. 2011. The diel imprint of leaf metabolism on the $\delta^{13}\text{C}$ signal of soil respiration under control and drought conditions. *New Phytologist* 192: 925–938.
- Barton CVM, Ellsworth DS, Medlyn BE, Duursma RA, Tissue DT, Adams MA, Eamus D, Conroy JP, McMurtrie RE, Parsby J, *et al.* 2010. Whole-tree chambers for elevated atmospheric CO_2 experimentation and tree scale flux measurements in south-eastern Australia: The Hawkesbury Forest Experiment. *Agricultural and Forest Meteorology* 150: 941–951.
- Van Bel AJE. 2003. The phloem, a miracle of ingenuity. *Plant, Cell & Environment* 26: 125–149.
- Blessing CH, Werner RA, Siegwolf R, Buchmann N. 2015. Allocation dynamics of recently fixed carbon in beech saplings in response to increased temperatures and drought. *Tree Physiology* 35: 585–598.
- Dannoura M, Maillard P, Fresneau C, Plain C, Berveiller D, Damesin C, Gerant D, Chipeaux C, Bosc A, Loustau D, *et al.* 2011. *In situ* assessment of the velocity of carbon transfer by tracing ^{13}C in trunk CO_2 efflux after pulse labelling: variations among tree species and seasons. *New Phytologist* 190: 181–192.

Drake JE, Aspinwall MJ, Pfautsch S, Rymer PD, Reich PB, Smith RA, Crous KY, Tissue DT, Ghannoum O, Tjoelker MG. 2015. The capacity to cope with climate warming declines from temperate to tropical latitudes in two widely distributed *Eucalyptus* species. *Global Change Biology* 21: 459–472.

Drake JE, Furze ME, Tjoelker M, Carillo Y, Barton C, Pendall E. 2019. Climate warming and tree carbon use efficiency in a whole-tree $^{13}\text{CO}_2$ tracer study. *New Phytologist*.

Drake JE, Tjoelker MG, Aspinwall MJ, Reich PB, Barton CVM, Medlyn BE, Duursma RA. 2016. Does physiological acclimation to climate warming stabilize the ratio of canopy respiration to photosynthesis? *New Phytologist* 211: 850–863.

Drake JE, Tjoelker MG, Vårhammar A, Medlyn BE, Reich PB, Leigh A, Pfautsch S, Blackman CJ, López R, Aspinwall MJ, *et al.* 2018. Trees tolerate an extreme heatwave via sustained transpirational cooling and increased leaf thermal tolerance. *Global Change Biology* 24: 2390–2402.

Duursma RA, Falster DS. 2016. Leaf mass per area, not total leaf area, drives differences in above-ground biomass distribution among woody plant functional types. *New Phytologist* 212: 368–376.

Endrulat T, Saurer M, Buchmann N, Brunner I. 2010. Incorporation and remobilization of ^{13}C within the fine-root systems of individual *Abies alba* trees in a temperate coniferous stand. *Tree Physiology* 30: 1515–1527.

Epron D, Bahn M, Derrien D, Lattanzi FA, Pumpanen J, Gessler A, Högberg P, Maillard P, Dannoura M, Gérard D, *et al.* 2012. Pulse-labelling trees to study carbon allocation dynamics: a review of methods, current knowledge and future prospects. *Tree Physiology* 32: 776–798.

Epron D, Cabral OMR, Laclau JP, Dannoura M, Packer AP, Plain C, Battie-Laclau P, Moreira MZ, Trivelin PCO, Bouillet JP, *et al.* 2015. *In situ* $^{13}\text{CO}_2$ pulse labelling of field-grown eucalypt trees revealed the effects of potassium nutrition and throughfall exclusion on phloem transport of photosynthetic carbon. *Tree Physiology* 36: 6–21.

Epron D, Ngao J, Dannoura M, Bakker MR, Zeller B, Bazot S, Bosc A, Plain C, Lata JC, Priault P, *et al.* 2011. Seasonal variations of belowground carbon transfer assessed by *in situ* $^{13}\text{CO}_2$ pulse labelling of trees. *Biogeosciences* 8: 1153–1168.

Furze ME, Trumbore S, Hartmann H. 2018. Detours on the phloem sugar highway: stem carbon storage and remobilization. *Current Opinion in Plant Biology* 43: 89–95.

- Gamalei Y. 1989. Structure and function of leaf minor veins in trees and herbs. *Trees* 3: 96–110.
- Hartmann H, Trumbore S. 2016. Understanding the roles of nonstructural carbohydrates in forest trees—from what we can measure to what we want to know. *New Phytologist* 211: 386–403.
- Hesse BD, Goisser M, Hartmann H, Grams TEE. 2018. Repeated summer drought delays sugar export from the leaf and impairs phloem transport in mature beech. *Tree Physiology* 39:192–200.
- IPCC. 2014. *Climate Change 2014: Synthesis Report*. Geneva, Switzerland:IPCC.
- Kagawa A, Sugimoto A, Maximov TC. 2006a. Seasonal course of translocation, storage and remobilization of ^{13}C pulse-labeled photoassimilate in naturally growing *Larix gmelinii* saplings. *New Phytologist* 171: 793–804.
- Kagawa A, Sugimoto A, Maximov TC. 2006b. $^{13}\text{CO}_2$ pulse-labelling of photoassimilates reveals carbon allocation within and between tree rings. *Plant, Cell & Environment* 29: 1571–1584.
- Keel SG, Campbell CD, Högberg MN, Richter A, Wild B, Zhou X, Hurry V, Linder S, Näsholm T, Högberg P. 2012. Allocation of carbon to fine root compounds and their residence times in a boreal forest depend on root size class and season. *New Phytologist* 194: 972–981.
- Knoblauch M, Knoblauch J, Mullendore DL, Savage JA, Babst BA, Beecher SD, Dodgen AC, Jensen KH, Holbrook NM. 2016. Testing the Münch hypothesis of long distance phloem transport in plants. *eLife* 5: e15341.
- Kozłowski TT. 1992. Carbohydrate sources and sinks in woody plants. *Botanical Review* 58: 107–222.
- Kuptz D, Fleischmann F, Matyssek R, Grams TEE. 2011. Seasonal patterns of carbon allocation to respiratory pools in 60-yr-old deciduous (*Fagus sylvatica*) and evergreen (*Picea abies*) trees assessed via whole-tree stable carbon isotope labeling. *New Phytologist* 191: 160–172.
- Merchant A, Peuke AD, Keitel C, MacFarlane C, Warren CR, Adams MA. 2010. Phloem sap and leaf $\delta^{13}\text{C}$, carbohydrates, and amino acid concentrations in *Eucalyptus globulus* change systematically according to flooding and water deficit treatment. *Journal of Experimental Botany* 61: 1785–1793.
- Münch E. 1930. *Die Stoffbewegungen in der Pflanze*. Jena, Germany: Gustav Fischer Verlagsbücher.

Plain C, Gerant D, Maillard P, Dannoura M, Dong Y, Zeller B, Priault P, Parent F, Epron D. 2009. Tracing of recently assimilated carbon in respiration at high temporal resolution in the field with a tuneable diode laser absorption spectrometer after *in situ* $^{13}\text{CO}_2$ pulse labelling of 20-year-old beech trees. *Tree Physiology* 29: 1433–1445.

Poorter H, Niklas KJ, Reich PB, Oleksyn J, Poot P, Mommer L. 2012. Biomass allocation to leaves, stems and roots : meta-analyses of interspecific variation and environmental control. *New Phytologist* 193: 30–50.

Reich PB, Sendall KM, Stefanski A, Wei X, Rich RL, Montgomery RA. 2016. Boreal and temperate trees show strong acclimation of respiration to warming. *Nature* 531: 633–636.

Rennie EA, Turgeon R. 2009. A comprehensive picture of phloem loading strategies. *Proceedings of the National Academy of Sciences* 106: 14162–14167.

Richter A, Wanek W, Werner RA, Ghashghaie J, Gessler A, Brugnoli E, Hettmann E, Go SG, Søe A, Salmon Y, *et al.* 2009. Preparation of starch and soluble sugars of plant material for the analysis of carbon isotope composition : a comparison of methods. *Rapid Communications in Mass Spectrometry* 23: 2476–2488.

Savage JA, Beecher SD, Clerx L, Gersony JT, Knoblauch J, Losada JM, Jensen KH, Knoblauch M, Holbrook NM. 2017. Maintenance of carbohydrate transport in tall trees. *Nature Plants* 3: 965–972.

Slot M, Kitajima K. 2015. General patterns of acclimation of leaf respiration to elevated temperatures across biomes and plant types. *Oecologia* 177: 885–900.

Smith AM, Stitt M. 2007. Coordination of carbon supply and plant growth. *Plant, Cell & Environment* 30: 1126–49.

Streit K, Rinne KT, Hagedorn F, Dawes MA, Saurer M, Hoch G, Werner RA, Buchmann N, Siegwolf RTW. 2013. Tracing fresh assimilates through *Larix decidua* exposed to elevated CO_2 and soil warming at the alpine treeline using compound-specific stable isotope analysis. *New Phytologist* 197: 838–849.

Turgeon R. 2010. The role of phloem loading reconsidered. *Plant Physiology* 152: 1817–1823.

Turgeon R, Medville R, Nixon K. 2001. The evolution of minor vein phloem and phloem loading. *American Journal of Botany* 88: 1331–1339.

Vizoso S, Gerant D, Guehl JM, Joffre R, Charlot M, Gross P, Maillard P. 2008. Do elevation of CO₂ concentration and nitrogen fertilization after storage and remobilization of carbon and nitrogen in pedunculate oak saplings? *Tree Physiology* 28: 1729–1739.

Warren JM, Iversen CM, Garten CT, Norby RJ, Childs J, Brice D, Evans RM, Gu L, Thornton P, Weston DJ. 2012. Timing and magnitude of C partitioning through a young loblolly pine (*Pinus taeda* L.) stand using ¹³C labeling and shade treatments. *Tree Physiology* 32: 799–813.

Xu Q, Chen S, Ren Y, Chen S, Liesche J. 2018. Regulation of sucrose transporters and phloem loading in response to environmental cues. *Plant Physiology* 176: 930–945.

Yamori W, Hikosaka K, Way DA. 2014. Temperature response of photosynthesis in C₃, C₄, and CAM plants: temperature acclimation and temperature adaptation. *Photosynthesis Research* 119: 101–117.

Supplementary Materials for Chapter 3

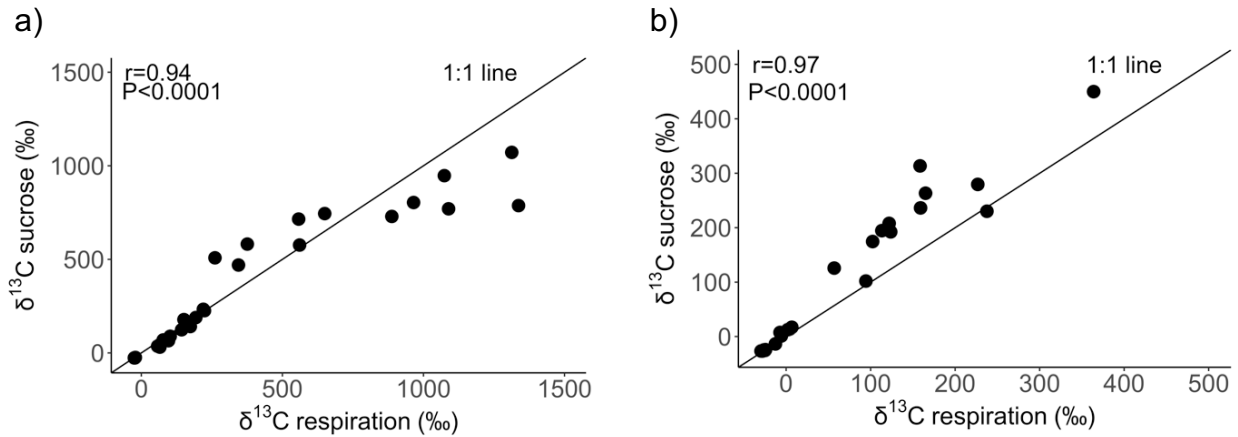


Figure S1 Comparison of $\delta^{13}\text{C}$ of respiration and $\delta^{13}\text{C}$ of sucrose in a) leaves and b) roots. Strength of association was evaluated using Pearson's correlation, $\alpha=0.05$. See Methods S1.

Methods S1 Measurement of $\delta^{13}\text{C}$ of respiration in leaves and roots

$\delta^{13}\text{C}$ of leaf and root respiration were measured throughout the pulse-chase period. At each sampling, we collected two leaves per tree and placed them in Tedlar bags. The bags were flushed with CO_2 -free air containing N_2 and O_2 at atmospheric concentrations three times and then filled with 240 mL of CO_2 -free air. The bags were incubated for 30 minutes inside insulated containers placed within each WTC, and then sampled by an isotopic laser (G2101-i Picarro).

Fine root samples (<2 mm diameter) were sampled by crawling under the plastic subfloor and excavating them from the surface soils (0-15 cm depth) using a hand trowel. Fine roots were washed with water, blotted dry, and incubated in Tedlar bags flushed with CO_2 -free air. However, the fine roots were incubated at laboratory temperatures ($\sim 25^\circ\text{C}$) for several hours before the CO_2 concentrations were high enough to measure accurately on the G2101-i Picarro.

Leaves were sampled 4, 17, 26, 49, and 438 hours after labeling and roots were sampled 22, 47, 164, 621 hours after labeling. At these time points, the $\delta^{13}\text{C}$ of sugars was measured. However, the $\delta^{13}\text{C}$ of respiration was not always quantified at the same time. Thus, to compare isotopic compositions in Figure S1, we paired measurements of the $\delta^{13}\text{C}$ of respiration and $\delta^{13}\text{C}$ of sucrose

that were taken at or near the same sampling time. We chose sucrose as a representative of soluble sugars because it accounted for more than 50% of the sugar pool in each organ and had a complete $\delta^{13}\text{C}$ dataset.

For example, the $\delta^{13}\text{C}$ of leaf sucrose was measured 17 hours after labeling and the $\delta^{13}\text{C}$ of leaf respiration was measured 15 hours after labeling, so these measurements were paired. In Fig. S1a, $\delta^{13}\text{C}$ values in the leaves deviate from the 1:1 line at high values. This deviation may reflect contributions by an enriched sugar pool other than sucrose (i.e. glucose) to the respiration efflux, and/or the offset between when $\delta^{13}\text{C}$ of leaf sucrose were measured compared to $\delta^{13}\text{C}$ of leaf respiration as mentioned above.

4

Seasonal patterns of nonstructural carbohydrate reserves in four woody boreal species

Reprinted from:

Furze, ME, Jensen, AM, Warren, JM, Richardson, AD. 2018. Seasonal patterns of nonstructural carbohydrate reserves in four woody boreal species. *The Journal of the Torrey Botanical Society* 145:332-339.

Article and supplement available at <https://doi.org/10.3159/TORREY-D-18-00007.1>

Related publication:

Richardson, AD, Hufkens, K, Milliman, T., Aubrecht, DM, **Furze, ME**, Seyednasrollah, B, Krassovski, MB, Latimer, JM, Nettles, WR, Heiderman, RR, Warren, JM, Hanson, PJ. 2018. Ecosystem warming extends vegetation activity but heightens vulnerability to cold temperatures. *Nature* 560: 368-371.

Seasonal patterns of nonstructural carbohydrate reserves in four woody boreal species¹

Morgan E. Furze²

Department of Organismic and Evolutionary Biology, Harvard University, 26 Oxford Street, Cambridge, MA 02138

Anna M. Jensen

Environmental Sciences Division, Oak Ridge National Laboratory, Oak Ridge, TN 37831

Jeffrey M. Warren

Environmental Sciences Division, Oak Ridge National Laboratory, Oak Ridge, TN 37831

Andrew D. Richardson

Center for Ecosystem Science and Society, Northern Arizona University, Flagstaff, AZ 86011
School of Informatics, Computing, and Cyber Systems, Northern Arizona University, Flagstaff, AZ 86011

Abstract. Plants store nonstructural carbohydrates (NSCs), such as sugars and starch, to use as carbon and energy sources for daily maintenance and growth needs as well as during times of stress. Allocation of NSCs to storage provides an important physiological strategy associated with future growth and survival, and thus understanding the seasonal patterns of NSC reserves provides insight into how species with different traits (*e.g.*, growth form, leaf habit, wood anatomy) may respond to stress. We characterized the seasonal patterns of NSCs in four woody boreal plant species in Minnesota, USA. Sugar and starch concentrations were measured across the year in the roots and branches of two conifer trees, black spruce (*Picea mariana* (Mill.) B.S.P.) and eastern tamarack (*Larix laricina* (Du Roi) K. Koch), as well as in the leaves and branches of two evergreen broadleaf shrubs, bog Labrador tea (*Rhododendron groenlandicum* (Oeder) Kron & Judd) and leatherleaf (*Chamaedaphne calyculata* (L.) Moench). In general, seasonal variation was dominated by changes in starch across all organs and species. While similar seasonal patterns of NSCs were observed in the shrubs, different seasonal patterns were observed between the trees, particularly in the roots. Our results suggest that species-specific traits likely have consequences for organ-level storage dynamics, which may influence whole-plant growth and survival under global change.

Key words: boreal, carbohydrates, carbon allocation, NSC, SPRUCE

Woody plants can allocate products of photosynthesis to storage in the form of nonstructural carbohydrates (NSCs) (Chapin *et al.* 1990, Hartmann and Trumbore 2016). NSCs, consisting primarily of sugars and starch, are stored throughout the plant, for example, in the ray parenchyma cells of branches, stems, and roots. These reserves can then serve as carbon sources for metabolic processes, such as growth and respiration, as well as for times of stress, such as drought (Sevanto *et*

al. 2014) and disturbance (Carbone *et al.* 2013). Thus, an understanding of the seasonal changes in the amount of stored NSCs and how these reserves are distributed throughout the plant may provide insight into species' responses to stress associated with global change.

In boreal ecosystems, long-lived woody plants often accumulate NSCs during the summer to support maintenance processes during the winter. However, the demands of several months can be

Present address: Department of Forestry and Wood Technology, Linnaeus University, Växjö, Sweden

¹ This material is based on work supported by the US Department of Energy, Office of Science, Office of Biological and Environmental Research. Oak Ridge National Laboratory is managed by UT-Battelle, LLC, for the US Department of Energy under contract DE-AC05-00OR22725. Additional support was provided by the National Science Foundation Graduate Research Fellowship under grant number DGE1144152. A special thank-you is extended to the OEB210 teaching staff and students who provided their feedback and support throughout the paper-writing process.

² Author for correspondence: mfurze@fas.harvard.edu
doi: 10.3159/TORREY-D-18-00007.1

©Copyright 2018 by The Torrey Botanical Society

Received for publication Jan 17, 2018; and in revised form May 22, 2018; first published November 6, 2018.

satisfied by a single day's carbon gain in some cold-dwelling species (Körner 1998). Our current knowledge of allocation and storage processes in the boreal zone comes largely from shrub species (Reader 1978, Landhäusser and Liefers 1997, Zasada *et al.* 1994), with less work focusing on mature trees (Landhäusser and Liefers 2003; Klöseiko *et al.* 2006). Findings from boreal plant species (Whitney 1982, Zasada *et al.* 1994, Landhäusser and Liefers 1997) indicate dynamic root reserves, with concentrations often peaking between late summer and the dormant season. But we still lack an understanding of how storage differs throughout the year between boreal species and whether the same seasonal patterns hold in both below- and aboveground organs.

To establish seasonal patterns of NSCs and improve our understanding of storage processes in woody boreal species, we studied the mature conifer trees, the evergreen *Picea mariana* (Mill.) B.S.P. (black spruce) and the deciduous *Larix laricina* (Du Roi) K. Koch (eastern tamarack), as well as the evergreen broadleaf shrubs *Rhododendron groenlandicum* (Oeder) Kron & Judd (bog Labrador tea) and *Chamaedaphne calyculata* (L.) Moench (leatherleaf) in the Marcell Experimental Forest (Minnesota, USA). We selected samples that were collected at four time points in 2013 and then measured the concentrations of sugars and starch in roots and branches in the tree species and leaves and branches in the shrub species.

We addressed two questions. First, do NSC concentrations change throughout the year? Second, are the seasonal patterns different for each species? We hypothesized that (a) total NSCs will vary throughout the year with different seasonal patterns for sugars and starch; (b) seasonal dynamics of NSCs will be similar between the two evergreen shrub species but dissimilar between the two trees, which have different leaf habits; and (c) maximum total NSC accumulation will occur in the early summer for the evergreen species and in the fall for the deciduous species. Our results provide insight into how boreal species distribute NSCs to various organs throughout the year, which may have implications for whole-plant growth and survival in the context of global change.

Materials and Methods. STUDY SITE AND SPECIES. We obtained samples from an 8.1-ha *Picea-Sphagnum* ombrotrophic bog (S1 bog)

(47°30.5'N, 93°27.2'W) within the Marcell Experimental Forest about 40 km north of Grand Rapids, MN, USA. The mean annual temperature is 3.3 °C, and mean annual precipitation is 780 mm, with two-thirds falling as rain in the summer and one-third falling as snow in the winter. The S1 bog is an acidic and nutrient-deficient peatland. Its surface has a hummock-hollow microtopography with a layer of various *Sphagnum* moss species (Kolka *et al.* 2011). Following silvicultural strip cuts in 1969 and 1974, the S1 bog naturally regenerated a mixed-age forest dominated by black spruce, eastern tamarack, bog Labrador tea, and leatherleaf. Both black spruce and eastern tamarack are conifers; the former is evergreen, and the latter is deciduous. While the shrubs are evergreen, leaves persist for only two growing seasons; they usually last throughout the first winter but drop during the summer and autumn of the second year (Lems 1956, Tendland *et al.* 2012).

FIELD COLLECTION. For black spruce and eastern tamarack, coarse roots with developed secondary xylem as well as multiyear (1–2 yr) woody branch samples were collected from mature trees approximately 5–8 m tall. For bog Labrador tea and leatherleaf, current-year leaves (2013) and multi-year (1–2 yr) woody branch samples were collected. Branch samples included phloem for NSC analyses. We selected our samples from organs that were previously collected for a different purpose during 2013 field campaigns at the Marcell Experimental Forest. Thus, the individual plants used in this study may vary from month to month for each species (Table S1).

LABORATORY PREPARATIONS AND NONSTRUCTURAL CARBOHYDRATE ANALYSIS. Samples were micro-waved for 90 sec (full effect) to stop enzymatic activity, oven-dried at 70 °C, and homogenized to a fine powder (SPEX SamplePrep 1600 MiniG, Metuchen, NJ). To measure sugar and starch concentrations (adapted from Chow and Landhäusser 2004), 10 mg of freeze-dried tissue (FreeZone 2.5, Labconco, Kansas City, MO; Hybrid Vacuum Pump, Vacuubrand, Wertheim, Germany) was extracted with 80% ethanol followed by colorimetric analysis with phenol-sulfuric acid to determine bulk sugar concentrations. The resulting bulk sugar extract was read at 490 nm with a microplate reader (Epoch Microplate Spectrophotometer, Bio-Tek Instruments, Winooski, VT). Bulk sugar concentrations (ex-

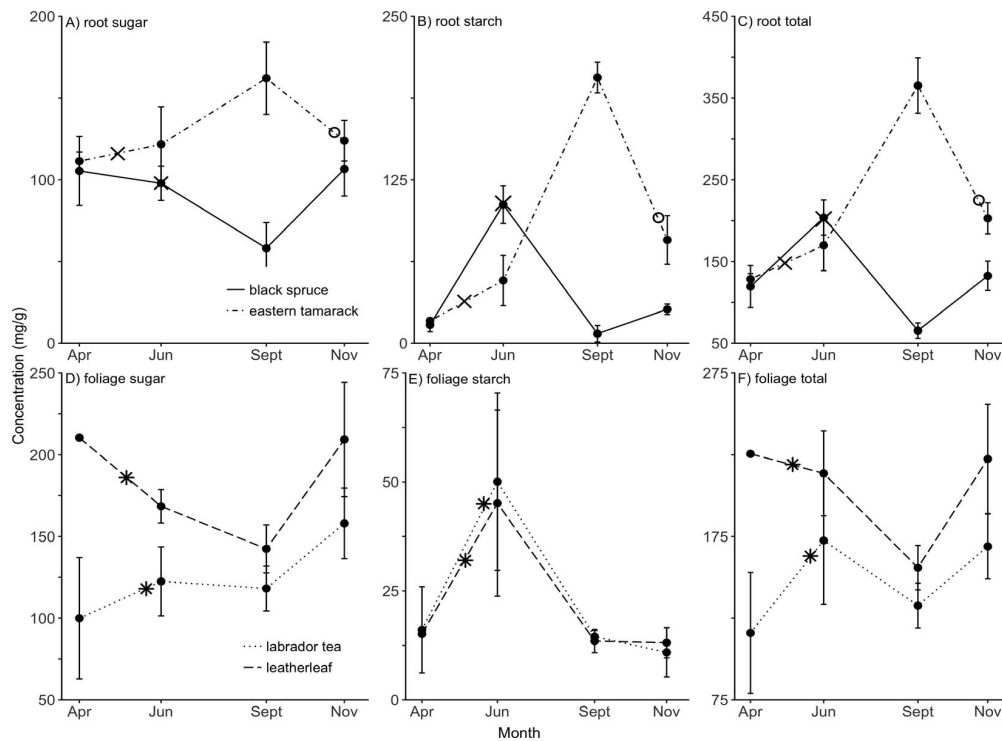


FIG. 1. Seasonal dynamics of sugar (left column), starch (center column), and total NSC (right column) concentrations in roots from black spruce and eastern tamarack (top row, A–C) and in leaves from bog Labrador tea and leatherleaf (bottom row, D–F) sampled at the Marcell Experimental Forest in 2013. Symbols mark the start of the following phenological events: leaf out (X), flowering (asterisk), leaf fall (open circle). Error bars denote ± 1 SE of the mean. In some cases, the error is smaller than the size of the symbol.

pressed as mg sugar per g dry wood) were calculated from a 1:1:1 glucose:fructose:galactose (Sigma Chemicals, St. Louis, MO) standard curve.

The remaining tissue residue was solubilized and then digested with an α -amylase/amyloglucosidase digestive enzyme solution to determine starch concentrations. Glucose hydrolysate was determined using a PGO-color reagent solution (Sigma Chemicals) and read at 525 nm with the microplate reader. Starch concentrations (expressed as mg starch per g dry wood) were calculated based on a glucose (Sigma Chemicals) standard curve. Uncertainty of NSC measurements is addressed in Methods S1.

Data from this project are available for download and public use (Furze *et al.* 2018). In Figs. 1 and 2, sampling months April, June, September, and November correspond to day of year (DOY) 103, 169, 254, and 317, respectively. Phenological

events in 2013 were also recorded, and the onset of each event is denoted by a unique symbol in Figs. 1 and 2 to show their timing in relation to observed NSC dynamics: black spruce leaf out DOY 169–176; eastern tamarack leaf out DOY 134, leaf off DOY 309; bog Labrador tea flowering DOY 157; and leatherleaf flowering DOY 141–148.

STATISTICAL ANALYSIS. To compare NSC storage between the two tree species, we used a two-way analysis of variance (ANOVA) to individually analyze sugar, starch, and total NSC (sum of sugars and starch) concentrations in roots among sampling months and species. Root diameter was not included as a covariate in our analyses based on its weak association with NSC concentrations (Fig. S1). For the two shrub species whose extremely fine root systems are unlikely to provide much NSC storage, the same analyses were

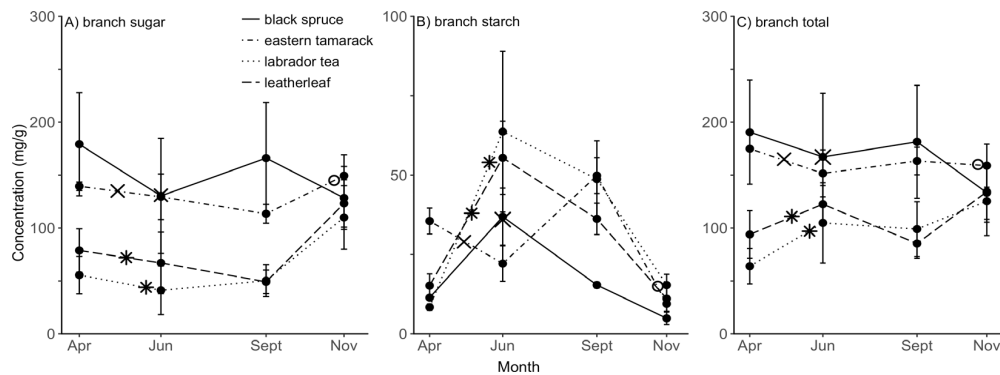


FIG. 2. Seasonal dynamics of (A) sugar, (B) starch, and (C) total NSC concentrations in branches from black spruce, eastern tamarack, bog Labrador tea, and leatherleaf sampled at the Marcell Experimental Forest in 2013. Symbols mark the start of the following phenological events: leaf out (X), flowering (asterisk), leaf fall (open circle). Error bars denote ± 1 SE of the mean. In some cases, the error is smaller than the size of the symbol.

conducted but using the NSC concentrations in leaves instead of roots.

To compare NSC storage between the four species, we used a two-way ANOVA to individually analyze sugar, starch, and total NSC concentrations in branches among sampling months and species. Woody branch samples were the common organ collected across both trees and shrubs. This study precludes a repeated measures approach, and ANOVA results are presented in Table 1. For significant ANOVAs, differences between pairs of means were evaluated using Tukey's HSD, $\alpha = 0.05$. For significant interaction effects (month \times species), concentrations in individual organs were assessed across sampling months for each species (Table S2).

Results. Overall, sugar and total NSC concentrations did not significantly vary throughout the year in tree roots, shrub leaves, or the branches of trees and shrubs, whereas starch concentrations were seasonally dynamic for all.

SEASONAL PATTERNS OF NSC RESERVES IN TREES: BLACK SPRUCE AND EASTERN TAMARACK. Starch but not sugar concentrations in the roots significantly varied throughout the year and differed between black spruce and eastern tamarack (Fig. 1A, B). Variation in root sugar concentrations was not well explained by either factor ($F_{7,57} = 0.78$, $R^2 = 0.09$, $P = 0.61$; month, $P = 0.99$; species, $P = 0.09$; Table 1A). Sampling month explained much of the variation in root starch concentrations ($F_{7,57} = 6.48$, $R^2 = 0.44$, $P < 0.0001$; month, $P < 0.01$; species, $P = 0.049$; Table 1A). However, the effect of sampling month on starch concentrations depended on species (interaction $P < 0.0001$; Table 1A). In general, concentrations of starch in the roots were higher in eastern tamarack than black spruce and peaked later in September as opposed to June for each species, respectively (Table S2). When eastern tamarack's root starch concentrations peaked in September, they were 28 times greater than black spruce's at the same time, as well as two times greater than black spruce's

Table 1. Results of analysis of variance testing for main effects of sampling month, species, and their interaction on sugar, starch, and total concentrations for roots from two tree species, leaves from two shrub species, and branches from all four species. P value is the level of statistical significance based on an F test, with bold type indicating results significant at $P \leq 0.05$.

	Tree roots			Shrub leaves			Tree and shrub branches		
	Sugar	Starch	Total	Sugar	Starch	Total	Sugar	Starch	Total
Month	0.99	< 0.01	0.20	0.21	0.01	0.30	0.34	< 0.0001	0.96
Species	0.09	0.049	0.01	0.02	0.80	0.03	< 0.001	0.048	< 0.01
Interaction	0.50	< 0.0001	< 0.001	0.80	0.99	0.83	0.71	< 0.01	0.75

peak in June (Fig. 1B). Additionally, total NSC concentrations in the roots differed between tree species ($P = 0.01$) but were not seasonally dynamic ($P = 0.20$; Table 1A).

SEASONAL PATTERNS OF NSC RESERVES IN SHRUBS: BOG LABRADOR TEA AND LEATHERLEAF. Starch but not sugar concentrations in the leaves varied throughout the year, and the seasonal dynamics were similar for bog Labrador tea and leatherleaf (Fig. 1D, E). Sampling month and species explained some of the variation in sugar ($F_{7,31} = 1.76$, $R^2 = 0.28$, $P = 0.13$; month, $P = 0.21$; species, $P = 0.02$) and starch concentrations ($F_{7,31} = 1.88$, $R^2 = 0.30$, $P = 0.11$; month, $P = 0.01$; species, $P = 0.80$; Table 1B). There was a general trend of increasing sugar concentrations from September to November (Fig. 1D), while starch concentrations peaked in June and declined onward (Tukey's HSD, September–June $P = 0.05$, November–June $P = 0.01$; Fig. 1E). Total concentrations in the leaves were higher in leatherleaf than bog Labrador tea (Tukey's HSD, $P = 0.03$), and, much like the roots of our tree species, total NSC concentrations were not seasonally dynamic ($P = 0.30$; Table 1B).

SEASONAL PATTERNS OF NSC RESERVES IN TREES AND SHRUBS. Starch but not sugar concentrations in branches varied throughout the year in both trees and shrubs. Sampling month and species explained most of the variation in branch sugar ($F_{15,35} = 2.36$, $R^2 = 0.50$, $P = 0.02$; month, $P = 0.34$; species, $P < 0.001$) and starch concentrations ($F_{15,35} = 5.40$, $R^2 = 0.70$, $P < 0.0001$; month, $P < 0.0001$; species, $P = 0.048$; Table 1C). However, the effect of sampling month on starch concentrations depended on species (interaction $P < 0.01$; Table 1C). Branch sugar concentrations did not vary throughout the year and did not differ between black spruce and eastern tamarack (Tukey's HSD, $P = 0.80$) or between bog Labrador tea and leatherleaf (Tukey's HSD, $P = 0.88$) but did differ between all shrub-tree species combinations (Tukey's HSD, bog Labrador tea-black spruce, $P < 0.001$; leatherleaf-black spruce, $P < 0.01$; bog Labrador tea-eastern tamarack, $P < 0.01$; leatherleaf-eastern tamarack, $P = 0.04$; Fig. 2A). In contrast, branch starch concentrations generally varied throughout the year with evergreen species peaking in June and deciduous eastern tamarack peaking in September (Fig. 2B; Table S2).

We did not find dynamic changes in total NSC concentrations in the branches of our four species. While some variation in total NSCs existed, it cannot be fully explained by sampling month and species ($F_{15,35} = 1.51$, $R^2 = 0.40$, $P = 0.15$; month, $P = 0.96$; species, $P < 0.01$; Table 1C). Similar to branch sugar concentrations, total NSC concentrations did not differ between either tree species (Tukey's HSD, $P = 0.98$) or between either shrub species (Tukey's HSD, $P = 0.97$) but did differ between all shrub-tree species combinations (Tukey's HSD, bog Labrador tea-black spruce, $P = 0.02$; leatherleaf-black spruce, $P = 0.04$; bog Labrador tea-eastern tamarack, $P = 0.03$; leatherleaf-eastern tamarack, $P = 0.07$; Fig. 2C).

Discussion. **SEASONAL PATTERNS OF NSC RESERVES IN TREES: BLACK SPRUCE AND EASTERN TAMARACK.** Whereas in deciduous tree species new growth in the spring is supported by NSCs in overwintering organs, evergreen species can begin photosynthesizing immediately using the previous year's foliage; the ability to photosynthesize immediately diminishes the need to draw on stored reserves and influences NSC dynamics (Wyka and Oleksyn 2014, Jensen *et al.* 2015). The observed seasonal patterns of starch in the two trees, black spruce and eastern tamarack, were dynamic in the roots and were unique for each species, possibly reflecting differences in leaf habit as outlined above, as well as contributions by other seasonally dynamic processes, such as secondary root or fine root production (Iversen *et al.* 2018). While future root sampling should include larger sample sizes to better represent the population and resolve dynamics, the data we present are still valuable, as seasonal NSC dynamics for roots are less reported.

At the start of the growing season, we observed differences in storage dynamics in the roots between the trees. As starch concentrations rapidly increased and peaked in June for black spruce, an evergreen conifer, concentrations gradually increased and did not peak until the autumn for eastern tamarack, a deciduous conifer. The large and relatively quick increase in starch reserves for black spruce may be attributed to its ability to photosynthesize immediately with older needles before new shoot, stem, and root growth begins, whereas starch reserves gradually increased over the growing season in eastern tamarack as demands slow.

Toward the end of the growing season, total NSC concentrations of roots in September were nearly six times larger in eastern tamarack than in black spruce. This is in agreement with higher storage requirements for deciduous species compared to evergreen species prior to the dormant season due to their annual leaf drop and regrowth (Dickson 1989). After this point, starch root concentrations declined in eastern tamarack; this decline prior to the dormant season is likely associated with root growth. As a future warmer climate may threaten to lower the water table and stress the root system in these environments, it will be important to link root phenology with NSC dynamics going forward in order to better predict species' resiliency in bog ecosystems.

SEASONAL PATTERNS OF NSC RESERVES IN SHRUBS: BOG LABRADOR TEA AND LEATHERLEAF. Bog Labrador tea and leatherleaf have the same growth form (shrub) and leaf habit (evergreen). Thus, similar seasonal patterns may be expected in both species if such traits are drivers of allocation. In both species, leaf starch concentrations peaked in June and declined onward. Previous studies have shown a buildup of starch in foliage and branches before bud burst (Oleksyn *et al.* 2000, Bansal and Germino 2009), and remobilization of these reserves to build new tissues (Cerasoli *et al.* 2004). Declines in both species occurred post-flowering, a similarly expensive phenological stage that has been followed by degradation of starch in the leaves and/or branches for several months in other plant species (Zieslin *et al.* 1975, Sanz *et al.* 1987, Hagidimitriou and Roper 1994, Monerri *et al.* 2011).

Furthermore, the highest sugar concentrations for both shrub species were measured in the leaves. This finding is in line with previous studies that examined storage in boreal species (compiled in Martínez-Vilalta *et al.* 2016) as well as with the role that sugars play in osmoregulation and phloem loading (Chaves *et al.* 2003, Sala *et al.* 2012, Savage *et al.* 2016). Additionally, sugar and total NSC concentrations were highest in November for both species. Accumulation of NSCs in evergreen shrub leaves prior to the dormant season may be particularly important for frost tolerance and springtime growth of species in environments that experience extreme winter temperatures (Ino *et al.* 2003, Palacio *et al.* 2007).

SEASONAL PATTERNS OF NSC RESERVES IN TREES AND SHRUBS. Branches were the common organ sampled across the four species and can provide insight into storage differences between trees and shrubs. Just like we observed for starch in the tree roots and shrub leaves, starch in the branches was seasonally dynamic, generally peaking earlier in June for evergreen species compared to September for deciduous eastern tamarack. While branch sugar and total concentrations did not significantly vary throughout the year, there were storage differences between trees and shrubs. Concentrations of sugars and total NSCs in the branches were higher in each tree species than each shrub species but similar among themselves.

These findings suggest that growth form (*i.e.*, tree *vs.* shrub) may influence NSC storage, at least in the branches. However, this does not hold true when looking across multiple organs. For example, while leaf NSC concentrations were often similar among the shrubs, root NSC concentrations were not similar among the trees. Thus, organ level NSC storage is likely influenced by many potentially confounding factors, including growth form, leaf habit, and wood anatomy, to name a few. Including a deciduous shrub species in future comparisons may help to tease apart their contributions.

Additionally, the timing of maximum accumulation of total NSCs was inconsistent between organs and species. For instance, we hypothesized that maximum total NSC accumulation for the deciduous conifer would occur in the fall; this held true in the roots but not in the branches of eastern tamarack. We also hypothesized that maximum total NSC accumulation for the three evergreen species would occur in the early summer; this was observed only in the roots of black spruce. The different maximum total NSC storage times observed for individual organs imply a role for within-plant allocation of reserves throughout the year, and species-specific traits, again, influence these dynamics.

Further, previous studies have identified total NSC concentrations that are only weakly seasonal in several tree species (Hoch *et al.* 2003, Würth *et al.* 2005, Richardson *et al.* 2013), implying that the trees examined were fully charged with carbon and that carbon was not a limiting resource for growth under natural conditions (Hoch 2015, Körner 2015). However, more pronounced seasonal variation, particularly driven by starch, may be expected in environments with greater asynchro-

nies in supply and demand, as in the boreal zone (Martínez-Vilalta *et al.* 2016). Overall, we observed total concentrations in individual organs of both trees and shrubs that were only weakly seasonal, with contributions from a highly dynamic starch pool as expected. We suggest that increasing sample sizes, sampling multiple organs including stemwood (Furze *et al.* 2018), and examining whole-plant total NSC pools by summing individual organ-level pools together would help to further resolve seasonal patterns of total NSCs and produce the predicted patterns of maximum total NSC storage.

To better understand (a) NSC dynamics in the context of source-sink relationships and (b) the responses of plants (*e.g.*, growth) to global change, studies should focus on integrating the study of NSCs with measurements of physiology and phenology under both natural and experimental conditions. We conducted this study on vegetation that is directly adjacent to the Spruce and Peatland Responses Under Climatic and Environmental Change (SPRUCE) experiment, in which open-top chambers receive various levels of warming and elevated carbon dioxide (Hanson *et al.* 2017). Future work at SPRUCE will combine the aforementioned measurements to explore whether these tree and shrub species are carbon limited.

Conclusions. In this study, we quantified the seasonal patterns of NSC reserves for four woody boreal species in the upper midwestern USA. We measured concentrations of sugars and starch in branches and roots of black spruce, an evergreen conifer, and eastern tamarack, a deciduous conifer, as well as branches and leaves of bog Labrador tea and leatherleaf, both evergreen broadleaf shrubs. In general, seasonal dynamics were dominated by changes in starch in both below- and aboveground organs, with species-specific traits contributing to storage differences.

Our data support the idea that species-specific traits influence NSC dynamics, highlighting the need to gain a comprehensive understanding of storage and allocation processes in various organs of diverse species across time and space to better predict the responses of woody boreal species to global change.

Literature Cited

- BANSAL, S. AND M. J. GERMINO. 2009. Temporal variation of nonstructural carbohydrates in montane conifers: Similarities and differences among developmental stages, species and environmental conditions. *Tree Physiol.* 29: 559–568.
- CARBONE, M. S., C. I. CZIMCZIK, T. F. KEENAN, P. F. MURAKAMI, N. PEDERSON, P. G. SCHABERG, X. XU, AND A. D. RICHARDSON. 2013. Age, allocation and availability of nonstructural carbon in mature red maple trees. *New Phytol.* 200: 1145–1155.
- CERASOLI, S., P. MAILLARD, A. SCARTAZZA, E. BRUGNOLI, M. M. CHAVES, AND J. S. PEREIRA. 2004. Carbon and nitrogen winter storage and remobilisation during seasonal flush growth in two-year-old cork oak (*Quercus suber* L.) saplings. *Ann. For. Sci.* 61: 721–729.
- CHAPIN, F. S., E. D. SCHULZE, AND H. A. MOONEY. 1990. The ecology and economics of storage in plants. *Annu. Rev. Ecol. Syst.* 21: 423–447.
- CHAVES, M. M., J. P. MAROCO, AND J. S. PEREIRA. 2003. Understanding plant responses to drought—From genes to the whole plant. *Funct. Plant Biol.* 30: 239–264.
- CHOW, P. S. AND S. M. LANDHÄUSSER. 2004. A method for routine measurements of total sugar and starch content in woody plant tissues. *Tree Physiol.* 24: 1129–1136.
- DICKSON, R. E. 1989. Carbon and nitrogen allocation in trees. *Ann. For. Sci.* 46: 631s–647s.
- FURZE, M. E., S. TRUMBORE, AND H. HARTMANN. 2018. Detours on the phloem sugar highway: Stem carbon storage and remobilization. *Curr. Opin. Plant Biol.* 43: 89–95.
- FURZE, M. E., A. M. JENSEN, J. M. WARREN, AND A. D. RICHARDSON. 2018. SPRUCE S1 Bog Seasonal Patterns of Nonstructural Carbohydrates in *Larix*, *Picea*, *Rhododendron*, and *Chamaedaphne*, 2013. Oak Ridge National Laboratory, TES SFA, US Department of Energy, Oak Ridge, TN. <<https://doi.org/10.25581/spruce.037/1473917>>.
- HAGIDIMITRIOU, M. AND T. R. ROPER. 1994. Seasonal changes in nonstructural carbohydrates in cranberry. *J. Am. Soc. Hortic. Sci.* 119: 1029–1033.
- HANSON, P. J., J. S. RIGGS, W. R. NETTLES, J. R. PHILLIPS, M. B. KRASSOVSKI, L. A. HOOK, L. GU, A. D. RICHARDSON, D. M. AUBRECHT, D. M. RICCIUTO, J. M. WARREN, AND C. BARBIER. 2017. Attaining whole-ecosystem warming using air and deep-soil heating methods with an elevated CO₂ atmosphere. *Biogeosciences* 14: 861–883.
- HARTMANN, H. AND S. TRUMBORE. 2016. Understanding the roles of nonstructural carbohydrates in forest trees—From what we can measure to what we want to know. *New Phytol.* 211: 386–403.
- HOCH, G. 2015. Carbon reserves as indicators for carbon limitation in trees, pp. 321–346. *In* U. Lüttge and W. Beyschlag [eds.], *Progress in Botany*. Springer International Publishing, Cham, Switzerland.
- HOCH, G., A. RICHTER, AND C. KÖRNER. 2003. Nonstructural carbon compounds in temperate forest trees. *Plant Cell Environ.* 26: 1067–1081.
- INO, Y., T. MAEKAWA, T. SHIBAYAMA, AND Y. SAKAMAKI. 2003. Two types of matter economy for the wintering of evergreen shrubs in regions of heavy snowfall. *J. Plant Res.* 116: 327–330.
- IVERSEN, C. M., J. CHILDS, R. J. NORBY, T. A. ONTL, R. K. KOLKA, D. J. BRICE, K. J. MCFARLANE, AND P. J.

- HANSON. 2018. Fine-root growth in a forested bog is seasonally dynamic, but shallowly distributed in nutrient-poor peat. *Plant Soil*. 424: 123–143.
- JENSEN, A. M., J. M. WARREN, P. J. HANSON, J. CHILDS, AND S. D. WULLSCHLEGER. 2015. Needle age and season influence photosynthetic temperature response and total annual carbon uptake in mature *Picea mariana* trees. *Ann. Bot.* 116: 821–832.
- KLÖSEIKO, J., M. MANDRE, AND R. KORSJUKOV. 2006. Needle carbohydrate concentrations in Norway spruce as affected by wood ash application to soil. *Proc. Est. Acad. Sci. Biol. Ecol.* 55: 123–136.
- KOLKA, R. K., S. D. SEBESTYEN, E. S. VERRY, AND K. N. BROOKS, eds. 2011. *Peatland Biogeochemistry and Watershed Hydrology at the Marcell Experimental Forest*. CRC Press, Boca Raton, FL.
- KÖRNER, C. 1998. A re-assessment of high elevation treeline positions and their explanation. *Oecologia* 115: 445–459.
- KÖRNER, C. 2015. Paradigm shift in plant growth control. *Curr. Opin. Plant Biol.* 25: 107–114.
- LANDHÄUSSER, S. M. AND V. J. LIEFFERS. 1997. Seasonal changes in carbohydrate storage and regrowth in rhizomes and stems of four boreal forest shrubs: Applications in *Picea glauca* understorey regeneration. *Scand. J. For. Res.* 12: 27–32.
- LANDHÄUSSER, S. M., AND V. J. LIEFFERS. 2003. Seasonal changes in carbohydrate reserves in mature northern *Populus tremuloides* clones. *Trees Struct. Funct.* 17: 471–476.
- LEMS, K. 1956. Ecological study of the peat bogs of eastern North America: Notes on the behavior of *Chamaedaphne calyculata*. *Can. J. Bot.* 34: 197–207.
- MARTÍNEZ-VILALTA, J., A. SALA, D. ASENSIO, L. GALIANO, G. HOCH, S. PALACIO, F. I. PIPER, AND F. LLORET. 2016. Dynamics of non-structural carbohydrates in terrestrial plants: A global synthesis. *Ecol. Monogr.* 86: 495–516.
- MONERRI, C., A. FORTUNATO-ALMEIDA, R. V. MOLINA, S. G. NEBAUER, A. GARCÍA-LUIS, AND J. L. GUARDIOLA. 2011. Relation of carbohydrate reserves with the forthcoming crop, flower formation and photosynthetic rate, in the alternate bearing “Salustiana” sweet orange (*Citrus sinensis* L.). *Sci. Hortic. (Amsterdam)* 129: 71–78.
- OLEKSYN, J., R. ZYTKOWIAK, P. KAROLEWSKI, P. B. REICH, AND M. G. TJOELKER. 2000. Genetic and environmental control of seasonal carbohydrate dynamics in trees of diverse *Pinus sylvestris* populations. *Tree Physiol.* 20: 837–847.
- PALACIO, S., P. MILLARD, M. MAESTRO, AND G. MONTSERRAT-MARTÍ. 2007. Non-structural carbohydrates and nitrogen dynamics in Mediterranean sub-shrubs: An analysis of the functional role of overwintering leaves. *Plant Biol.* 9: 49–58.
- READER, R. J. 1978. Contribution of overwintering leaves to the growth of three broad-leaved, evergreen shrubs belonging to the Ericaceae family. *Can. J. Bot.* 56: 1248–1261.
- RICHARDSON, A. D., M. S. CARBONE, T. F. KEENAN, C. I. CZIMCZIK, D. Y. HOLLINGER, P. MURAKAMI, P. G. SCHABERG, AND X. XU. 2013. Seasonal dynamics and age of stemwood nonstructural carbohydrates in temperate forest trees. *New Phytol.* 197: 850–861.
- SALA, A., D. R. WOODRUFF, AND F. C. MEINZER. 2012. Carbon dynamics in trees: Feast or famine? *Tree Physiol.* 32: 764–75.
- SANZ, A., C. MONERRI, J. GONZALEZ-FERRER, AND J. L. GUARDIOLA. 1987. Changes in carbohydrates and mineral elements in *Citrus* leaves during flowering and fruit set. *Physiol. Plant.* 69: 93–98.
- SAVAGE, J. A., M. J. CLEARWATER, D. F. HAINES, T. KLEIN, M. MENCUCINI, S. SEVANTO, R. TURGEON, AND C. ZHANG. 2016. Allocation, stress tolerance and carbon transport in plants: How does phloem physiology affect plant ecology? *Plant Cell Environ.* 39: 709–725.
- SEVANTO, S., N. G. MCDOWELL, L. T. DICKMAN, R. PANGLE, AND W. T. POCKMAN. 2014. How do trees die? A test of the hydraulic failure and carbon starvation hypotheses. *Plant Cell Environ.* 37: 153–161.
- TENDLAND, Y., S. PELLERIN, P. S. HADDAD, AND A. CUERRIER. 2012. Impacts of experimental leaf harvesting on a North American medicinal shrub, *Rhododendron groenlandicum*. *NRC Res. Press* 251: 247–251.
- WHITNEY, G. G. 1982. The productivity and carbohydrate economy of a developing stand of *Rubus idaeus*. *Can. J. Bot.* 60: 2697–2703.
- WÜRTH, M. K. R., S. PELÁEZ-RIEDL, S. J. WRIGHT, AND C. KÖRNER. 2005. Non-structural carbohydrate pools in a tropical forest. *Oecologia* 143: 11–24.
- WYKA, T. P. AND J. OLEKSYN. 2014. Photosynthetic ecophysiology of evergreen leaves in the woody angiosperms—A review. *Dendrobiology* 72: 3–27.
- ZASADA, J. C., J. C. TAPPEINER III, B. D. MAXWELL, AND M. A. RADWAN. 1994. Seasonal changes in shoot and root production and in carbohydrate content of salmonberry (*Rubus spectabilis*) rhizome segments from the central Oregon Coast Ranges. *Can. J. For. Res.* 24: 272–277.
- ZIESLIN, N., A. HURWITZ, AND A. H. HALEVY. 1975. Flower production and the accumulation and distribution of carbohydrates in different parts of Baccara rose plants as influenced by various pruning and pinching treatments. *J. Hortic. Sci.* 50: 339–348.

Supplementary Materials for Chapter 4

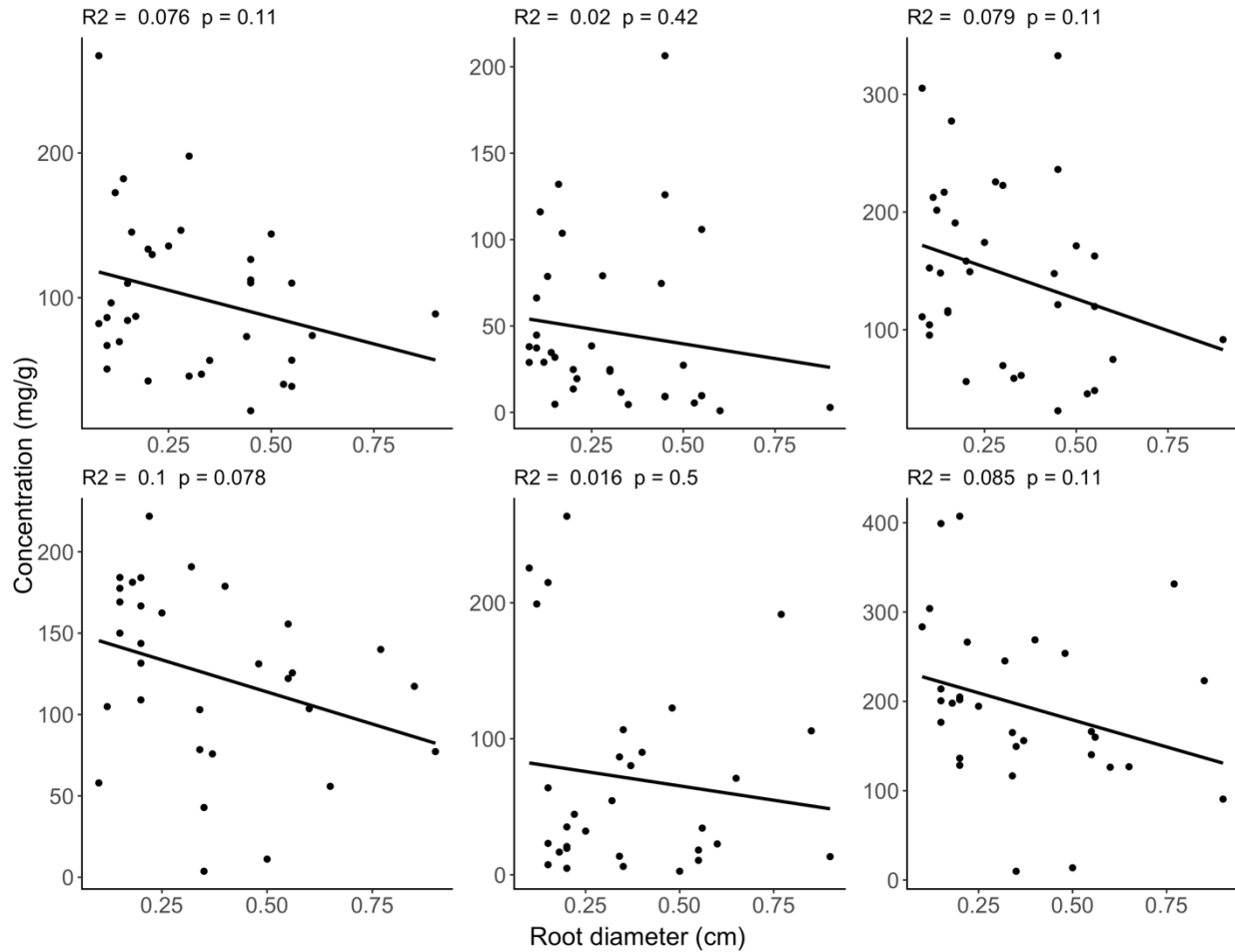


Figure S1 Scatter plots of sugar (left column), starch (center column), and total NSC (right column) concentrations versus root diameter for black spruce (top row) and eastern tamarack (bottom row). Black lines and displayed statistics were obtained from ordinary least squares model fits.

Table S1 Number of individual plants analyzed for nonstructural carbohydrates by species, organ, and month.

	Black spruce		Eastern tamarack		Bog Labrador tea		Leatherleaf		TOTAL
	Branch	Root	Branch	Root	Branch	Leaf	Branch	Leaf	
April	3	6	3	3	3	4	4	1	27
June	3	10	4	10	3	6	3	4	43
September	3	2	4	2	3	4	3	4	25
November	3	16	3	16	3	8	3	8	60
TOTAL	12	34	14	31	12	22	13	17	155

Table S2 Tukey’s HSD results from one-way ANOVA testing for the effect of sampling month on starch concentrations in individual organs for each species. This testing was conducted when the interaction effect (month x species) was significant for starch in Table 1. NS= not significant, * = $P \leq 0.05$, ** = $P \leq 0.01$, *** = $P \leq 0.001$, or **** = $P \leq 0.0001$ in each white cell indicates if column month and row month are significantly different from each other or not based on the difference between their least squares means. Each light gray cell contains this difference (mean \pm 1SE), calculated by row month minus column month. If the entire grid is shaded orange, then month was not a significant factor in the one-way ANOVA with $P \geq 0.05$ and post-hoc testing was not conducted.

Root starch									
Black spruce					Eastern tamarack				
	Apr	Jun	Sept	Nov		Apr	Jun	Sept	Nov
Apr		-92 \pm 14	7 \pm 23	-12 \pm 13	Apr		-31 \pm 43	-186 \pm 60	-62 \pm 41
Jun	***		99 \pm 22	80 \pm 11	Jun	NS		-155 \pm 51	-31 \pm 27
Sept	NS	***		-19 \pm 21	Sept	*	*		124 \pm 49
Nov	NS	****	NS		Nov	NS	NS	NS	
Branch starch									
Black spruce					Eastern tamarack				
	Apr	Jun	Sept	Nov		Apr	Jun	Sept	Nov
Apr		-26 \pm 7	-4 \pm 7	7 \pm 7	Apr		13 \pm 7	-14 \pm 7	26 \pm 8
Jun	*		22 \pm 7	32 \pm 7	Jun	NS		-28 \pm 7	13 \pm 7
Sept	NS	*		11 \pm 7	Sept	NS	**		40 \pm 7
Nov	NS	**	NS		Nov	*	NS	**	
Bog Labrador tea					Leatherleaf				
	Apr	Jun	Sept	Nov		Apr	Jun	Sept	Nov
Apr					Apr		-40 \pm 9	-21 \pm 9	4 \pm 9
Jun					Jun	**		19 \pm 9	44 \pm 9
Sept					Sept	NS	NS		25 \pm 9
Nov					Nov	NS	**	NS	

Methods S1 Uncertainty of NSC measurements

To evaluate our extraction methods, we compared sugar and starch concentrations for standards throughout the study. For every batch (≥ 15 samples each) that underwent concentration analyses, peach foliage (NIST, Gaithersburg, MD USA) was included as a standard for sugar analysis, and potato starch (Sigma Chemicals, St. Louis, MO USA) was included for starch analysis. Across all batches, the mean and standard deviation of the sugar concentration for peach foliage (n=9) was $111.8 \pm 15.9 \text{ mg g}^{-1}$, while the mean and standard deviation of the starch concentration for potato starch (n=5) was $814 \pm 46.2 \text{ mg g}^{-1}$.

There is no universal standard for nonstructural carbohydrate analyses. Towards the end of the study, we became interested in creating a standard with higher repeatability that could be used as the control for both sugar and starch analyses. We created our own internal standard using *Quercus rubra* (red oak) stemwood collected from the Harvard Forest (Petersham, MA, USA). It was included in the last two batches of samples for sugar (30.8 mg g⁻¹ and 34.1 mg g⁻¹) and starch (22.7 mg g⁻¹ and 22.8 mg g⁻¹) analyses.



Detours on the phloem sugar highway: stem carbon storage and remobilization

Reprinted from:

Furze, M.E., Trumbore, S, Hartmann, H. (2018). Detours on the phloem sugar highway: stem carbon storage and remobilization. *Current Opinion in Plant Biology* 43:89-95.

Article available at <https://doi.org/10.1016/j.pbi.2018.02.005>



Detours on the phloem sugar highway: stem carbon storage and remobilization

Morgan E Furze¹, Susan Trumbore² and Henrik Hartmann²



For trees to survive, they must allocate resources between sources and sinks to maintain proper function. The vertical transport pathway in tree stems is essential for carbohydrates and other solutes to move between the canopy and the root system. To date, research and models emphasize the role of tree stems as ‘express’ sugar highways. However, recent investigations using isotopic markers suggest that there is considerable storage and exchange of phloem-transported sugars with older carbon (C) reserves within the stem. Thus, we suggest that stems play an important role not only in long-distance transport, but also in the regulation of the tree’s overall C balance. A quantitative partitioning of stem C inputs among storage and sinks, including tissue growth, respiration, and export to roots, is still lacking. Combining methods to better quantify the dynamics and controls of C storage and remobilization in the stem will help to resolve central questions of allocation and C balance in trees.

Addresses

¹Department of Organismic and Evolutionary Biology, Harvard University, 26 Oxford St, Cambridge, MA 02138, USA

²Max-Planck Institute for Biogeochemistry, Hans Knoll Str. 10, 07745 Jena, Germany

Corresponding author: Furze, Morgan E (mfurze@fas.harvard.edu)

Current Opinion in Plant Biology 2018, 43:89–95

This review comes from a themed issue on **Physiology and metabolism**

Edited by **Noel Michele Holbrook** and **Michael Knoblauch**

<https://doi.org/10.1016/j.pbi.2018.02.005>

1369-5266/© 2018 Elsevier Ltd. All rights reserved.

Introduction

Trees are organisms that can live for decades, centuries, and even millennia. This long lifespan increases a tree’s risk of encountering stressful conditions where normal functioning is disturbed and metabolism has to rely on stored resources [1]. Because trees are autotrophic organisms, storage of primary metabolites like carbohydrates is particularly important for survival during harsh environmental conditions and stress. Carbohydrates are allocated to various organs and processes operating on timescales

ranging from hours to decades, each contributing to the tree’s overall carbon (C) balance.

Tree stems are predominantly viewed as the infrastructure that provides mechanical support for the canopy and facilitates transport between sources and sinks, but they also store ~40% of a tree’s total **nonstructural carbohydrates** (NSCs; [Box 1](#)) [2*]. During C transport, there is substantial exchange of C between phloem and parenchyma of the stem [3], but a quantitative understanding of C partitioning between storage, tissue growth, and respiration as well as the underlying regulation of C partitioning is still lacking. Here we emphasize that the stem is itself a major C sink and an important organ for the regulation of the tree’s C balance, not merely an ‘express’ highway for long-distance C transport. We stress the need for process-oriented research that will provide quantitative insights into dynamics and controls of C storage and remobilization in tree stems and along the transport pathway. Without such information, the stem will remain a missing link in whole-tree C balance.

Non-structural carbohydrates in the stem

NSCs exist in basically all components of living vegetative tissues of the plant; they can be found in vacuoles, plastids, and the cytosol of cells, as well as in the apoplast [4*]. Supply and demand of NSCs are often asynchronous and surplus sugars produced in leaves during daytime are stored as starch granules in chloroplasts. During the night, these starch granules are then hydrolyzed to glucose to fuel growth and respiration or exported as sucrose to other plant organs via the phloem [5].

Large amounts of NSCs are stored long-term in amyloplasts of **ray and axial parenchyma** cells. Because secondary growth in woody plants produces new cell layers interspersed with living parenchyma cells every year, the resulting tissues provide storage capacities for different temporal horizons: small branches and fine roots serve as seasonal storage, while large branches, coarse roots, and tree stems are used for decadal storage [6*]. Only the heartwood, comprising the inner part of tree branches and stems, does not contain living cells and therefore cannot remobilize remaining NSCs.

In the stem, NSC concentrations usually decrease across the sapwood towards the sapwood-heartwood transition zone and then remain constant (often at zero concentration in older trees) throughout the heartwood to the pith [7]. However, some studies have observed high levels of

Box 1 Glossary of key terms. Terms are bolded within text upon first mention

Term	Definition
Nonstructural carbohydrates (NSC)	Mainly sugars and starch, the major substrates for primary and secondary plant metabolism; 5-C sugars (i.e. glucose, fructose) function as metabolites and osmoregulators, while disaccharides and oligosaccharides (i.e. sucrose, raffinose) function as transport sugars
Ray and axial parenchyma	Living cells of the secondary xylem and phloem that function in many metabolic processes including NSC storage
Collection phloem	Sieve element-companion cell complex of the minor leaf vein that sucrose is loaded into after its production in the leaf mesophyll
Transport phloem	sieve element-companion cell complex in the major veins, petioles, branches, stems, and roots that transports and redistributes NSCs and other molecules to sinks along the vertical pathway
Release phloem	Sieve element-companion cell complex that unloads sucrose and other molecules into sink cells
Leakage-retrieval mechanism	Process by which NSCs traveling along the leaky transport phloem passively diffuse out and are actively loaded back into companion cells
Radiocarbon signatures	Well-documented changes in the radiocarbon signatures atmospheric carbon dioxide since the testing of atmospheric nuclear weapons in the 1960s provide an estimate for the mean time elapsed since C in NSC pools or plant tissues were fixed from the atmosphere
Lateral storage and remobilization	Lateral flow and accumulation of NSCs in sinks (i.e. parenchyma cells of stem xylem) and subsequent release of stored reserves back into the transport phloem
Apoplastic sensing	Proposed mechanism by which lateral flows are regulated through sensing of apoplastic sucrose concentrations; low apoplastic sucrose concentrations will reduce phloem loading

sugars [8**] and/or starch [9] deep in the xylem. NSC concentrations vary seasonally in the stems of several tree species [10], reflecting the accumulation, utilization, and redistribution of NSCs to buffer changing supply and demand throughout the year.

Whole-tree phloem transport

The Münch theory posits that the flux of carbohydrates from sources to sinks is driven by a hydrostatic pressure gradient in the phloem that causes mass flow of phloem sap along the sieve tubes [11,12*,13*]. The hydrostatic pressure is created by loading of sucrose into companion cells followed by diffusion into sieve tubes of the **collection phloem**. The increase in solute concentration in the sieve tubes decreases phloem water potential and causes inflow of water from surrounding tissues, mainly the xylem. Increasing turgor in the collection phloem of source tissues due to this inflow along with unloading of sucrose and ensuing decreases in turgor in the **release phloem** of sink tissues creates the gradient of hydrostatic pressure that drives phloem flow [14*].

Stems are the linkage between the tree's main photosynthetic source, the canopy, and one of its major heterotrophic sinks, the root system. Secondary growth in stems produces layers of cells each growing season, divided into xylem, which transports mainly water and nutrients from the soil to the canopy and **transport phloem**, which redistributes carbohydrates and other organic and inorganic molecules across tree organs. Xylem water transport is much faster than phloem sap flow and can reach

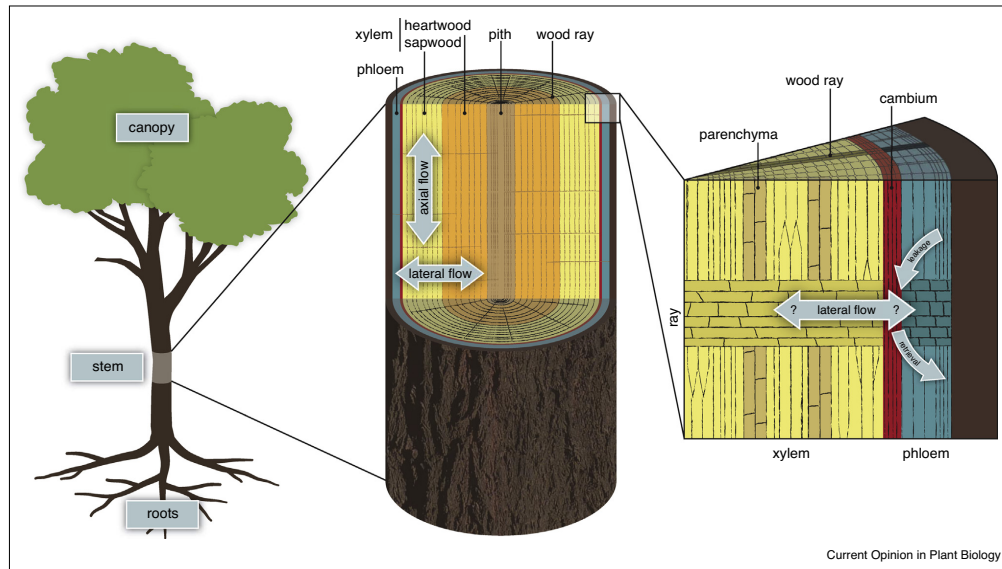
maximum peak velocities ranging from 16 to 45 m hour⁻¹ depending on vessel size [15]. However, phloem velocities average between 22 cm hour⁻¹ in gymnosperm trees and 56 cm hour⁻¹ for angiosperms [16*], making tree stems large highways for both water and sugar transport.

Tree stems are more than just unidirectional 'express' highways

Viewing transport phloem in the tree stem as a simple sugar highway is too simplistic (Figure 1). During the last decades, evidence has accumulated that the transport phloem is not an 'express' highway, but rather a leaky pipe where carbohydrates passively diffuse out and are actively loaded back into companion cells during transport [17]; this has been termed the **leakage-retrieval mechanism**. In bean plants, about 6% of sugars are lost and 3.4% retrieved per centimeter of phloem length [18]. Thus, leakage and retrieval may provide resources locally for maintenance and growth of axial sinks like stem cambium [19].

The inverse flows involved in leakage and retrieval are thought to serve as short term buffers for imbalances between sources and sinks, but can also facilitate exchange of NSCs between the phloem and stem parenchyma [20,21]. Ray cells extend radially throughout the xylem and connect to the phloem, allowing for both the **lateral storage and remobilization** of NSCs into and out of the stem [22], which in turn supports the leakage and retrieval of solutes along the pathway [17].

Figure 1



Tree stems and phloem transport. Tree stems contain phloem, the main transport system connecting the major carbon source in the canopy to a large carbon sink in the roots. While phloem transport is often considered to be an express highway between canopy and roots, it is in fact more like a winding road interrupted by detours. Carbohydrates leak out of and are loaded back into the sieve elements of the phloem to provide energy and carbon skeletons for respiration, growth, and storage in living cells of the phloem, the cambium, and the xylem. Questions that need answering include: How much of the transported carbohydrates end up in parenchyma cells of wood rays in the xylem? and How are stored carbohydrates remobilized when source activity in the canopy is lower than overall carbon demand?

Recently, **radiocarbon signatures** of sugars and starch have demonstrated lateral storage by net inward mixing of younger NSCs into the stem in many temperate tree species [2*,23*]. The use of these mixed younger and older NSCs for respiration or growth of stem resprouts [24,25] support the idea of remobilization. While we have a basic understanding of the spatial and temporal distributions of NSCs in the stem, processes regulating the exchange of NSCs along the transport pathway — how younger C is mixed inward, and older C is used — remain poorly understood. In particular, the degree to which timescales of NSC storage result from physical transport and isolation (e.g. flow rates into and out of rays) versus active regulation requires further investigation [6*].

When the tree canopy is not the major source of NSCs (i. e. when deciduous trees lack leaves, or during extended drought), storage and remobilization of reserves in the stem may be particularly important. In fact, the transport pathway runs in reverse, supplying stored NSCs to grow buds and new leaves until they are able to fix excess C supply on their own. In addition to flowing in reverse, our

understanding of phloem–xylem function has also been challenged. Recent work shows that long distance transport for springtime growth in young walnut trees is accomplished by NSC transport in the xylem, which is maintained with the recirculation of water by phloem Münch flow [26*].

Unknown role of tree stems in C balance

Isotopic tools have provided evidence for exchange dynamics along the leaky highway, particularly ^{13}C tracer studies that have monitored a label fixed in the canopy and respired from different organs over time. However, mass balance of the fate of the tracer in such studies is notoriously difficult. Strong evidence for phloem leakage and recovery comes from the observed ~10 fold reduction in the ^{13}C label associated with canopy-derived NSCs as it is transported between the top and bottom of the stem [27**]. Other canopy labeling studies tracing the ^{13}C distribution down the stem have quantified the label in CO_2 emitted from the stem, indicating not just transport, but also metabolism of canopy-derived sugar (reviewed in [28*]). Such studies have demonstrated

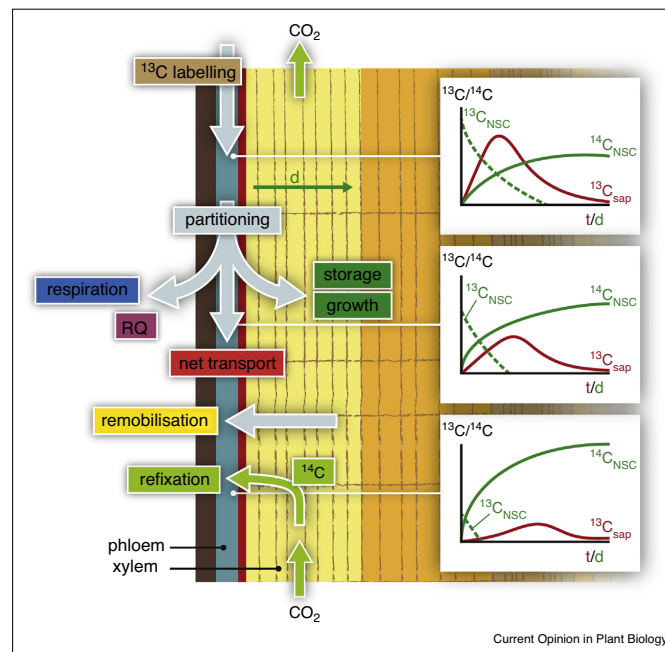
arrival of the tracer with downward transport rates of 0.2–1.2 m per hour (i.e. in the same range as water flow in phloem).

Studies tracking canopy-derived C also indicate the presence of additional mechanisms that allow the label to be detected in stem CO₂ efflux over subsequent weeks to months. This indicates that there is a second, slower process at work, as might be expected from phloem leakage and recovery. However, xylem-transported CO₂ can also influence signals in stem CO₂ efflux based on an estimated 50% of root respired CO₂ being retained and transpired upwards [29*]. The signal of respiration of ¹³C-labeled photosynthetic products can therefore be

diluted both via mixing of labeled and unlabeled NSCs before respiration, or by diffusion of unlabeled CO₂ from stem interiors. Teasing these signals apart requires using O₂ uptake rather than CO₂ release as a measure of local respiration rates [30**], as O₂ is far less soluble in stem water, or using the higher radiocarbon (¹⁴C) content of in-stem CO₂ [25] to estimate the contribution from lateral diffusion.

In some cases, the ¹³C label can be stored even longer, and is detectable in respiration [31] or new wood growth in subsequent years [32]. Thus, mixing and retrieval mechanisms have the potential to contribute to even long-term NSC stores in stems. Such studies are in accord

Figure 2



Partitioning of phloem transport. On its way from source to sink, fractions of phloem sap leaked out of sieve cells can be allocated to metabolic activity (e.g. respiration, cambial and wood growth) or stored within parenchyma cells of the xylem. These fractions are currently unknown and dedicated experimental approaches are required to provide information on these processes (see also Table 1). Labeling of phloem sap with stable carbon isotopes (¹³C) via photosynthesis will yield information on the fraction of carbohydrates that remain in the sap on its way down (red lines in inlet panels). The ¹³C signal decreases with distance (*d*) from the source (indicated by position on stem, distance increasing downwards) and over time (¹³C signal of sap being diluted with 'fresh' photosynthates, *t* of *x*-axis on inlet panels is time). Storage of carbohydrates is indicated by ¹³C signal of stem NSCs, which are likely to decline with distance from source and with distance from phloem (green dashed lines, *d* on *x*-axis of inlet panels is distance from phloem). The fraction of 'older' carbohydrates in stored NSCs consequently increases with distance from source and from phloem (¹⁴C signal, green solid lines on inlet panels) as less 'fresh' photosynthates are stored. Partitioning of each fraction can be derived from comparing ¹³C signals of stored NSCs, wood tissues, phloem sap, and respired CO₂ whereas the fraction of CO₂ transported in the xylem and contributing to stem emissions can be estimated by RQ (respiratory quotient, the amount of CO₂ evolved over the amount of oxygen used during respiration; the RQ can provide information on the substrates used in respiration, like carbohydrates or lipids, or indicate the fraction of root-derived CO₂ transported in the xylem and emitted by the stem) measurements.

Table 1

Future directions and tools for assessing whole-tree NSC transport

Question	Current understanding	New experiments/observations
How are NSCs that are loaded into the phloem in the canopy partitioned (Figure 2) as they move down the stem?	Label signal from ^{13}C fixed in the canopy is diluted in phloem sugars and stem CO_2 efflux as the distance from the canopy increases [27**]	Combine canopy ^{13}C labeling with natural radiocarbon measurements in phloem sap, wood and xylem NSCs and CO_2 efflux at different stem heights (panels in Figure 2). Use O_2 uptake (RQ; Figure 2) and C isotopes to differentiate local respiration from transported CO_2
What fraction of the C respired by roots originated in the canopy in the last few days?	Transport from canopy labeling combined with radiocarbon signature of root respiration indicates a mix of multi-year storage reserves and label C [31]	Perform more combined label/radiocarbon experiments. Add compound specific isotope measurements (e.g. sucrose, amino acids, organic acids) to understand changing sources of these compounds in phloem and stem CO_2
What is the role of CO_2 fixation and internal recycling in tree C balance?	A portion of ^{13}C - CO_2 label applied at stem base is transported to the canopy and fixed by photosynthetic tissues [29*] Low respiration quotients [30**] suggest CO_2 is also fixed within stems to produce organic acids	Labeling of in-stem CO_2 and tracking the label into tissues and organic compounds in xylem and phloem. Simultaneous monitoring of isotopes in CO_2 efflux and O_2 uptake in extracted tissues as well as stem fluxes with distance from the label injection
Does the remobilization of older reserves increase when canopy C sources decline (dormant season or extended drought)?	Radiocarbon signatures of NSC and in-stem CO_2 indicate storage reserves that are decades old contribute to respiration [2*,23*,24,25]	Use stem girdling to disrupt phloem transport and track O_2 uptake (RQ) as well as the ^{14}C of respired CO_2 with time (in extracted cores and stem chambers)

with the inferred use of storage reserves from either long-term labeling experiments [33] or the bomb ^{14}C signature. Krepowski *et al.* [32] showed large differences in the timescales of label persistence between deciduous and evergreen broadleaf trees; Epron *et al.* [28*] showed faster transport of label downward in gymnosperms compared to angiosperms. Thus, the mechanisms at work and how NSCs are allocated among them differ with the life strategy of the tree, a fact that must be kept in mind when comparing studies.

Regulation of exchange processes

While there is evidence that exchange of NSCs along the transport pathway is occurring, the regulation of these processes is not well understood. We know that they are controlled partly by the distribution of and coordination between sources and sinks. Further, it has been proposed that NSC storage and remobilization in ray and axial parenchyma cells of the stem involves both plasmodesmatal and transporter-mediated routes for exchange [3], with active uptake that is likely controlled by the concentration of sugars in the apoplastic space, at least for short term buffering [34].

But, it is unclear if **apoplastic sensing** plays a role in longer term NSC storage. The phloem is, however, not limited to the long distance transport of sugars as it also carries nutrients and signaling molecules like hormones, RNA, and proteins [35,36]. These signaling molecules may induce changes to the abundance and distribution of transporters and enzymes that then have the potential to modify the partitioning and allocation of stem reserves

[37]. Understanding both the relative importance of various signaling molecules for exchange dynamics and how they exert control on processes like lateral storage and remobilization will help shed light on the mechanisms at play along the stem during long distance transport.

Tools and approaches for understanding stem storage and remobilization of whole-tree NSC transport

Future work should aim to combine the measurement of NSCs with isotope studies to piece together a detailed picture of storage and allocation processes in the stem, which will in turn inform our understanding of whole-tree transport. Historically, storage in the stem has been estimated by measuring NSCs from sapwood tissue collected at breast height, but it is clear that concentrations may vary with distance from the source and should be quantified both radially and axially at different stem heights [7,38]. Concurrent application and monitoring of isotopic signals like ^{13}C and ^{14}C along the stem will allow us to partition C to different sinks and tease apart the importance of and mechanisms behind different processes like lateral storage and remobilization and CO_2 fixation (Figure 2 and Table 1). Additional manipulation of source–sink relationships through girdling and defoliation may help to further resolve stem dynamics.

There are many complex questions that these methods will help address (see also Table 1): How much of the timescale involved in storage is related to physical transport (i.e. mixing going down the stem) versus actual chemical transformations (i.e. sugar to starch and back)?

How important is internal recycling/refixation of CO₂ in the stem xylem to the whole-tree C budget? Like short term buffering, does apoplastic sensing control the long term storage and remobilization of reserves and how do wood anatomy and leaf habit influence such processes? Answering these and similar questions will highlight the stem's role not only in C transport, but also in regulating the whole-tree C balance.

Summary and conclusion

The statement by Minchin *et al.* [39**] “There has been very little work to determine whether axial sinks alter the ‘classical’ model of source to sink transport, probably because of the experimental difficulties . . .” is still valid. We currently do not understand the dynamics and regulation of storage and exchange processes that occur along the transport pathway, and the stem remains a black box for our understanding of whole-tree C balance. Recent applications of X-ray micro-computed tomography imaging combined with machine learning have opened new avenues for *in vivo* observations of stem storage processes [40*]. In addition, further research using isotopic tracers and clever experimental designs (Figure 2) is required to produce quantitative evidence for C partitioning in tree stems and will show that tree stems are not just transport highways, but also play an important role in the C metabolism of trees.

Acknowledgements

We thank Catherine Chamberlain and Jessica Gersony for feedback on a previous version of the manuscript. We are grateful to Annett Boerner for producing the figures.

References and recommended reading

Papers of particular interest, published within the period of review, have been highlighted as:

- of special interest
- of outstanding interest

1. McDowell NG: **Mechanisms linking drought, hydraulics, carbon metabolism, and vegetation mortality.** *Plant Physiol* 2011, **155**:1051-1059.
2. Richardson AD, Carbone MS, Huggert BA, Furze ME, Czimczik CI, Walker JC, Xu X, Schaberg PG, Murakami P: **Distribution and mixing of old and new nonstructural carbon in two temperate trees.** *New Phytol* 2015, **206**:590-597.
Radiocarbon evidence for decades-old nonstructural carbon in outermost few centimeters of stemwood. Combined with observations of seasonal change in concentration, this requires at least two pools with distinct cycling times.
3. Van Bel A: **Xylem-phloem exchange via the rays: the undervalued route of transport.** *J Exp Bot* 1990, **41**:631-644.
4. Secchi F, Zwieniecki MA: **Accumulation of sugars in the xylem apoplast observed under water stress conditions is controlled by xylem pH.** *Plant Cell Environ* 2016, **39**:2350-2360.
Demonstrates links between xylem apoplast pH, sugar accumulation and tree water stress, linking these changes to embolism formation and recovery in poplar trees.
5. Stitt M, Zeeman SC: **Starch turnover: pathways, regulation and role in growth.** *Curr Opin Plant Biol* 2012, **15**:282-292.
6. Hartmann H, Trumbore S: **Understanding the roles of nonstructural carbohydrates in forest trees – from what we can measure to what we want to know.** *New Phytol* 2016, **211**:386-403.
Review emphasizing the view that ‘storage’ is not a function, but the outcome of asynchrony in source-sink demands.
7. Hoch G, Richter A, Körner C: **Non-structural carbon compounds in temperate forest trees.** *Plant Cell Environ* 2003, **26**:1067-1081.
8. Smith MG, Miller RE, Arndt SK, Kasel S, Bennett LT: **Whole-tree distribution and temporal variation of non-structural carbohydrates in broadleaf evergreen trees.** *Tree Physiol* 2017, **00**:1-12.
Provides a detailed assessment of whole-tree carbohydrate storage including longitudinal and radial profiles of the stem across seasons.
9. Würth M, Paláez-Riedl S, Wright J, Körner C: **Non-structural carbohydrate pools in a tropical forest.** *Oecologia* 2005, **143**:11-24.
10. Richardson AD, Carbone MS, Keenan TF, Czimczik CI, Hollinger DY, Murakami P, Schaberg PG, Xu X: **Seasonal dynamics and age of stemwood nonstructural carbohydrates in temperate forest trees.** *New Phytol* 2013, **197**:850-861.
11. Münch E: *Die Stoffbewegungen in der Pflanze.* Jena, Germany: Gustav Fischer Verlagsbücher; 1930.
12. Jensen KH, Berg-Sørensen K, Bruus H, Holbrook NM, Liesche J, Schulz A, Zwieniecki MA, Bohr T: **Sap flow and sugar transport in plants.** *Rev Mod Phys* 2016, **88**:035007.
Review emphasizing the physics governing xylem and phloem flow in plants.
13. Knoblauch M, Knoblauch J, Mullendore DL, Savage JA, Babst BA, Beecher SD, Dodgen AC, Jensen KH, Holbrook NM: **Testing the Münch hypothesis of long distance phloem transport in plants.** *eLife* 2016, **5**:e15341.
This paper provides support for the Münch hypothesis.
14. Hölttä T, Lintunen A, Chan T, Mäkelä A, Nikinmaa E: **A steady-state stomatal model of balanced leaf gas exchange, hydraulics and maximal source-sink flux.** *Tree Physiol* 2017, **37**:851-868.
A new model linking carbon sources (leaf gas exchange) and carbon sinks (sugar utilization and soil water uptake) relations through xylem and phloem transport, that can explain stomatal behavior by maximizing carbon uptake.
15. Taiz L: *Plant physiology and development.* 2015.
16. Liesche J, Windt C, Bohr T, Schulz A, Jensen KH: **Slower phloem transport in gymnosperm trees can be attributed to higher sieve element resistance.** *Tree Physiol* 2015, **35**:376-386.
A meta-analysis of data on phloem transport speed in trees, demonstrating that the faster transport in angiosperms compared to gymnosperms is related to anatomical elements that increase hydraulic resistance.
17. De Schepper V, De Swaef T, Bauweraerts I, Steppe K: **Phloem transport: a review of mechanisms and controls.** *J Exp Bot* 2013, **64**:4839-4850.
18. Minchin PEH, Thorpe MR: **Measurement of unloading and reloading of photo-assimilate within the stem of bean.** *J Exp Bot* 1987, **38**:211-220.
19. van Bel AJE: **Transport phloem: low profile, high impact.** *Plant Physiol* 2003, **131**:1509.
20. Minchin PEH, Thorpe MR, Farrar JF: **A simple mechanistic model of phloem transport which explains sink priority.** *J Exp Bot* 1993, **44**:947-955.
21. McQueen JC, Minchin PEH, Thorpe MR, Silvester WB: **Short-term storage of carbohydrate in stem tissue of apple (*Malus domestica*), a woody perennial: evidence for involvement of the apoplast.** *Funct Plant Biol* 2005, **32**:1027-1031.
22. Ziegler H: **Storage, mobilization and distribution of reserve material in trees.** In *The Formation of Wood in Forest Trees.* Edited by Zimmermann MH. Academic Press; 1964:303-320.
23. Trumbore S, Czimczik CI, Sierra CA, Muhr J, Xu X: **Non-structural carbon dynamics and allocation relate to growth rate and leaf habit in California oaks.** *Tree Physiol* 2015, **35**:1206-1222.
Measurements of radiocarbon in NSC and stem CO₂ efflux in sympatric deciduous and evergreen oaks in California. These are brought together

with a model linking CO₂ production in the stem with the rates of internal transport using both observations constraints.

24. Carbone MS, Czimczik CI, Keenan TF, Murakami PF, Pederson N, Schaberg PG, Xu X, Richardson AD: **Age, allocation and availability of nonstructural carbon in mature red maple trees.** *New Phytol* 2013;1-11.
25. Muhr J, Angert A, Negrón-Juárez RI, Muñoz WA, Kraemer G, Chambers JQ, Trumbore SE: **Carbon dioxide emitted from live stems of tropical trees is several years old.** *Tree Physiol* 2013, **33**:743-752.
26. Tixier A, Sperling O, Orozco J, Lampinen B, Amico Roxas A, Saa S, Earles JM, Zwieniecki MA: **Spring bud growth depends on sugar delivery by xylem and water recirculation by phloem Münch flow in *Juglans regia*.** *Planta* 2017, **246**:495-508.

Suggests that long distance transport for springtime growth in walnut trees is accomplished by NSC transport in the xylem which is maintained by phloem Münch flow.

27. Epron D, Cabral OMR, Laclau J-P, Dannoura M, Packer AP, Plain C, Battie-Laclau P, Moreira MZ, Trivelin PCO, Bouillet J-P, Gérard D, Nouvellon Y: **In situ ¹³C₂ pulse labelling of field-grown eucalypt trees revealed the effects of potassium nutrition and throughfall exclusion on phloem transport of photosynthetic carbon.** *Tree Physiol* 2016, **36**:6-21.

¹³C labeling study combined with potassium fertilization and rainfall exclusion treatments. In addition to demonstrating dilution of the ¹³C in phloem in the stem from below-canopy to above-roots, this paper also demonstrates the role of potassium in phloem transport.

28. Epron D, Bahn M, Derrien D, Lattanzi FA, Pumpanen J, Gessler A, Höglberg P, Maillard P, Dannoura M, Gérard D *et al.*: **Pulse-labelling trees to study carbon allocation dynamics: a review of methods, current knowledge and future prospects.** *Tree Physiol* 2012, **32**:776-798.

Synthesis and review of canopy pulse labeling experiments, highlighting the rate of downward transport of tracer fixed in the canopy in angiosperms versus gymnosperms.

29. Bloemen J, McGuire MA, Aubrey DP, Teskey RO, Steppe K: **Transport of root-respired CO₂ via the transpiration stream affects aboveground carbon assimilation and CO₂ efflux in trees.** *New Phytol* 2013, **197**:555-565.

Demonstration of refixation of labeled in-stem CO₂ in photosynthetic elements (bark, xylem, petiole) in trees.

30. Hilman B, Angert A: **Measuring the ratio of CO₂ efflux to O₂ influx in tree stem respiration.** *Tree Physiol* 2016, **36**:1422-1431.

Demonstration that influx of O₂ exceeds CO₂ release in tree stems. As O₂ is less soluble in water, it should provide a better measure of *in situ* respiration, thus there is a sink for CO₂ in stems.

31. Carbone MS, Czimczik CI, McDuffee KE, Trumbore SE: **Allocation and residence time of photosynthetic products in a boreal forest using a low-level ¹⁴C pulse-chase labeling technique.** *Glob Change Biol* 2007, **13**:466-477.

32. Krepkowski J, Gebrekirstos A, Shibistova O, Br A: **Stable carbon isotope labeling reveals different carry-over effects between functional types of tropical trees in an Ethiopian mountain forest.** *New Phytol* 2013:431-440.

33. Keel SG, Siegwolf RTW, JÄGgi M, KÖRner C: **Rapid mixing between old and new C pools in the canopy of mature forest trees.** *Plant Cell Environ* 2007, **30**:963-972.

34. McQueen J, Minchin P, Thorpe M, Silvester W: **Short-term storage of carbohydrate in stem tissue of apple (*Malus domestica*), a woody perennial: evidence for involvement of the apoplast.** *Funct Plant Biol* 2005, **32**:1027-1031.

35. Turgeon R, Wolf S: **Phloem transport: cellular pathways and molecular trafficking.** *Annu Rev Plant Biol* 2009, **60**:207-221.

36. Lucas W, Yoo B, Kragler F: **RNA as a long-distance information macromolecule in plants.** *Nat Rev Mol Cell Biol* 2001, **2**:849-857.

37. Ayre B, Keller F, Turgeon R: **Symplastic continuity between companion cells and the translocation stream: long-distance transport is controlled by retention and retrieval mechanisms in the phloem.** *Plant Physiol* 2003, **131**:1518-1528.

38. Barbaroux C, Breda N, Dufrene E: **Distribution of above-ground and below-ground carbohydrate reserves in adult trees of two contrasting broad-leaved species (*Quercus petraea* and *Fagus sylvatica*).** *New Phytol* 2003, **157**:605-615.

39. Minchin PEH, Lacombe A: **Consequences of phloem pathway unloading/reloading on equilibrium flows between source and sink: a modelling approach.** *Funct Plant Biol* 2017, **44**:507-514.

The first attempt to include the effects of unloading and reloading of carbohydrates in the modelling of pressure driven phloem flow.

40. Earles J, Knipfer T, Tixier A, Orozco J, Reyes C, Zwieniecki M, Brodersen C, McElrone A: **In vivo quantification of plant starch reserves at micrometer resolution using X-ray microCT imaging and machine learning.** *New Phytol* 2018 <http://dx.doi.org/10.1111/nph.15068>. (in press).

Highlights a novel technique for *in vivo* monitoring of starch storage.